Evaluation of Land in Wairoa District for Potential Horticultural Development

A thesis
submitted in partial fulfilment
of the requirements for the degree
of
Master of Science
in Earth Science
at
The University of Waikato
by
Johnathon Taukiri Rau

THE UNIVERSITY OF
WAIKATO
Te Whare Wānanga o Waikato

2018

Abstract

The Wairoa District, on the East Coast of the North Island of New Zealand has less horticultural development than areas to the north and south. The objective of this study was to provide information to help inform landowners who may wish to invest in horticulture which could improve the economic situation of the district.

Field work involving local scale climate mapping and soil characterisation of areas with potential for horticulture in Wairoa District was completed in 2017. Constructed climate and topographical maps with existing soil maps were evaluated against known crop growth requirements to produce crop potential maps identifying areas with potential for crop production. Horticultural crops included in this study include kiwifruit, apples, cherries. Alternative crops include hemp and poppies.

Between mid-April – 31 October 2017, 45 portable iButton temperature loggers were deployed throughout Land Use Capability classes 1-3 in the Wairoa District and were set to record hourly temperature. When regressed against nearby climate stations, long term (18 -26 years) temperature datasets were derived from the short term iButton datasets. MODIS satellite images were also analysed to help identify areas prone to frost. From the long-term datasets local scale chill hour, growing degree days and October frost risk maps were constructed for the Wairoa District. For the central area from Wairoa to Frasertown, chill hours were estimated to range between 600 – 900, growing degree days 1300 – 1400 and October frost risk less than 25%.

From four representative soil types, horizon samples were taken to determine the soils physical properties including each horizons Total Available Water Holding Capacity (TAWHC). Horizon TAWHC for each soil type were summed to give TAWHC to 1 meter which along with 21 years of estimated daily rainfall and potential evapotranspiration were used in a soil water balance model to estimate seasonal crop irrigation requirements. Irrigation estimates for kiwifruit compared well against published values ranging between mean 204 – 247 mm.

The crop potential maps with seasonal crop irrigation estimates can enhance a land owner's ability to make informed decisions resulting in economic benefit to whanau, community and the Wairoa District.

Acknowledgements

Completion of this work would not have been possible without the support and advice from various people to whom I am forever indebted towards. Firstly, I wish to thank my supervisor Dr Megan Balks for her unending patience, humour and enthusiasm. Megan provided guidance when needed and encouragement in all other times.

I am further indebted to a long list of people including Dr Shaun Awatere, John Claydon, Danny Thornburrow (Manaaki Whenua/Landcare Research), Jamie Cox at the Wairoa District Council who supported me financially with a scholarship and accommodation during many weeks of field work. Cheryl Ward – thank you for helping bring my thesis together, you are a lifesaver. Glen Balks deserves mention for assisting me in making an automated method of calculating the climate variables reducing many hours of stress. Likewise, Richard Allen many thanks to you for your energy and enthusiasm – you are an inspiration to all around you. Lastly, this work would not have been possible without the participation and commitment from all the various landowners who provided me access to their land blocks - thank you!

Many thanks to fellow students for general support and encouragement – especially Noel Bates, Nicola Lovett, Andrew Douie and Ben Stewart. Thanks team!

Lastly this work is dedicated to my mother without whom I would not be here today - thanks Mum!

Table of Contents

List of Figures

List of Tables

Chapter 1

Introduction

1.1 Background to Wairoa District

The Wairoa District, in the Hawkes's Bay Region, on the east coast of the North Island, is 4,133.4 km^2 in area (Figure 1.1) and is approximately 340 km north east of Wellington and 340 km south east of Auckland. The Wairoa District is bounded by the Gisborne District in the north east, the Pacific Ocean in the east, Hastings District to the south west, and Whakatane District in the north west.

The Wairoa District has less horticultural development than the Gisborne District to the north or the Napier District to the south. However, within the Wairoa District there are areas of soils with few limitations, and equable climate, capable of growing a range of horticultural crops, pasture, and forestry (Pullar, 1965; Rijkse, 1979; Rijkse, 1980).

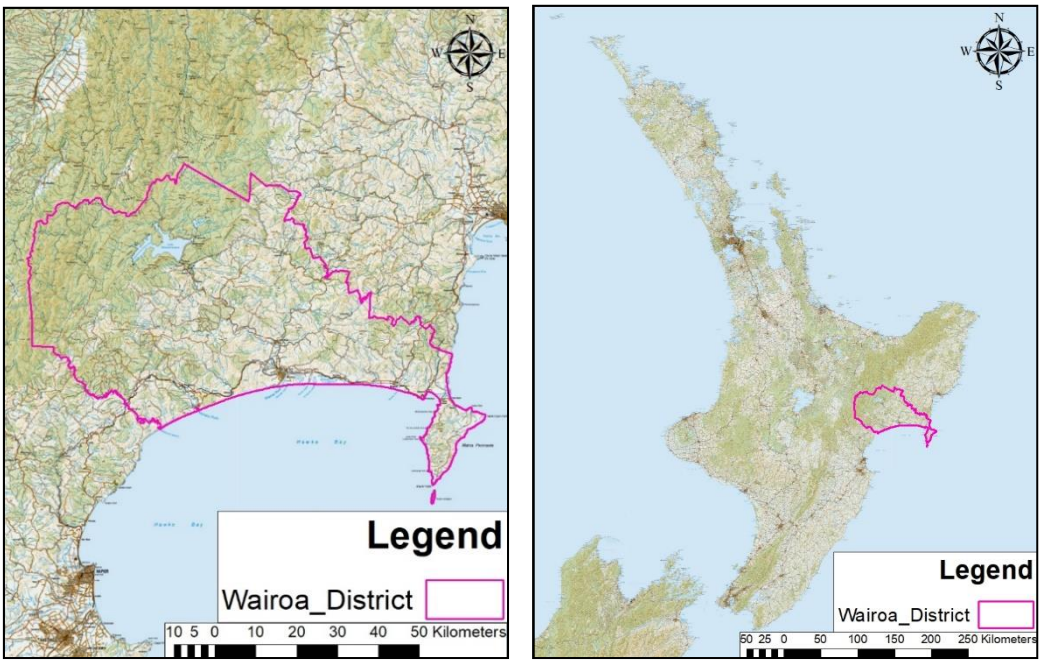

Figure 1:1: Maps showing location of Wairoa District within the North Island, New Zealand.

In the Wairoa District, from 1991 to 2013, the population declined from 10,266 (King *et al.,* 1995) to 7890 (idcommunity - Demographic Resources, n.d.)

and the number of people employed decreased from 3326 (King *et al*., 1995) to 3180 (idcommunity - Demographic Resources, n.d.). This can be attributed to the District's lack of job and career opportunities compounded by the attraction of better wages and lifestyle of other areas e.g. Auckland or Australia (Loomis, 2012). An increase in horticultural production is one potential way to increase income and employment opportunities in the District.

To reduce risk associated with investment in horticulture, and thus realise horticultural land potential, local scale (0.1 – 10km) climate information is needed (Purdie *et al*., 1999; Wratt *et al*., 2006; Webb *et al*., 2016). Recent advances in climate mapping include estimating long-term climate variables (growing degree days (GDD), chilling hours, frost risk) from a dense network of short term (one year) monitoring sites (Sansom & Tait, 2004; Webb *et al*., 2016). In addition night time thermal infrared satellite images have potential to be analysed to improve estimates of frost risk. Satellite image analysis examples include National Oceanic and Atmospheric Administration Advanced Very High Resolution Radiometer (NOAA AVHRR) (Tait & Zheng, 2003; Francois, 1999) and MODerate-resolution Imaging Spectroradiometer (MODIS) (Pouteau *et al*., 2011; Lensky *et al*., 2011; Kotikot & Onywere, 2015; Simões *et al*., 2015).

1.2 Objectives

The overall purpose of this project is to conduct a land suitability analysis of the Wairoa District to identify areas with potential for horticultural development. Integration of climate, soil, and crop information communicated as crop potential maps may enhance land owner's ability to make informed decisions resulting in economic benefits to whanau, community and the Wairoa District.

I have four specific objectives.

Objective 1: Climate analysis: Produce local scale climate maps (growing degree days, chill hours and spring frost risk) for the Wairoa District.

Activities to achieve objective 1 include:

- Monitor local temperatures to provide ground-truthing for satellite data and improved ability to extrapolate from the Wairoa District's long- term climate record.

- Analyse MODIS satellite images and climate records to identify areas prone to frost.

Objective 2: Soil characterisation: For representative soil types in Wairoa District determine soil properties including, soil water holding capacity, to provide information to determine crop suitability and seasonal irrigation requirements.

Objective 3: Investigate soil, water, and climate requirements for a range of crops (Table 1.1):

Table 1:1: Range of crops used in this study

Fruit	Other
Apples	Hemp
Cherries	Poppies
Kiwifruit	

Objective 4: Develop crop potential maps for Wairoa District, based on above objectives and soil/land evaluation analysis.

Chapter 2

Literature Review: Wairoa District

2.1 Wairoa District history & development

During pre-European times the Wairoa District had numerous Maori settlements mainly concentrated along the coast and some inland routes. Much of the Wairoa Plains were used for growing crops with considerable areas of the hill country burned (Pullar & Ayson, 1965) and reverting to Manuka (Page, 1988).

From the late 1820's European settlement commenced with a whaling and trading station operating from the 1830's. Pre 1850 population growth in Wairoa was minimal until a sea trade with Napier began (idcommunity - Demographic Resources, n.d.). By 1868 local exports included wheat, wool, maize, flax and tobacco (Pullar & Ayson, 1965). Preceding developmental land use the most probable landcover in the 1860's was dense kahikatea stands, matai and manuka on the low-lying wetlands and flood plains with manuka on the Wairoa River natural levees and manuka and fern on the remaining terraces and steep lands (Pullar & Ayson, 1965).

In the 1860's Wairoa became a military base with the population increasing during the late nineteenth and early twentieth centuries (idcommunity - Demographic Resources, n.d.). From 1878 to 1961 the area of sown grass for agriculture increased from 42,000 to 421,000 acres (Pullar & Ayson, 1965). In 1903, a dairy factory was established producing in 1909/10 20 tons of butter increasing to 200 tons in 1924/25 and 500 tons by the early 1960's (Pullar & Ayson, 1965). Commercial flax growing at Awatere commenced in 1911 for a short term then in 1915 a freezing works processing local meat began (Pullar & Ayson, 1965) and currently still operates.

The railway opened in the late 1930's which co-incided with the river port use declining. Post WW1 and WW2 gradual growth occurred into the late 1960's. Since the 1970's however gradual population decline has occurred (idcommunity - Demographic Resources, n.d.) with the Wairoa District population falling from

10,266 in 1991 (King *et al.,* 1995) to 8,150 in 2013 (idcommunity - Demographic Resources, n.d.). This can be attributed to the District's lack of job and career opportunities compared to other areas e.g. Auckland or Australia (Loomis, 2012). Agriculture is the predominant land-use being mostly sheep and beef farming (Chappell, 2013) accounting for 1,494.3 km^2 or 36.2% of the Wairoa District followed by native forests (29.5%), exotic forests (13.2%) and manuka/kanuka (8.1%) (Thompson *et al.,* 2003).

2.2 Climate

Located on the east coast, the Wairoa District is protected by the axial ranges from the pre-dominant westerly weather systems influencing western and central New Zealand. As a result, the east coast, including Wairoa District, is normally drier, less windy and sunnier than other areas on the west coast (Page, 1988).

Climate conditions within the District can vary considerably being mild near the coast but becoming more severe with increasing altitude and distance from the coast (Page, 1988). The Wairoa District comprises three climate classes, C_1, C_3 and M (New Zealand Meteorological Service (1983) in Page (1988); Figure 2.1). Most of the District is class "C_1" (Figure 2.1), which is characterised by very warm summers with day temperatures occasionally rising above 30°C and dry fohn winds (New Zealand Meteorological Service, 1983) with moderate winter temperatures and a mean annual rainfall of between 1000-1500 mm (Figure 2.2; Rijkse, 1980a, 1980b; New Zealand Meteorological Service, 1983). Near the Wairoa township ground frosts have occurred during late autumn in May and early spring in September but not frequently. The average number of ground frosts in June is 4.7, July = 6.7 and for August 3.5, but may be less on the terraces (Pullar & Ayson, 1965). At the McRae farm in Frasertown, Jessen (2002) noted the mean annual rainfall to be 1450 mm, mean summer temperature as 19°C, mean winter temperature as 9°C, with 21 annual ground frosts mostly occurring between May and September.

Mahia Peninsula is also within climate class C_1 (New Zealand Meteorological Service, 1983), with its climate strongly influenced by its closeness to the coast (Whaley, 2001). Summers are very warm with day temperatures occasionally rising above 30°C and dry fohn winds. Mean winter minimum temperatures are

moderate ranging between 6.3-9°C. Coastal annual rainfall averages 1000 mm increasing to 1600-2000 mm in the central hills (Figure 2.2; Whaley, 2001).

Further inland but south of the axial ranges and Whakapunake is the hill country within climate class "C_3"(Figure 2.1) which has cooler mean annual temperatures than class C_1 and mean annual rainfall is 1500-2500 mm (Figure 2.1, 2.2; New Zealand Meteorological Service, 1983 in Page, 1988).

The axial ranges within Wairoa District are classified as climate class "M" (Figure 2.1) being a high mountain climate. Annual rainfall at Lake Waikaremoana exceeds 2000 mm (Figure 2.2) with summer daily maximum temperatures of 25°C while winter daily minimums are -5°C. In winter ground frosts and snowfall occur regularly (Hopkirk, 2011).

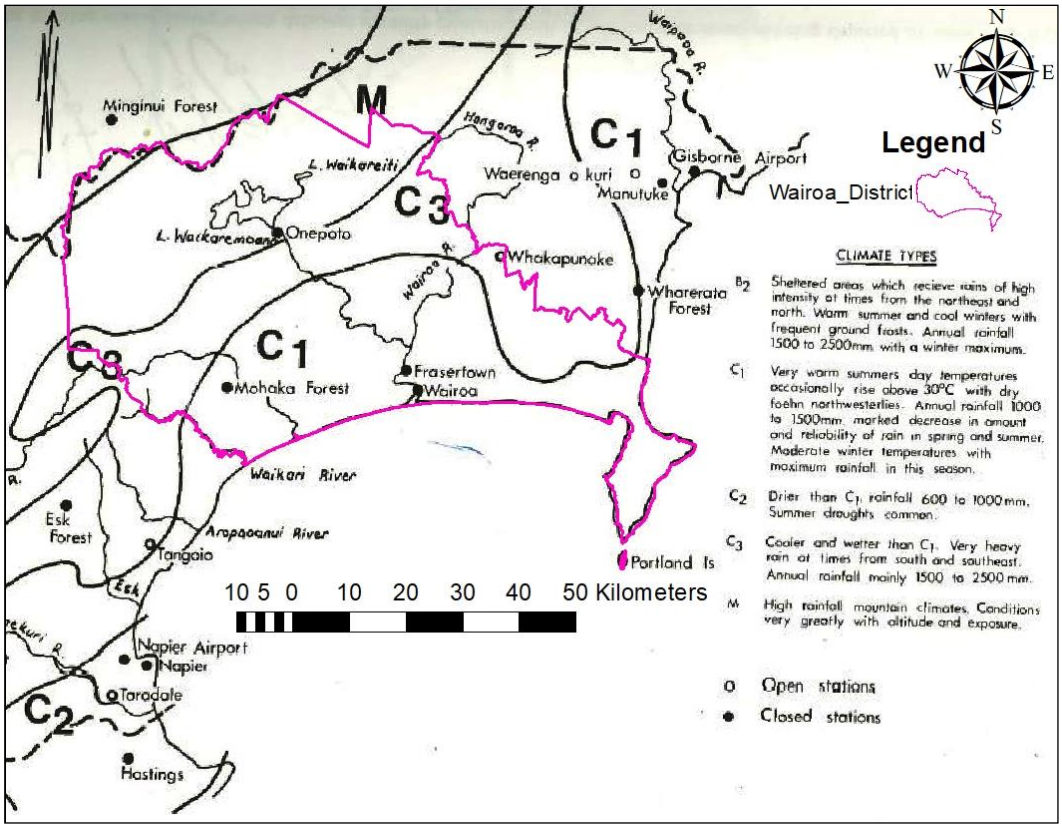

Figure 2:1: Climate classification of Wairoa District. Adapted from the New Zealand Meteorological Service (1983) in Page (1988).

Throughout the District rainfall typically peaks in winter and is lowest in summer (Pullar & Ayson, 1965). Atypically, monthly rainfall can vary with intense rain events occurring from cyclonic depressions moving from north to south down the east coast of the North Island (Pullar & Ayson, 1965). Such cyclones have caused

mass flooding events e.g. as seen in 1858, 1875, 1904, 1914, 1932, 1938, 1948, 1954 (Pullar & Ayson, 1965) and in March 1988 Cyclone Bola deposited 635 mm of rainfall over three days at Pukeorapa. Cyclone Bola flooded the Wairoa township causing extensive landslides throughout the Wairoa District and surrounding region (Pearse *et al.,* 2001).

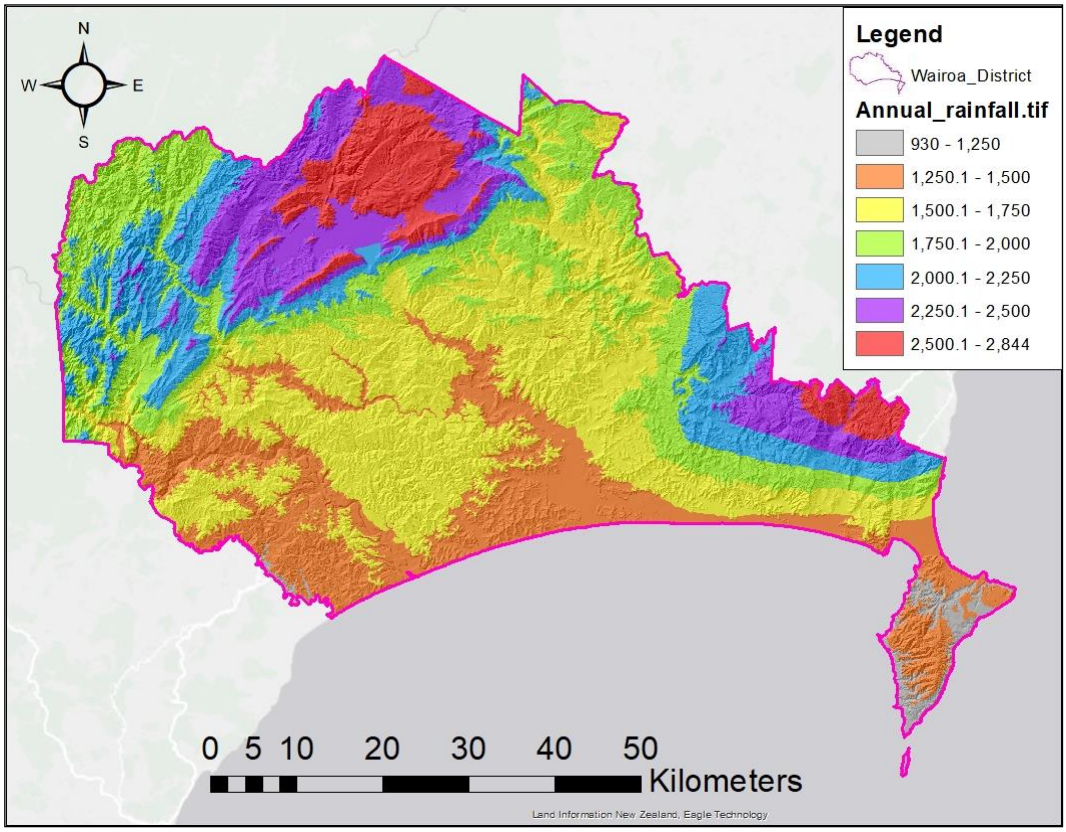

Figure 2:2: Mean annual rainfall for the Wairoa District. Adapted from Leathwick & Stephens (1998).

In contrast the Wairoa District is also prone to prolonged periods of no rainfall leading to a drought as seen in the summer of 1998 - 1999 (Sadeghi & Shamseldin, 2014). Extended periods of insufficient rainfall (dry spells) result in severe depletion of soil moisture and cessation of plant growth (Chappell, 2013).

In summary, the climate of the Wairoa District is mild and equable (Pullar & Ayson, 1965). The climate of such areas holds few limitations to land use having high sunshine hours (2000 hours/year^{-1}), infrequent frosts (5.1/year) with temperatures warm in summer and mild in winter (Page, 1988).

2.3 Geology

The geology of the Wairoa District is depositionally and structurally complex exhibiting rapid facies changes, unconformities and faults (Mazengarb & Speden, 2000; Lee *et al.,* 2011). Figure 2.3 shows the oldest rocks (aged Jurassic - Creteceous) of the Wairoa District to lie in the Huiarau and Ikamatua Ranges west and north west of Lake Waikaremoana. However, the bulk (68%, Table 2.1) of the district's surface geology is Miocene (23.8 Ma) to Pliocene (5.3 Ma) aged with the river valleys and coastal flats being Quaternary (1.8 Ma) aged.

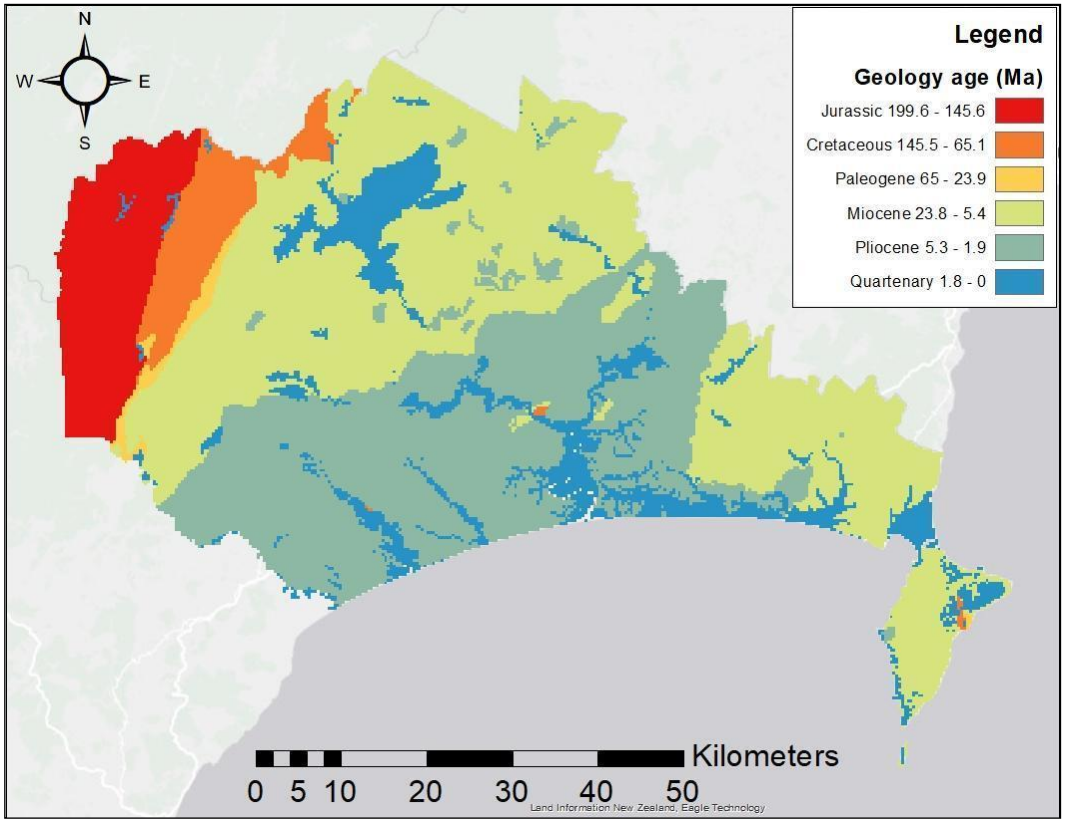

Figure 2:3: Age (Ma) of surface geology in Wairoa District. Adapted from Heron (2014).

Table 2:1: Area of geologic time units within Wairoa District

Time period	Max age (Ma)	Area (km2)	% of total
Creteceous	145.5	192.5	4.7
Jurassic	199.6	350.7	8.5
Paleogene	65	39.8	1.0
Miocene	23.8	1744.2	42.3
Pliocene	5.3	1041.9	25.2
Quaternary	1.8	758.2	18.4
Grand Total		**4127.2**	**100.0**

During the late Oligocene (28 Ma) to Early Miocene (23 Ma) the modern plate boundary began to form throughout the District (Mazengarb & Speden, 2000; Lee *et al.,* 2011) expressed as an accretionary wedge (Figure 2.4) with discrete slope basins bounded in the west by actively rising thrust ridges (Barnes *et al.,* 2002).

From Early Miocene to late Miocene (11.6 Ma) the interaction between the Pacific Plate being subducted beneath the Australian Plate (Figure 2.4) resulted in increased sedimentation, localised uplift and sub-basin formation (Lee *et al.,* 2011).

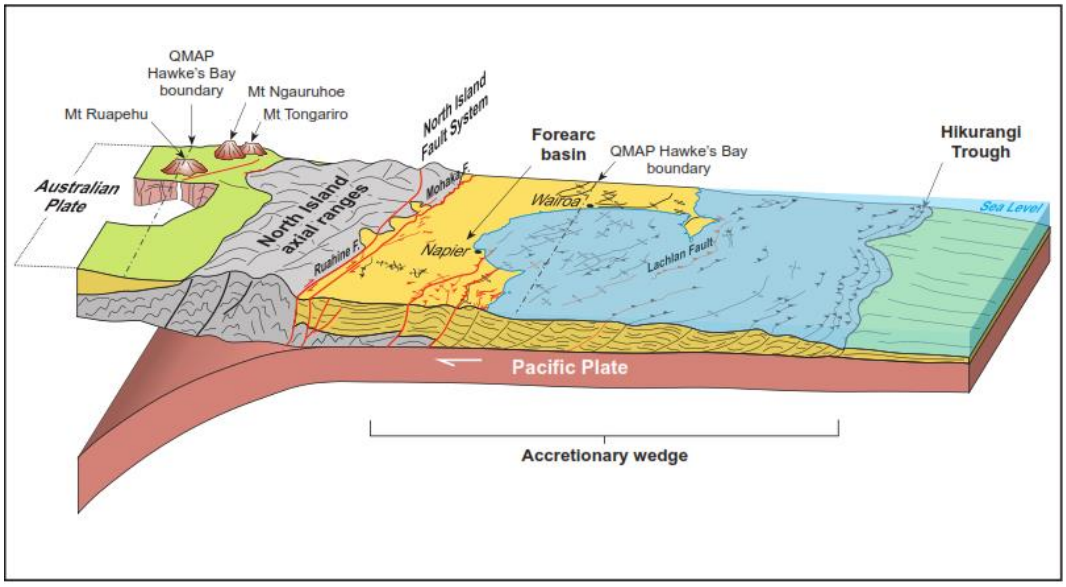

Figure 2:4: Diagram showing the interaction between the Pacific Plate subducting beneath the Australian Plate creating an accretionary ridge and landforms on which the Wairoa District is based. From Lee et al., (2011).

Within the Middle Miocene (16.0 - 11.6 Ma) sub-basins in the northern and eastern Wairoa area underwent rapid subsidence (Drinnan, 2011) creating a marine environment (Mazengarb & Speden, 2000). During the Early Miocene (23 Ma) to Late Pliocene (2.6 Ma), on the forearc basin (Figure 2.4) between Te Hoe (Lee *et al.,* 2011) to Wairoa and Te Puia up to 5km of muddy sandstone sediments, bathyal mudstone and alternating mudstone/sandstone turbidites were deposited in a marine shelf environment (Mazengarb & Speden, 2000; Lee *et al.,* 2011).

During the Middle to Late Miocene (16 - 5.3 Ma) differential uplift created a structural eastern high, part of which is currently the Mahia Peninsula (Figure 2.5)

(Mazengarb & Speden, 2000). The eastern high restricted the eastern extent of the nearby subsiding Wairoa Basin (Mazengarb & Speden, 2000).

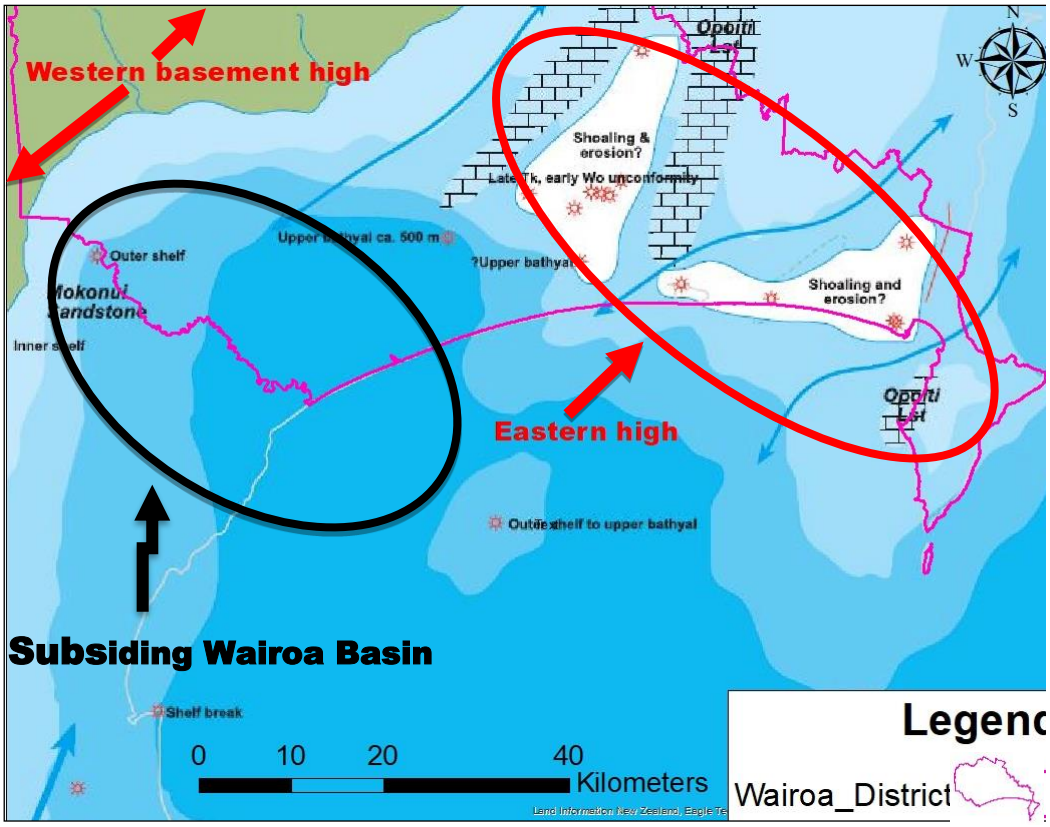

Figure 2:5: Paleographic setting of Hawke's Bay in Late Miocene (5.3 Ma) showing western basement high, subsiding Wairoa basin, rising eastern high and Wairoa District current location outlined. Adapted from Bland & Kamp (2014).

Uplift of the area where the modern North Island axial ranges are, continued from Early Miocene (23.8 Ma) into the Quaternary (1.8 - 0.1 Ma) (Lee *et al.,* 2011) causing the landmass east of the axial ranges to also be uplifted bringing the Miocene and Pliocene aged sediments to the present-day surface forming the majority (68%) of the Wairoa Districts surface geology (Table 2.1, Figure 2.6). In steep hill country with slopes greater than 25° erosion has allowed soils to develop from the exposed geology (Jessen, 2002).

During Middle Miocene and younger times (<16 Ma) volcanic tephra deposits were interbedded with the marine sediments (Mazengarb & Speden, 2000). Volcanic tephra older than 2 Ma were likely sourced from volcanoes of the Tauranga-Kaimai area whereas deposition of rhyolitic volcanic tephra into sedimentary basins west

and east of the axial ranges marks the formation of the Taupo Volcanic Zone at approximately 2 Ma (Lee *et al.,* 2011).

During the Quaternary (2.6 Ma - 0.1 Ma) due to rapid uplift, erosion and sea level changes have created extensive alluvial terraces and floodplain deposits in catchments (classified as "gravel" in Figure 2.6) and near the coast, dune complexes, wetlands and uplifted marine terraces e.g. Mahia Peninsula (Mazengarb & Speden, 2000).

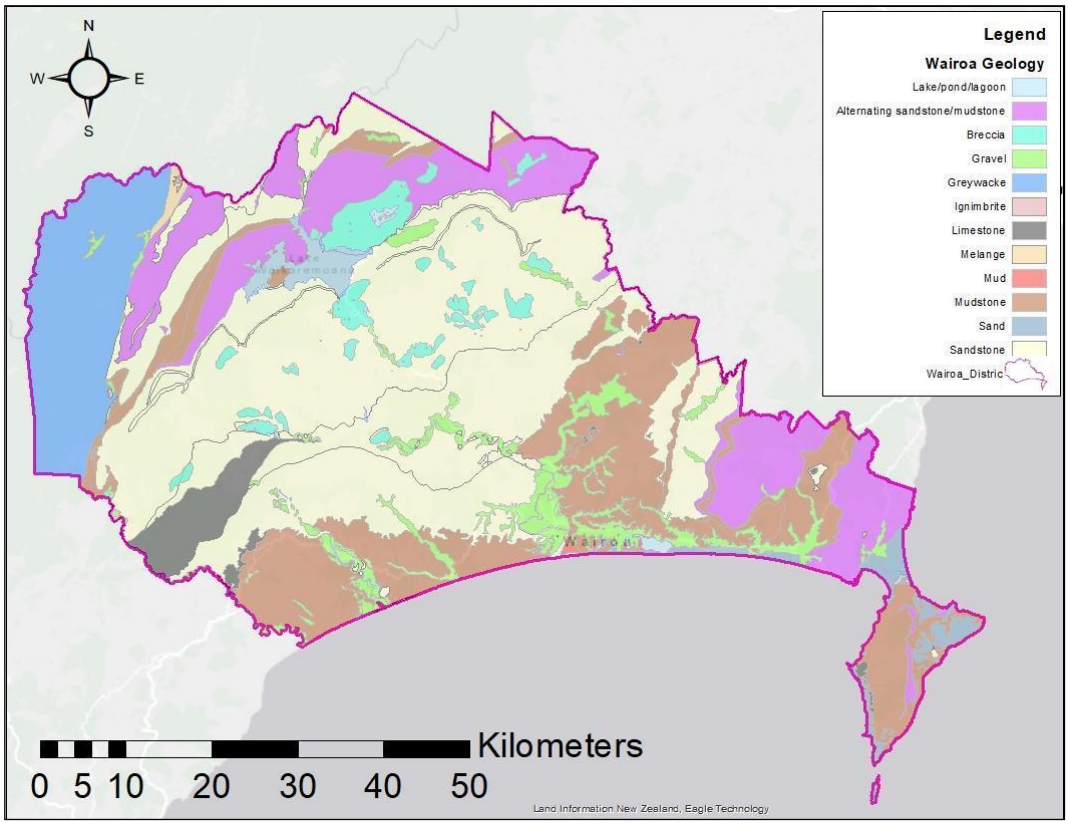

Figure 2:6: Classification of surface geology in Wairoa District (Heron, 2014).

Taupo Pumice (1718 cal. yr BP) and Waimihia Lapilli (3421 cal. yr BP) are the two dominant tephra in the Wairoa District contributing towards soil development (Figure 2.7, Molloy, 1998; Lowe *et al.,* 2013). Beneath the Waimihia likely lie the Rotoma Ash (9482 cal. yr BP), Waiohau Ash (14,001 cal. yr BP) and Kawakawa/Oruanui tephra (Figure 2.8, Molloy, 1998; Lowe *et al.,* 2013). Tephra deposits draping the steeplands (slope > 25°) have largely been removed by erosion to expose siltstone as the underlying parent material. In contrast the gently sloping hillslopes and terraces remain with the original tephra deposits (Jessen, 2002).

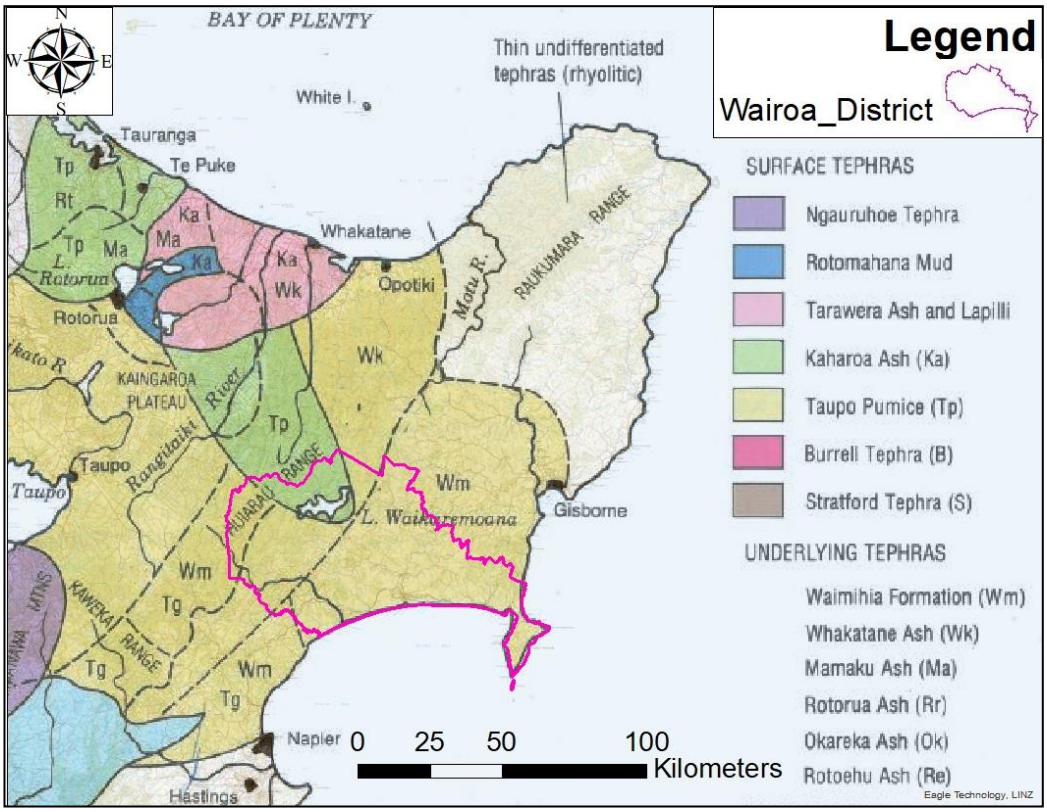

Figure 2:7: Spatial distribution of tephra deposits in eastern North Island including Wairoa District, contributing towards the top one metre of soil development. Adapted from Molloy (1998).

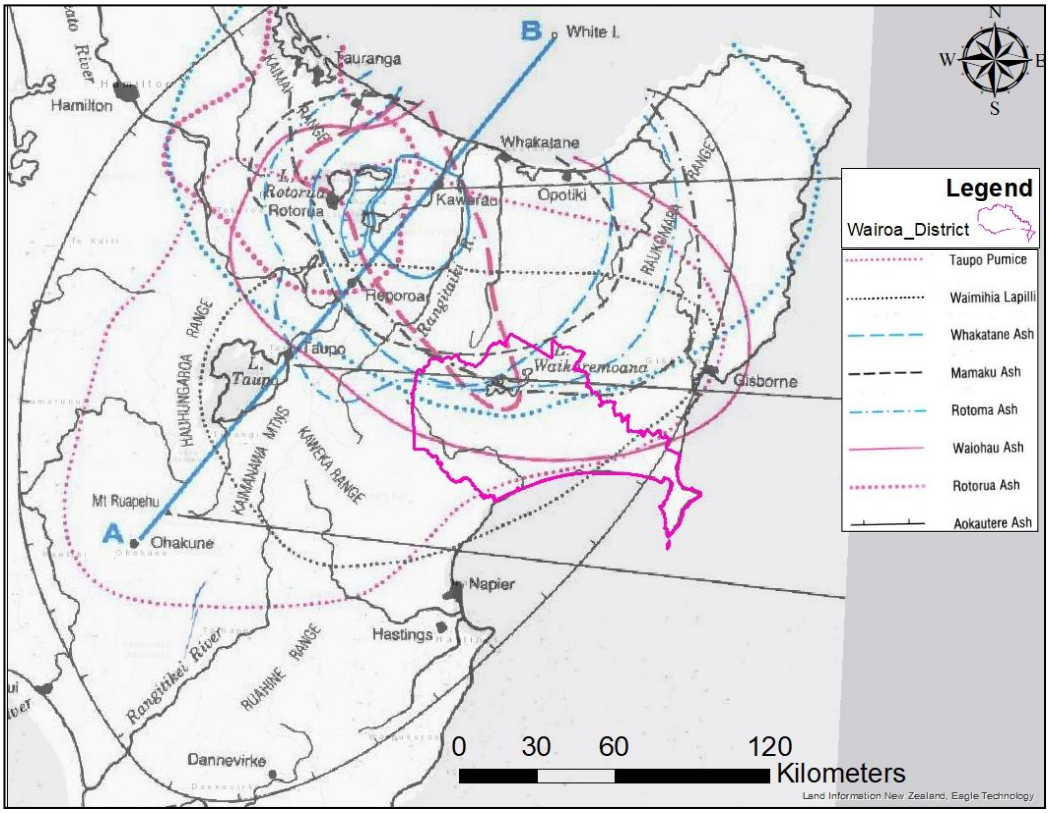

Figure 2:8: Spatial extent of major tephra deposits over Eastern North Island and Wairoa District. Adapted from Molloy (1998).

2.4 Landforms

The topography within Wairoa District is indicative of its underlying geology, structural trends and tectonic setting (Mazengarb & Speden, 2000; Lee *et al.,* 2011). The landscape was created by tectonic compression and faulting (Hammond, 1997) in concert with climate forces (Page, 1988). The basement rocks and overlying sedimentary rock sequence over geological time were distorted into minor north-east to south-west trending anticline (hills) and syncline (valleys and basins) folds with dips ranging between 5-20° (Hammond, 1997). During that time erosion and deposition have worked together to present the current landforms (Page, 1988).

Within the Wairoa District, Page (1988) described three main physiographic zones (Figure 2.9). Zone 4 is described from Whaley (2001). Typical landforms within zones 1-4 include:

(1) Mountain ranges: The North Island Axial ranges extend from Cook Strait to East Cape trending south-west to north-east through the Wairoa District as the Huiarau Ranges (Lee *et al.,* 2011). The ranges are steep sided, predominantly bush-clad, with many peaks over 1500m a.s.l. (Hammond, 1997). The Jurassic to Cretaceous aged ranges are composed of greywacke (Lee *et al.,* 2011) which act as a gravel source for the Mohaka, Waiau and Wairoa Rivers transporting sediments to the coast (Hammond, 1997).

At least 3,300 years ago (Lowe & Walker, 1992) a massive landslide formed a natural dam to block the Waikaretaheke river forming the present-day Lake Waikaremoana (Davies *et al.,* 2006). Other lakes, as landforms include Lakes Tuai and Putere which are also associated with large landslides (Whaley, 2001).

(2) Hill country: this zone covers the greatest area within the Wairoa District extending from the axial ranges to the coast (Page, 1988). Thick layers of Miocene to Pliocene aged sedimentary rocks with localised limestone bands dominate the topography trending south-west to north-east, dipping south-east (Whaley, 2001). The hill country is moderately steep to steep near the axial ranges but becomes rolling closer to the coast/plains (Hammond, 1997). Slope angles range between 20 - 30° (Rijkse, 1979) with stable slopes having up to a metre of tephra deposits

over siltstone. Unstable slopes have had the tephra deposits eroded with the current soil developed from underlying siltstone (Jessen, 2002)

Within the hill country are narrow and deeply entrenched valleys meaning any alluvial terraces and floodplains occur as discontinuous strips (Whaley, 2001).

(3) The terraces and floodplains of the Wairoa District were formed by interaction between tectonic uplift and climatic erosion (Mazengarb & Speden, 2000). Major rivers flowing into Hawke Bay include the Nuhaka, Wairoa, Waihua and Mohaka Rivers (Page, 1988). During the late Pleistocene (0.126Ma – 0.01Ma) a period of relative tectonic stability allowed rivers to cut into the landscape forming a series of high terraces. Uplift resumed to cause rivers to further downcut to their present level (Page, 1988).

Originating from the Okataina, Taupo and Tongariro Volcanic Centres and within the last 20,000 years several tephra deposits made their way over to the Wairoa District (Figures 2.7, 2.8). In the north and north west of the Wairoa District thickness of the deposits is greatest being closer to the source to thin out towards the coast. Since deposition erosion has transported sediments and tephra to be re-deposited on floodplains and terraces (Page, 1988). Where slope angles are less than 12° erosion has left such deposits largely intact (Rijkse, 1979).

(4) Coastal landforms: Between Opoutama and the Wairoa River mouth exists a barrier beach. Through this flows the Nuhaka and Wairoa Rivers while elsewhere between the barrier and mainland are lagoons and wetlands which have been partially infilled with alluvial silt (Whaley, 2001).

Within the Mahia Peninsula is a late Pleistocene aged marine terrace approximately 40-180m a.s.l. featuring mostly in the north eastern (Whaley, 2001) third of the Peninsula. The flat to undulating terraces from sea level appear plateau like hence the name “Table Cape” given to the eastern Kahutara Point by James Cook (Whaley, 2001).

Connecting the Mahia Peninsula to the mainland is a narrow tombolo composed of Holocene aged, wind-blown, well drained sands. Through the central tombolo flows the Kopuawhara Stream with associated imperfectly to poorly drained alluvial soils (Whaley, 2001).

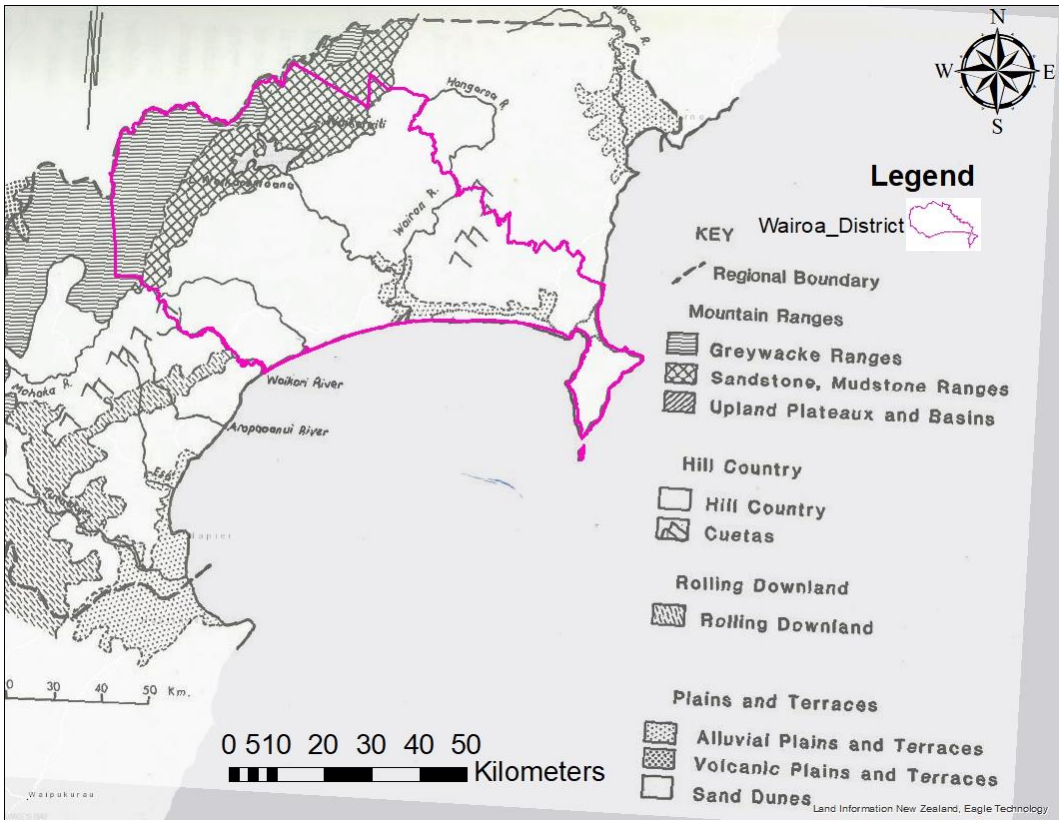

Figure 2:9: Physiography of Northern Hawkes Bay including Wairoa District. Adapted from Page (1988).

Page (1988) classified the Northern Hawkes bay Region (including Wairoa District) into 16 Land Use Capability (LUC) Suites. Page (1998) identified LUC Suite 1 as consisting mainly of alluvial plains and terraces. Page (1988) further identified such landforms as the most productive, versatile and intensively used land having the best soils with few climate limitations for plant growth. Existing limitations are due to poor drainage. Land in Suite 1, class 1-2 although originally in pastoral landuse also has potential for viticulture, horticulture and orcharding (Page, 1988).

Lynn *et al.,* (2009) outline the updated Land Use Capability (LUC) Classification system based on a land areas properties which limit its capacity for sustained long term production. McLaren & Cameron (1996) noted the LUC Classification system as being biased towards arable cropping. For this reason and for the purpose of finding areas suitable for horticulture LUC class 3 in addition to LUC classes 1-2 were selected in ArcGIS (ArcGIS, E. S. R. I., 2018) to identify such areas. Figure 2.10 was made by manipulating the spatial dataset made by Newsome *et al.,* (2008) to show Land Use Capability (LUC) classes 1 – 3 within the Wairoa District which

largely represent landforms of flood plains, river terraces, and coastal flats. Further manipulation of the attributes in Figure 2.10 produced Table 2.2.

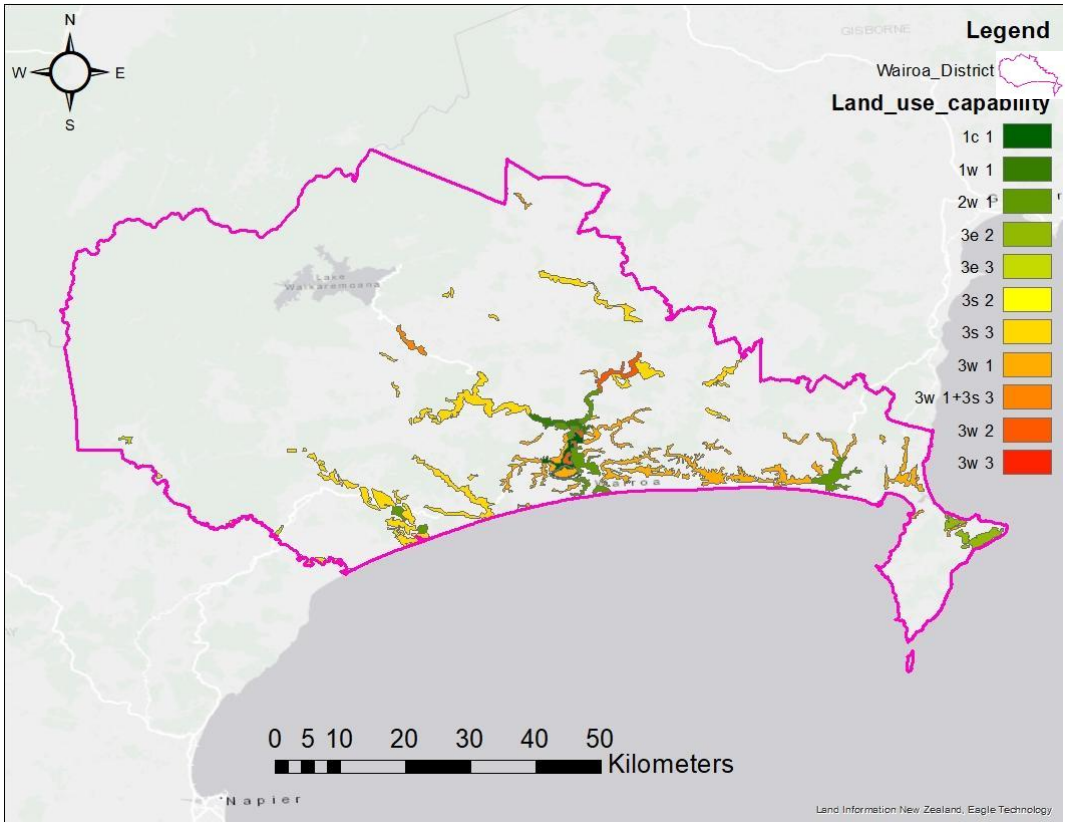

Figure 2:10: LUC classes 1-3 within Wairoa District. Adapted from Newsome et al., (2008).

Table 2.2 shows up to 24,333.8 hectares of land as potential area for use in this study.

Table 2:2.2: Area of Land Use Capability Classes 1 – 3 in Wairoa District.

LUC	Area (Ha)	% of Total	Limitation
1c 1	786.9	3.2	Climate
1w 1	656.9	2.7	Wetness
2w 1	3,110.6	12.8	Wetness
3e 2	1,100.6	4.5	Erosion
3e 3	161.2	0.7	Erosion
3s 2	28.3	0.1	Soil
3s 3	9,209.2	37.8	Soil
3w 1	8,034.2	33.0	Wetness
3w 1+3s 3	341.7	1.4	Wetness/soil
3w 2	889.7	3.7	Wetness
3w 3	14.5	0.1	Wetness
Total	**24,333.8**	**100.0**	

2.5 Soils

Alluvial plains and terraces feature extensively along the Wairoa, Nuhaka and Mohaka Rivers (Rijkse, 1979, 1980). Adjacent to the river beds on low lying banks lie well drained Typic Fluvial Recent soils (Whaley, 2001, e.g. the Waipaoa silt loam) which flood regularly (Pullar & Ayson 1965). On narrow levees lie older Weathered Fluvial Recent soils (Whaley, 2001) which flood rarely to infrequently e.g. the well drained Waihirere silt loam (Rijkse, 1979). Further away from the river on floodplains, terraces and low-angled fans lie imperfect to poorly drained Typic Fluvial Gley Soils (Whaley, 2001) and Typic Orthic Gley Soils e.g. Awamate silt loam (Jessen, 2002). Higher still above the river lie elevated terraces which occur along the Waihua, Mohaka (Whaley, 2001) and Wairoa Rivers on which lie poorly to imperfectly drained Typic Orthic Gley Soils (Whaley, 2001) and Perch-gley Pumice Soils e.g. Mohaka sandy loam (Jessen, 2001).

Limitations of the Wairoa floodplain soils include drainage, nutrient deficiency and irrigation. Provided such limitations could be overcome, these soils represented the greatest opportunities for horticultural development (Pullar & Ayson, 1965). Floodplain soils have been mapped as Waipaoa silt loam, Waihirere silt loam, or Awamate silt loam (Pullar & Ayson, 1965; Jessen, 2002). Terrace lands were mapped as Mohaka sandy loam (Pullar & Ayson, 1965) or Mohaka loamy sand (Jessen, 2002).

Rijkse (1979) reported that the composite Brown Soils, Pumice Soils, and Allophanic Soils on Mahia Peninsula possessed great potential for cropping (including horticulture). Soil series examples include: Mahia, and Kopuawhera soils. The New Zealand Soil Classification (NZSC) of soils covering 90% of the area within LUC 1 -3 are shown in Figure 2.11 and their area in Table 2.3.

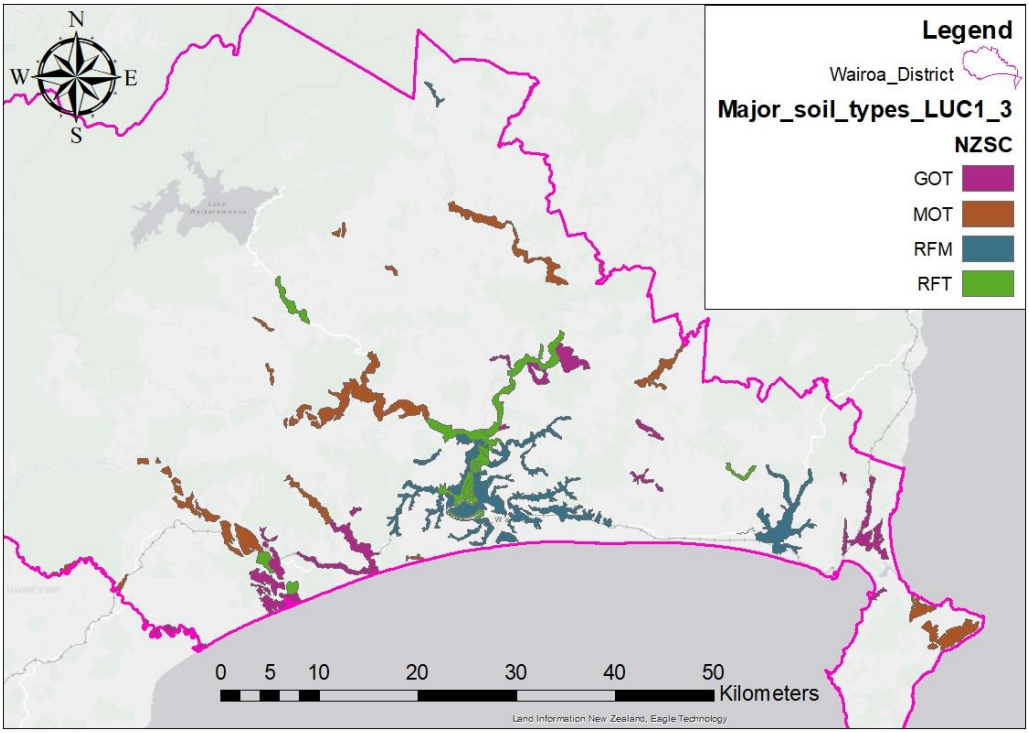

Figure 2:11: Main NZSC groups within LUC 1-3 in Wairoa District. Adapted from Newsome et al., (2008).

Table 2:3: Area of soils within LUC 1-3 in Wairoa District.

NZSC	Area (km2)	% of total
Typic Orthic Pumice (MOT)	69.5	28.6
Mottled Fluvial Recent (RFM)	67.7	27.8
Typic Orthic Gley (GOT)	46.7	19.2
Typic Fluvial Recent (RFT)	35.3	14.5
Mottled Acidic Fluvial Recent (RFMA)	22.4	9.2
Other soils	1.7	0.7
Total	**243.3**	**100.0**

Hill country soils: Jessen (2002) observed five soils within the hill country (slope angle 16-25°) at McRae Farm, Frasertown. These were: Gisborne loamy sand; Gisborne loamy sand, hill soil variant (both Orthic Pumice Soils); Pouawa silt loam, hill soil variant; Pakarae silt loam, hill soil variant (both Immature Pallic Soils) and Pakarae complex, an Orthic Gley Soil. Jessen (2002) further noted some hill country slopes that were stable had up to 1m of tephra over siltstone while on other slopes tephra was eroded with the soils derived from siltstone. For the Mohaka and Tiniroto areas Rijkse (1980) noted slopes between 20-30° were devoid of tephra due to erosion but ridge tops and stable slopes still had intact tephra layers.

2.6 Conclusion

Wairoa District has an equable climate with Land Use Capability Classes 1 – 3 totalling an area of 24,334 hectares. These areas lie mainly in alluvial terraces and floodplains being composed of Recent, Gley, Brown, Pumice and Allophanic soil orders. Areas with potential for horticulture likely lie in these areas.

Chapter 3

Literature Review: Climate Mapping, Estimating Crop Irrigation & Land Evaluation

3.1 Introduction

This chapter provides a literature review of methods for mapping climate variables, estimating crop irrigation requirements, and land evaluation.

Climate variables e.g. frost risk, growing degree days and chilling hours derived from long term (20 – 30 years) temperature records at point climate stations can be interpolated across the landscape to provide gridded climate maps. Widespread methods to interpolate climate variables include deterministic models, e.g. tri-variate thin plate smoothing spine, and geostatistical models, e.g. universal kriging.

Irrigation quantities for a range of crops can be estimated using a soil water balance model. Input data required for a soil water balance model include crop evapotranspiration, rainfall and the soils "available water holding capacity" or AWHC. A soil water balance can be implemented in an excel spreadsheet using Equation 3.1:

$$I = P – (E + D + R) \quad (3.1)$$

Where I = irrigation, P = precipitation, E = evapotranspiration, D = drainage, R = runoff.

Methods to evaluate land potential for horticulture in GIS include weighted linear combination as multi-criteria decision making analysis.

3.2 Climate Mapping

3.2.1 Mapping air temperature

Detailed spatial climate data is needed to model various environmental processes (Ninyerola *et al.,* 2007) e.g. ecology, forestry, hydrology, climate change and agriculture (Tveito *et al.,* 2008). "Geospatial climatology" is "the study of the spatial patterns of climate and their relationships with geographic features" (Daly *et al.,* 2002). The initial step in understanding the relationship between climate and its surrounding landscape is the analysis of climate variables (accurately recorded) at meteorological stations over time. New Zealand has over 300 meteorological stations with long term records, or one for every 850 km^2 (Fitzharris, 1989) which led to the production of a nation-wide spatial climate data set at the macro scale (Leathwick & Stephens, 1998, Table 3.1). The climate maps produced by Leathwick & Stephens (1998) include monthly minimum temperature, monthly maximum temperature, monthly mean temperature and monthly rainfall maps. These climate maps were produced by interpolating point meteorological station climate data across the landscape to estimate a given climate variable while accounting for several geographical co-variates e.g. elevation, location (Leathwick & Stephens, 1998).

Air temperature is an important control on the growth of crops (Blair *et al.,* 2002) hence its spatial representation is of interest in horticulture (Salinger *et al.,* 1995; Hutchinson & McIntosh, 2000). There are many areas with high quality topoclimates capable of growing high value export crops in New Zealand. Although such areas may not be in horticultural land use they need to be mapped to help protect them against future land uses that do not capitalise on their climatic resource (Fitzharris, 1989). Furthermore, mapping of air temperature at local scale is essential to reduce risk when assessing change in land use from pastoral to horticulture (Purdie *et al.,* 1999).

3.2.1.1 Scales of climate

Climate may be considered at a range of scales from microclimate (1 – 100m, Geiger, 2003) to global (>20,000 km, Table 3.1, Linacre & Geerts, 1997). Studies

describing climate scales frequently use the terms “regional”, “local” and “micro” to allow a comparison with similar studies. However, within each scale the range of values can overlap (Pike, 2013; Table 3.1).

Table 3:1: Summary of described climate scales (adapted from Pike, 2013).

Scale (Yoshino, 1975; Oke, 1987; Geiger et al., 2009)	**Scale (Linacre & Geerts, 1997)**	**Yoshino (1975)**	**Oke (1987)**	**Geiger et al., (2009)**	**Linacre & Geerts (1997)**
Micro	Microclimate (Site)	<100m	0.01 - 1000m	0.001 -100m	10m
Local	Topoclimate (Locality)	0.1 - 10km	0.1 - 50km	0.1 - 10km	5km
Meso	Mesoclimate (Region)	10 - 200km	10 - 200km	1km - 200km	50km
Macro	Synoptic (Continent)	>200km	100 - 100,000km	>200km	1000km
Global (Earth)					20,000km

3.2.1.2 Local scale climate

Topography can modify the surrounding climate at local scale (Söderström, & Magnusson, 1995) producing a “topoclimate” (Richards & Baumgarten, 2003) that may significantly influence crop growth and production (Purdie *et al.,* 1999). Thus, knowledge of local scale (Table 3.1; 0.1 – 10km; Yoshino, 1975; Geiger *et al*., 2009) climate information is needed to identify niche areas where the climate may be optimal for specific crops (Sansom & Tait, 2004). Local scale climate mapping is vital for assessing risk when considering change from pastoral to horticultural land use (Purdie *et al*., 1997). Turner & Fitzharris, (1986), Purdie *et al*., (1999) and Webb *et al*., (2016) all employed a dense network of temperature loggers to map the climate at the local scale (Table 3.2). In each study, each of the loggers was deployed for between six months (Turner & Fitzharris, 1989) to one year (Purdie *et al.,* 1999; Webb *et al*., 2016) with the data from each logger site statistically related to the nearest long-term climate station to derive a long-term (20 year) climate data set. The derived long-term dataset from each short-term logger site was then used to calculate climate variables of warm season degree days, growing degree days, chilling hours, and frost risk which were subsequently interpolated and mapped to the local scale (Table 3.2).

Table 3:2: Summary of studies mapping climate at the local scale

Reference	Study area (km2)	Number of temperature loggers	Logger density (km2/logger)	Method to estimate long term temperature dataset	Interpolation method	Climate variable mapped
Turner & Fitzharris (1986)	21	41	0.5	Linear regression	Human expert	Warm season degree days
Purdie *et al*., (1999)	8000	900	8.9	Linear regression, thin plate smoothing spline	Thin plate smoothing spline	Growing degree days, chilling hours, frost risk
Webb *et al*., (2016)	600	170	3.5	Linear regression, regression kriging	Random forests, regression kriging, regression trees	Growing degree days, chilling hours, frost risk

3.2.2 Methods for interpolation of climate variables

Spatial interpolation can be used to estimate the value of a parameter of interest over an unmeasured area using measured data from point sources (Meng *et al*., 2013). Spatial interpolation relies on the first law of geography: "Everything is related to everything else, but near things are more related than distant things" (Tobler, 1970). Methods of spatial interpolation can be categorised in one of three classes: human-expert, mechanistic (deterministic) or linear statistical (probability) based methods (Hengl, 2009).

3.2.2.1 Human expert guided interpolation

Human-expert methods utilise human knowledge & proficiency to deduce climate patterns from meteorological regimes, landscape topography, biological attributes and other information sources (Daly *et al*., 2002). For example, Turner & Fitzharris (1986) implemented linear regression where they used "Six's" type thermometers to measure daily minimum and maximum air temperatures for 45 sites to map the warm season degree days at the local scale of the Bannockburn District (21km^2) of Central Otago. The manually recorded daily measurements (from Nov 1980 – March 1981) were regressed against corresponding temperature measurements from the nearby (long term operating) Cromwell climate station to produce a 30 year daily November – March minimum & maximum temperature data set for each temporary measuring site. Warm season degree days (calculated from each estimated long-term data set at each short-term station) were then mapped at local scale by manually drawing contour lines using expert knowledge to account for topography and any trends suggested by the data (Turner & Fitzharris, 1986).

3.2.2.2 Mechanical (deterministic) models:

Deterministic methods use a numerical function to weight unevenly spaced point data to estimate values over an evenly spaced prediction grid (Daly *et al*., 2002). Example statistical methods used to interpolate climate variables include inverse distance weighting, Thiesson polygons, natural neighbours, and splining (Hengl, 2009).

(A) Inverse distance weighted

Using inverse distance weighting (IDW) method, values at unsampled locations are estimated by linear combination of measured values from known points (Collins, 1995). IDW assumes that areas close to sampled points will have similar values hence are given larger weights than areas further away from sampled sites which will receive smaller weights (Hengl, 2009). Weights of the linear combination are proportional of the inverse distance between the estimated and measured points and are normalised making the sum of all measured sites within the search neighbourhood equal to one (Tveito *et al*., 2008).

IDW is expressed in Equation 3.2 (Tveito *et al*., 2008):

$$\hat{z}(\mathbf{s}_0) = \frac{\sum_{i=1}^{n} \frac{1}{d_i} z(\mathbf{s}_i)}{\sum_{i=1}^{n} \frac{1}{d_i}} \qquad (3.2)$$

Where $z\hat{}\ (s_o)$ = interpolated value at site s_o, $z(s_i)$ is the measured value at site s_i and d_i is the Euclidean distance between the *i*-th location, i = 1, …., n and site s_o.

Advantages of IDW are that it is fast and easy to implement and change to specific needs. Disadvantages are that it has no measure of uncertainty but cross validation is possible (Tveito *et al*., 2008).

(B) Thin plate smoothing spline

Splining works to fit a predicted surface through measured values at known points while being as smooth as possible. This is similar to a rubber sheet being forced through points at known locations so that the sheet is flexed, not broken but also curvature between known points is minimised (Childs, 2004). Spline interpolation is expressed in Equation 3.3 (Meng *et al*., 2013):

$$\sum_{i=1}^{n} \left(z(s_i) - g(s_i)\right)^2 + \eta H_m(g) \quad (3.3)$$

Where z(s) are the predicted values, H_m(g) measures the spline function's smoothness, g is a smoothing function, when η = 0 the spline function passes through all data points and as η becomes close to infinity the function g approaches a least squares polynomial (Meng *et al*., 2013).

Smooth spline interpolator methods are advantageous in that they are efficient in dealing with noisy (weather station) data (Hengl, 2012) and are generally time efficient and user friendly (Hartkamp *et al*., 1999). Due to such advantages, smooth spline methods have been well recognized and implemented for modelling climate variables (Hengl, 2012). However, quantification of the interpolation error is less refined when compared to geostatistical methods (Boer, 2001) e.g. kriging. Also spline model parameters can be set subjectively by the user leading to criticism by geostatisticians (Hengl, 2012).

3.2.2.3 Linear statistical (probability) models:

Linear statistical models use probability theory to estimate parameters in an objective manner. Predictions are given with an estimate of the prediction error. A disadvantage is that input data sets need to satisfy strict statistical guidelines. Such methods include: kriging (plain geostatistics), environmental correlation (regression-based) and hybrid models (Hengl, 2009).

(A) Kriging

During the 1950's research in the mining industry completed by engineer D.G. Krige and statistician H.S. Sichel helped improve estimates of ore reserves. From such work the term "kriging" was born (Hengl, 2009). About a decade later the French mathematician G. Matheron added to Krige's work producing the formulas establishing the field of geostatistics (Webster & Oliver, 2007). Geostatistics employs the theory of regionalized variables to focus on spatial correlation, spatial

interpolation, simulation and depiction of values of random variables (Meng *et al*., 2013). Geostatistics e.g. kriging allows GIS analysts to consider the spatial correlation between measured observations to estimate values at unsampled sites. Subsequently kriging in its various forms has been extensively applied in various disciplines e.g. geology, ecology, geography (Meng *et al*., 2013) and local scale temperature interpolation (Webb *et al*., 2016).

(B) Ordinary kriging

Values estimated at unsampled points are a linear combination of actual measured values with weights relating to the spatial correlation between the data (Tveito *et al*., 2008), determined by a stationary random function semi variogram model (Meng *et al*., 2013).

Ordinary kriging is expressed in Equation 3.4:

$$\hat{z}_{\mathrm{OK}}(\mathbf{s}_0) = \sum_{i=1}^{n} w_i(\mathbf{s}_0) \cdot z(\mathbf{s}_i) = \lambda_0^{\mathrm{T}} \cdot \mathbf{z} \qquad (3.4)$$

Where λ = the vector of kriging weights (w_i), z = vector of *n* observations at locations (Hengl, 2009).

(C) Universal kriging

Universal kriging (UK) is a general liner regression model expressed as Equation 3.5:

$$\hat{z}(s_0) = \sum_{i=1}^{n} \lambda_i z(s_i) \qquad (3.5)$$

Where $\hat{z}(s_o)$ = the value at location s_o being interpolated, $z(s_i)$ are the sampled values, and λi are the weights assigned to each unsampled site (Meng *et al*., 2013). UK assumes that spatial variation in z values possess a trend which can be modelled with the locations information being added into the kriging process. In

contrast to ordinary kriging, weights in universal kriging are determined using a non-stationary random function semi variogram model (Meng *et al*., 2013).

(D) Regression kriging

Regression kriging (RK) brings together regression of the variable of interest on covariate data (e.g. DEM derivatives, satellite imagery) with simple kriging of the regression residuals (Hengl, 2007). Webb *et al*., (2016) applied RK to interpolate pre-calculated temperature variables of frost risk, growing degree days and chilling hours. This was done by stepwise linear regression of the auxiliary variables followed by simple kriging of the residuals.

The initial stepwise linear regression between the auxiliary predictors and the climate data derived a subset of predictors which explained 70% of the variance within the climate data (Table 3.5). This subset was later used to make a multiple linear regression model accounting for any major trends within the training data (Webb *et al*., 2016).

Regression between the observed values and the full covariate data set was then modelled to remove any trend. Subsequent geostatistical analysis of the de-trended residuals was completed to model the spatial autocorrelation between the observed values. As per Hengl (2007) this is expressed as Equation 3.6:

$$\widehat{Z}(s_0) = \sum_{k=0}^{p} \widehat{\beta}_k \cdot q_k(s_0) + \sum_{i=1}^{n} w_i(s_0) \cdot e(s_i), \quad (3.6)$$

Where β_k is the estimated linear regression model coefficient, $q_k(s_0)$ is the k^{th} auxiliary predictor at site s_o, p is the number of predictor variables, $w_i(s_o)$ is the weight derived from the covariance function and $e(s_i)$ is the regression residual.

Webb *et al*., (2016) then performed simple kriging of the residual values (i.e. observed temperature values minus values estimated from the multiple linear regression model). To account for spatial autocorrelation a model was fitted to an empirical variogram plot for each of the frost risk, growing degree days and chilling hour residuals. Using the variogram model, simple kriging of the residuals was

then performed with the resulting kriged surface added to the original trend estimates producing final grid surface/map each for frost risk, growing degree days and chilling hours.

3.2.3 Selecting a method of interpolation

For interpolating temperatures, there appears no singular appropriate method (Hartkamp *et al*., 1999; Ahmed, 2014). In order to select a study area's best performing interpolator a range of methods must be compared against one another as implemented by Hartkamp *et al*., 1999; Benavides *et al*., 2007; Attorre *et al*., 2007; Hofstra *et al*., 2008; Chai *et al*., 2011; Eldrandaly & Abu-Zaid, 2011; Meng *et al*., 2013; Ahmed *et al*., 2014; Webb *et al*., 2016. The results of which are summarised in Table 3.3. The studies in Table 3.3 show that for interpolating temperature, kriging in its variant forms is a superior method.

Table 3:3: Summary of studies comparing methods of interpolating temperature

Reference	Location/landscapes	Spatial interpolation method trialled	Parameter interpreted	Best performing interpolator
Hartkamp *et al.,* (1999)	Jalisco, Mexico	Inverse Distance Weighted (IDW), Thin Plate Spline (TPS), Co-Kriging (CK)	Monthly mean air min/max temperature	TPS
Atorre *et al.,* (2007)	Lazio Region, Italy. Mountains, coastal flats, fluvial valleys volcanic hills & plateau	IDW, multi-layer neural networks Universal kriging with external drift (UKED)	Mean monthly May/June/July/Aug air temperature and rainfall	UKED
Benavides *et al*., (2007)	Northern Spain	Ordinary kriging (OK), universal kriging (UK), regression models (RM)	Air temperature	OK
Hofstra *et al*., (2008)	United Kingdom, Alps	Global kriging (GK), Local kriging (LK), Natural neighbour (NN), regression, 2D & 3D TPS	Daily rainfall Daily mean/min/max air temperature	GK
Chai *et al*., (2011)	Xinjiang Uygur Autonomous Region (Xinjiang), China. High altitude mountains/basins.	IDW, OK Temperature lapse rate Multiple linear regression	Mean monthly air temperature	IDW
Eldrandaly & Abu-Zaid (2011)	Western Saudi Arabia	OK, UK, IDW, TPS, global polynomial (GP), local polynomial (LP)	Mean monthly air temperature	OK & UK
Meng *et al*., (2013)	Big Sur Ecoregion, California	Regression kriging (RK), CK, UK, IDW Radial basis function (RBF), TPS	Mean annual air temperature	RK
Ahmed *et al*., (2014)	Balochistan, Pakistan. Upper & lower highlands, plains & deserts.	IDW, GP, LP, RBF, OK, UK Ordinary, simple, universal & disjunctive kriging & co-kriging	Mean annual air temperature/rainfall	Disjunctive & universal co-kriging
Webb *et al*., (2016)	Tasmania, Australia. Meander Valley, undulating plains	Regression kriging (RK), regression trees (RT), random forests (RF)	Daily/hourly min/max air temp	RK

3.2.4 Use of covariate data to aid interpolation

Most statistical interpolation methods perform better if auxiliary data e.g. elevation, distance from coast (which have some influence on the predicted variable), are used as explanatory data in the interpolation process (Hengl, 2012).

3.2.4.1 Terrain derivatives

When using regression kriging to interpolate growing degree days, chill hours and frost risk at the local scale Webb *et al.,* (2016) used 30 terrain derivatives aid the interpolation. Jarvis & Stuart (2001b) stated that kriging does not need many co-variate data sources instead is able to use the power of spatial autocorrelation producing similar results to interpolators that use more than 3 co-variate parameters. Webb *et al.,* (2016) agree with Jarvis & Stuart's (2001b) statement showing that two co-variates could account for 71-75% of the variance (Table 3.4). This enabled Webb *et al.,* (2016) to conclude that regression kriging was the superior method for spatial interpolation of temperature at the local scale for their study area, especially given their other trialled methods did not have any geostatistical analysis or method to quantify the interpolation error (Webb *et al*., 2016).

Table 3:4: Co-variate predictors used in regression kriging to aid interpolation of climate variables showing explained variance (Webb et al., 2016). NHT = normalized height; SWI = SAGA wetness index; DEM = digital elevation model.

Climate parameter	Co-variate	Variance (%)
Chill hours	DEM, SWI	75
Growing degree days	DEM, SWI	71
Frost risk	NHT, SWI	73

3.2.4.2 Remotely sensed data

Remotely sensed satellite e.g. MODerate resolution Imaging Spectroradiometer (MODIS) images can estimate an areas land surface temperature (LST), defined as the "skin" temperature of the ground (Yang *et al*., 2017). Ground based meteorological stations measure air temperature (T_{air}) typically 2m above ground. Although there is a strong relationship between LST and T_{air} the two each have

distinct physical meanings, magnitude and measurement techniques (Jin & Dickinson, 2010). Despite their differences satellite based LST estimates have been successfully used as covariate data to improve the mapping of minimum air temperature (Jones *et al*., 2004; Mostovoy *et al*., 2006; Zhu *et al*., 2013) and frosts (Francois *et al*., 1999; Tait & Zheng, 2003; Pouteau *et al*., 2011).

MODIS LST products are derived from two satellites, Terra and Aqua which have been in operation since 2000 and 2002 respectively. Together they provide a global dataset available for download from the United States National Aeronautics & Space Administration (NASA) (Sohrabinia *et al*., 2015). An algorithm produces MODIS LST estimates which have been validated using ground measurements to ensure product quality. MODIS products from early 2000 (Terra) and 2002 (Aqua) are available through algorithm version 6 (Wan, 2014). MODIS products although freely available to download require several pre-processing steps before becoming useful. Such steps are technically simple however manual execution is time consuming. To overcome such issues Busetto & Rangetti (2016) developed MODIStsp, an open source "R" based package to automate the downloading and pre-processing of selected MODIS products.

3.2.5 Summary & conclusion

The kriging methods of "kriging with external Drift" (KED), "universal kriging" (UK) and "regression kriging" (RK) are now established as reliable methods for unbiased estimation of spatially continuous attributes, and have become increasingly used for interpolation of climatic and meteorological variables (Hengl, 2012; Table 3.3).

This review supports the decision to employ the open source "R" package MODIStsp to download MODIS images as potential co-variate data to support the mapping of climate variables. Universal kriging is chosen as the primary means of interpolating monthly frost risk, chill hours and growing degree day maps at the local scale for the Wairoa District.

3.3 Estimating crop irrigation requirements

3.3.1 Introduction

A soil's capacity to store water is vital for supporting plant growth (Jones *et al*., 2009) and within most agricultural systems is the major constraint to limiting plant growth and productivity (Farooq *et al*., 2009). Soil moisture levels are well correlated with crop yields (Wong & Asseng, 2006). Therefore, crop productivity can be ensured by applying irrigation to the soil to maintain soil moisture levels. However excessive irrigation can lead to depletion of water resources. Effective water resource management first needs an accurate estimate of the water needed for agricultural irrigation (Er-Raki *et al*., 2010). Knowing when and how much to irrigate a specific crop requires some understanding of the soils daily soil water balance. Volume of crop irrigation as crop evapotranspiration can be calculated as in Equation 3.7:

$$ET_c = K_c * ET_o \quad (3.7)$$

Where ET_c = crop evapotranspiration (mm d^{-1})

K_c = crop coefficient (dimensionless)

ET_o = reference crop evapotranspiration (mm d^{-1}), (Allen *et al*., 1998).

Crop coefficient values have been determined for a range of crops under standard climate conditions, defined as having calm to moderate wind speeds averaging 2m/s in a sub humid climate with average daytime minimum relative humidity (RH_{min}) = 45% (Allen *et al*., 1998).

Known crop coefficient values with reference crop evaporation estimates for a given period can be used as input data in a soil water balance to model crop evapotranspiration (Allen *et al*., 1998). Other data needed in a soil water balance model include rainfall and the soils "available water holding capacity" (AWHC), (Horne & Scotter, 2016).

Sections 3.3.2 to 3.3.3 describe methods of physical measurement and mathematical modelling of reference crop evapotranspiration and soil water balance models.

Section 3.3.4 gives a summary of the literature with recommendations for methods to use.

3.3.2 Modelling reference crop evapotranspiration

Evapotranspiration is the combination of two distinct processes being water lost from soil to the atmosphere by evaporation and water lost from plant to the atmosphere by transpiration. As the two occur simultaneously but are difficult to distinguish means they are often described together as evapotranspiration (Allen *et al*., 1998).

Reference crop evapotranspiration (ET_o) is defined as the rate of evapotranspiration from a hypothetical crop (normally pasture or alfalfa) with a surface resistance of 70 sm^{-1}, 0.12 m in height, albedo of 0.23 covering a large surface area with complete coverage over soil whose growth is active and not limited by available water (Allen *et al*., 1998). The concept of reference crop evapotranspiration was introduced to help understand the atmospheric evaporative demand regardless of plant type, development stage and land management practices. Basing evapotranspiration on a specific surface (grass) gives a reference from which other surfaces (crops) can be estimated from (Allen *et al*., 1998).

Factors influencing crop evapotranspiration include temperature, radiation, vapour pressure and wind speed. Reference crop evapotranspiration can be either measured directly or estimated mathematically using empirical or analytical methods (An, 2010).

The following sections 3.3.3.1 and 3.3.3.1 summarise methods to measure and estimate reference crop evapotranspiration.

3.3.2.1 Physical measurement methods

(A) Pan-measurement

Water is held in an open pan. Over time loss of water by evaporation is deduced by water level sensors. The quantity of evaporation is indicative of an areas collective solar radiation, air temperature, air humidity and wind effects which drive evaporation (Allen *et al*., 1998). Advantages include simple low cost materials. Disadvantages include regular field work to maintain equipment.

(B) Weighing lysimeter

A large block of soil with vegetation representative of its surrounding area is contained within a set structure which sits on top of weighing scales. Over time evapotranspiration is calculated as the difference between rainfall and water lost as discharge (Yang *et al*., 2000).

Advantages include accurate estimates, proven methods. Disadvantages are intensive field work involved.

(C) Eddy covariance method

At up to 30 minute intervals the eddy covariance instrument monitors and records vapour density, and three-dimensional wind speeds. (Baldochhi, 2008). The measured variables are then used to estimate evapotranspiration as expressed in Equation 3.8:

$$\lambda E = \rho\overline{w'q'} = \frac{0.622}{P}\rho\overline{w'e'} \qquad (3.8)$$

Where E = vapor flux in kg m^{-2} s^{-1}; q' is the immediate deviation of specific humidity from mean specific humidity (q) in $kgkg^{-1}$; e' is the immediate deviation of vapor pressure from mean vapor pressure (e) in kPa; w' is the immediate deviation of vertical wind velocity from mean vertical wind velocity (w) in m s^{-1}; P is atmospheric pressure, kPa; and ρa is air density, kgm^{-3}, assumed to be constant (Jensen & Allen, 2016).

Advantages include accurate 30 minute evapotranspiration estimates between 5,000 – 100,000 m^2. Disadvantages include data correction; equipment is expensive, fragile and needs to be maintained by experienced staff.

(D) Remote sensing methods

Since the 1990's researchers have used satellite images to estimate evapotranspiration over large areas using an energy balance (Bastiaanssen *et al*., 1998). Remotely sensed energy balance methods are useful for identifying areas under water stress and related decreases in evapotranspiration (Jensen & Allen, 2016). Limitations for remotely sensed evapotranspiration include the resolution

of the satellite images and derived evapotranspiration maps. Landsat provide high level resolution imagery of 30m with a thermal imager and 16 day return period to allow for change in vegetation cover and increase or decrease in water stress (Anderson *et al*., 2012).

3.3.2.2 Mathematical estimation methods

(A) Empirical methods

- **Thornthwaite method**

Early in the 20th century researchers began to relate air temperature from land and water surfaces to evaporation. Thornthwaite (1948) developed a relationship between mean monthly air temperature and evaporation by analysing catchment water balance studies. Thornthwaite's method for estimating evapotranspiration is shown in Table 3.5, Equation 3.9. Thornthwaite's method used temperature as the sole climate variable. Due to its simplicity, it has been widely used. However, when applied outside its intended area of use e.g. to semi-arid or arid climates errors have resulted (Jensen & Allen, 2016).

- **Hargreaves method**

Hargreaves & Sarmani (1985) recognised the need for a method which could be applied to areas with limited climate data. Using measured minimum and maximum temperatures in combination with measured radiation, evapotranspiration was estimated as per Equation 3.10, Table 3.5.

(B) Analytical methods

- **Priestley-Taylor method**

Barnes (2011) noted that Priestley & Taylor (1972) used the concept of an equilibrium evaporation rate to distribute the net radiation reaching the surface between sensible heat and latent heat of vaporization under conditions of minimal advection. Priestley & Taylor (1972) analysed lysimeter data for saturated land surfaces and data from oceanic cruises to quantify α, defined in Equation 3.11, Table 3.5. Priestley & Taylor (1972) found the best estimate of α for saturated land surfaces had a mean of 1.26.

Past studies have indicated the Priestley-Taylor method to satisfactorily estimate evapotranspiration (Clothier *et al*., 1982; McAneney & Judd, 1983). With new developments and technology however this has proven otherwise. Suleiman & Hoogenboom (2007) found for Georgia, USA that the Priestley-Taylor method when compared to FAO56 Penman-Monteith method underestimated daily and monthly evapotranspiration in winter and overestimate daily and monthly evapotranspiration for summer. Suleiman & Hoogenboom (2007) concluded by anticipating FAO56 Penman-Monteith method to supersede the Priestley-Taylor method to improve crop irrigation efficiency.

- **Penman method**

Most modern methods for estimating evapotranspiration using standard climate variables of air temperature, humidity, wind speed and solar radiation are based on the original Penman equation. British physicist Howard Penman developed the Penman equation during World War II to predict soil surface wetness in Western Europe to help determine if Allied trucks and tanks could advance without becoming bogged down (Jensen & Allen, 2016). Penman's energy balance equation allowed evaporation, sensible heat flux and the soil heat flux to sum to available net radiation energy. Within Penman's equation evaporation was expressed as an empirical aerodynamic formula which is then combined with the energy balance using the Bowen ratio, shown in Equation 3.12, Table 3.5. Input variables for Penman's equation include air temperature, humidity, wind speed and solar radiation (Jensen & Allen, 2016).

Irmak (2003) reviewed the performance of 21 evapotranspiration methods (17 for grass, 4 for alfalfa) for the humid climatic conditions of Florida and found the Penman (1948) equation to be closest to estimates by the FAO56 Penman-Monteith method.

For 16 sites across New Zealand, Scotter & Heng (2003) found mean monthly evapotranspiration estimates from Penman's equation to be within 0.3mm/day of FAO 56 Penman-Monteith evapotranspiration estimates. NIWA use Penman's method to estimate evapotranspiration for 77 climate stations throughout New Zealand which are then interpolated (Tait & Woods, 2007) and made available for

download through their virtual climate station network. Rajanayaka *et al.,* (2016) noted Scotter & Heng's (2003) results then for multiple sites in the Waikato Region downloaded Penman evapotranspiration and rainfall estimates from NIWA's virtual climate station network. These were used as input variables for use within a soil water balance model to estimate irrigation needs for selected vegetables, wine grapes, orchard crops and pasture.

- **Penman-Monteith**

Monteith (1965) reformatted Penman's method using a more theoretical equation for the aerodynamic component. The new equation included parameters describing aerodynamic resistance and surface resistance. The changes allowed the equation to be applied to more diverse surfaces and vegetation types. The resulting equation was called the Penman-Monteith equation (Equation 3.13, Table 3.5; Jensen & Allen, 2016).

Because the Penman-Monteith equation is based on sound physical principles it has greater applicability than the empirical formulations e.g. Thornthwaite method (Jones & Tardieu, 1998). Yoder *et al*., (2005) noted that Jensen *et al*., (1990) compared the performance of 20 methods estimating evapotranspiration against lysimeter measured evapotranspiration spread over 11 sites covering different world climate zones. Jensen *et al*., (1990) concluded that the Penman-Monteith method was the best performing method in all climatic conditions. Furthermore, Allen *et al.,* (1994) showed that the Penman-Monteith estimated evapotranspiration values were close to actual measured values.

- **FAO56 Penman-Monteith model**

Recognising the need for a standard method to estimate crop evapotranspiration, industry experts met in 1990 to revise the available options. The Penman-Monteith method was unanimously chosen (McVicar *et al*., 2005). Subsequent work culminated in the FAO56 Penman-Monteith method as the new recommended method to estimate crop evapotranspiration (Allen *et al*., 1998). Refining the Penman-Monteith into the FAO56 Penman-Monteith method were based on simplifying assumptions through the definition of reference surface conditions. This is defined as "a hypothetical reference crop with an assumed crop

height of 0.12m, a fixed surface resistance of 70sm^{-1} and an albedo of 0.23" (Allen *et al*., 1998). Estimating crop evapotranspiration via the FAO56 Penman-Monteith method is given in Equation 3.14, Table 3.5.

Table 3:5: Summary of evapotranspiration estimation methods

Method	Equation	Equation #	Reference
Thornthwaite	$e = 1.6(10t.I^{-1})^{\alpha}$	3.9	Thornthwaite (1948) in Bhatti & Patel (2014)
Hargreaves	$ET = 0.0023TD_c^{0.5}(T_c + 17.8)R_a$	3.10	Hargreaves & Samani (1985) in Bhatti & Patel (2014)
Priestley-Taylor	$ET_o = \alpha \frac{\Delta}{\Delta + \gamma} \frac{(R_n - G)}{\lambda}$	3.11	Priestly and Taylor (1972) in Bhatti & Patel (2014)
Penman	$\lambda E = \frac{[\Delta(R_n - G)] + (\gamma \lambda E_a)}{(\Delta + \lambda)}$	3.12	Penman (1948,1963) in Bhatti & Patel (2014)
Penman-Monteith	$ET = \frac{\Delta(R_n - G) + \rho c_p (VPD)/r_a}{\Delta + \gamma(1 + \frac{r_s}{r_a})}$	3.13	(Monteith 1965) in Bhatti & Patel (2014)
FAO56 Penman-Monteith	$ET_o = \frac{o.408\Delta(R_n - G) + \gamma \frac{900}{T + 273} u_2(e_s - e_a)}{\Delta + \gamma(1 + 0.34u_2)}$	3.14	Allen *et al.,* (1998) in Bhatti & Patel (2014)

Where e = unadjusted potential ET (cm/month)(month of 30 days each and 12 hrs daytime), t= mean air temperature(°C), *ET= s*easonal crop water requirements (inches), TD_c = maximum and minimum daily air temperature difference, $T_f and\ T_c$ = mean air temperature (°F and °C), R_a = extra-terrestrial radiation (mm d^{-1}), ET_o= reference evapotranspiration (mm day^{-1}), α = 1.26, Δ = slope of saturated vapour pressure curve (kPa $°C^{-1}$), R_n= net radiation flux (MJ m^{-2} day^{-1}), *G* = sensible heat flux into the soil (MJ m^{-2} d^{-1}), γ = psychrometric constant (kPa $°C^{-1}$), λ = latent heat of vaporization (MJ kg^{-1}), λE = evaporative latent heat flux (MJ m^{-2} day^{-1}), E_a = vapour transport of flux (mm d^{-1}), ρ = density of air (kg m^{-3}), c_p = specific heat of moisture (J kg^{-1} $°C^{-1}$), *VPD* = vapour pressure deficit, $r_s\ and\ r_a$ = canopy surface resistance and aerodynamic resistance (sm^{-1}), T = mean monthly temperature (°F), U_2 = wind speed at 2m (km h^{-1}), e_s = saturation vapour pressure (k Pa), e_a = mean actual vapour pressure (k Pa) (Bhatti & Patel, 2014).

3.3.3 Modelling crop evapotranspiration

Evapotranspiration (ET) from a given crop can be measured directly via the mass transfer, energy balance methods or lysimeter studies (Allen et al, 1998). When such methods are not feasible crop evapotranspiration (ET_c) can be estimated by multiplying the reference crop ET (ET_o) by a particular crop's coefficient (K_c) given in Equation 3.7. Pereira *et al*., (2015) reported that this method was first applied by Jensen (1968) who compared ET for a given crop over a defined time period to the "potential evapotranspiration" (PET) rate of a reference crop over the same time period. PET for a reference crop over time evolved into "reference crop evapotranspiration" using alfalfa or pasture as the reference crop (Pereira *et al*., 2015). Pereira *et al*., (2015) further noted that Jensen (1968) called this ratio the crop coefficient (K_c) who described it as a dimensionless ratio representing several factors. These included the resistance to movement of water from soil to the evaporating surface; the resistance to diffusion of water vapour from evaporating surfaces via the laminar boundary layer and the resistance of turbulent transfer with the surrounding atmosphere and relative amount of radiant energy obtainable as compared to the reference crop.

Calculation of ET_o in a range of climates has been standardised (Allen et al, 1998). K_c values for a range of crops have been reported (Allen et al, 1998, 2007; Jensen & Allen, 2016). Estimating ET_c using the ET_oK_c method is simple, makes use of readily available (Allen et al, 1998). The method is applicable in differing regions and climates due to the assumption that by calculating the reference crop ET this accounts for any variation in weather and climate (Allen & Pereira, 2009).

K_c can be given as one single coefficient or split into two factors describing loss of moisture from soil by evaporation (K_e) and crop transpiration (K_{cb}). Selection of the single (Kc) or dual ($K_c = K_{cb} + K_e$) approach is dependent on the accuracy needed, climate data available and temporal resolution in which the calculations will be used (Allen et al, 1998). The single crop coefficient is suitable for irrigation planning and design, scheduling for non-frequent irrigation and basic irrigation schedules. Time-steps are daily, co-daily and monthly calculations. The dual crop coefficient approach is suitable for detailed soil and hydrologic water balance

studies; real-time irrigation scheduling and determining a high frequency irrigation. Calculations of ET_c are daily (Allen et al, 1998).

The single crop coefficient method is suitable for this study because the objectives include estimating seasonal irrigation requirements for multiple crops. This information could be used to aid landowners in irrigation planning, design and management.

3.3.4 Soil water balance modelling

Estimating soil moisture content over time is useful for irrigation planning and drought forecasting (Woodward *et al.,* 2001). This can be achieved by employing a soil water balance. Various methods exist to model the water balance ranging from simple water balances to detailed mechanistic models (Woodward *et al*., 2001). Single layer models are adequate for practical purposes however multi-layer water balance models are preferred (Woodward *et al*., 2001). Scotter *et al*., (1979) developed a two-layer water balance model including a zone which is preferentially depleted & recharged thereby significantly improving on other single layer models (Woodward *et al*., 2001). Woodward *et al*., (2001) improved the Scotter *et al*., (1979) model by replacing empirical constants with soil available water holding capacity (AWHC) and used the FAO modified Penman-Monteith method to estimate evapotranspiration instead of the Priestly-Taylor method. Horne & Scotter (2016) improved the Woodward *et al.,* (2001) by modifying the drainage equation and simplifying the evapotranspiration equations. Horne & Scotter (2016) noted that their modified dual layer model was an improvement on the single layer model by simulating an extra 40mm/yr of evapotranspiration meaning 40mm/yr less in drainage.

Woodward *et al.,* (2001) implemented their work in an excel spreadsheet. Initial parameters include $AWHC_s$, $AWHC_{76}$, a scaling factor (β), AWHC, a water coefficient (α), an efficiency factor and a leaf area index. These are discussed as follows. Woodward *et al*., (2001) for their work defined $AWHC_s$ as the readily available water holding capacity of the soil recharge zone. As the soil data used by Wooodward *et al.,* (2001) had no values for the recharge zone this was instead assumed to be 25mm. $AWHC_{76}$ refers to the AWHC of a soil to 76 cm depth. Woodward *et al.,* (2001) used published $AWHC_{76}$ data from 20 different soil types.

Analytically AWHC is the difference between field capacity (0.01 – 0.02 MPa) and permanent wilting point (1.5 MPa) to a given depth (Woodward *et al.,* 2001). Pasture however can extract greater moisture than that given by the laboratory defined AWHC. To compensate for this Woodward *et al.,* (2001) used a scaling factor (β) to multiply $AWHC_{76}$ yielding AWHC. Woodward *et al.,* (2001) noted that for use in their model AWHC did not equal AWHC as determined by laboratory analysis but instead represented the potential water capable of being extracted by plants. The water coefficient (α) Woodward *et al.,* (2001) used was estimated by examining the ratio of actual ET to calculated PET when soils are especially dry. For six soil datasets Woodward *et al.,* (2001) found α to be similar with a pooled best fit value of 0.0073. Woodward *et al.,* (2001) incorporated a leaf area index (LAI) describing the amount of pasture cover over the site being modelled. A value of one represented full ground cover.

3.3.5 Summary & conclusion

Physical measurement of evapotranspiration and rainfall for this study's four sites were not possible meaning alternative methods for estimating evapotranspiration and rainfall were investigated. Penman, Penman-Monteith and FAO56 Penman-Monteith methods of estimating evapotranspiration all produce acceptable results. Currently FAO56 Penman-Monteith is the recommended method. However as not all the required data was available for each site alternative sources were investigated. This review supports the decision to employ the single crop coefficient (K_c), daily Penman evapotranspiration and rainfall estimates (downloaded from NIWA's virtual climate station network) with laboratory derived physical soil properties as input variables into the Woodward *et al*., (2001) soil water balance model to estimate seasonal irrigation requirements for a range of horticultural crops for four representative soil types in Wairoa District.

3.4 Land Evaluation: Theory & History

3.4.1 Introduction

Evaluation of land (for agricultural productivity) has been in practice since early agrarian civilizations (Ahrens *et al*., 2002). In recent times land evaluation practices have originated from soil science learnings (Mueller, 2010). With soil being the most significant element within a land resource, soil evaluation is critical for land evaluation (Rossiter, 1996). The terms "soil" and "land" in evaluation systems are often not differentiated however within the last 40 years such methods of evaluation have favoured the term "land" (Mueller, 2010). "Land evaluation" can be defined as: "the process of assessment of land performance when used for specific purposes (Brink & Young, 1977).

3.4.2 History & development of Land Evaluation

In the USA during the 1930's due to soil erosion threatening food production and thus societal stability, work involving soil surveys and land capability assessments gained traction (Beek, 1978) and continued into the 1950's culminating in a detailed land capability assessment and classification report (Klingebiel & Montgomery, 1961). Funded by the United States Department of Agriculture (USDA) the method was subsequently adopted and modified by other countries to suit their own land resources. For example, in 1965 Canada developed its "Soil Capability Classification for Agriculture" (Kenk & Cotic, 1983) and Great Britain produced its "Land Use Capability Classification" (Bibby & Mackney, 1969).

Having many differing land evaluation systems world-wide made an exchange of information between countries difficult (Brink & Young, 1977). During the early 1970's work led by the Food & Agricultural Organisation (FAO) began international discussions to standardise a method for land evaluation. The report "A Framework for Land Evaluation" by Brink & Young (1977) was the result of years of expert collaboration, development and refinement. Indeed, the document was a defining publication whose concepts still strongly influence current land evaluation projects world-wide (Malone *et al*., 2017).

3.4.3 New Zealand history & development

In 1952, the New Zealand Soil Conservation and Rivers Control Council (SCRCC) adopted the United States Department of Agriculture Land Use Capability/Land Inventory System. The system was modified to suit New Zealand Conditions. In 1970 at the request of the SCRCC the Ministry of Works (MOW) began work on series of national resource surveys at a scale of 1:250,000 providing a structured physical stocktake of New Zealand's land resources. National Land Use Capability assessment was achieved by late 1970's (Anthony, 2002) but work continued through to 1998 (Lynn *et al*., 2009) producing higher resolution (1: 63,360) Land Resource Inventory(LRI)/Land Use Capability(LUC) maps (Page, 1988).

In their review of land evaluation for horticulture Webb & Wilson (1994) cited "Soils of Alexandra district" by McCraw (1964) who classified soils within the Alexandra District for stonefruit and pipfruit suitability. The classification was based on orchard productivity. Webb & Wilson (1994) noted that Cowie (1974) improved on McCraw (1964) by classifying soils for horticultural use based on soil limitations including drainage, stoniness, flooding and soil structure. Webb & Wilson (1994) also cited Cox (1978) who classified the soils of Paparua County for horticulture based on available water holding capacity and drainage. Webb & Wilson (1994) criticised the classifications by McCraw (1964), Cowie (1974) and Cox (1978) by saying they lacked objective class definitions, had an absence of clear relationships between the parameters used in the classification and their application to broad crop production systems. Webb & Wilson (1994) noted that Wilson & Giltrap (1984) remedied this by developing a classification system based on land versatility for horticultural production. Their method applied clearly defined objective land attributes to score land relative to its versatility for orchard use (Webb & Wilson, 1994). Webb & Wilson, (1994) updated the classification system of Wilson & Giltrap (1984) by integrating some of the "A Framework for Land Evaluation" (Brink & Young, 1977) concepts. These included:

1. Classification of land suitability is associated with distinct land uses.
2. Suitability assessments are based on land qualities (land attributes which have a direct effect on crop growth).

3. High suitability assessments suggest that productive capacity can be upheld.

3.4.4 Recent developments in land evaluation

In recent times, due to the agricultural industry requesting more precise and quantified crop yield predictions meant more information was needed to evaluate land (Riviere & Maseda, 2006). The drive towards quantifiable crop predictions saw the rise of dynamic simulation models in agriculture systems (Stockle *et al*., 2003). To facilitate the processing of larger data sets computers became more widespread e.g. the Land Evaluation Computer System (LECS; Wood & Dent, 1983 in Nwer, 2006); Automated Land Evaluation System (ALES; Johnson & Cramb, 1991); Micro Land Evaluation Information System (Micro-LEIS; Rosa *et al*., 1992); Intelligent System for Land Evaluation (ISLE; Tsoumakas & Vlahavas, 1999); Land Evaluation Intelligent Geographical Information System (LEIGIS; Kalogirou, 2002) and Agricultural Land Suitability Evaluator (ALSE; Elsheikh *et al*., 2013) and Agricultural Land Use Evaluation System (ALUES; Salvacion & Asaad, 2016). Salvacion & Asaad (2016), Elsheikh *et al*., (2013) and Nwer (2000) each reviewed part or all of the above models, the advantages and disadvantages of which are summarised in Table 3.6.

Table 3:6: Summary of computerised land evaluation models

Model	Advantages	Disadvantages	Reference
LECS	Based on FAO framework; can change parameter values then quickly re-run analysis for multiple outcome comparisons.	Simplicity; developed for Sumatra.	Wood & Dent (1983) in Nwer (2006).
ALES	User can build own expert system; no fixed list for land use requirements or land characteristics; fast assessment; can be linked to socio-economic evaluation.	Not user friendly; no GIS functions; not able to create maps to show results.	Johnson & Cramb (1991), Elsheikh *et al*., (2013).
Micro-LEIS	GIS compatible; can process climate and soil spatial data.	User cannot build personal expert system.	Rosa *et al*., (1992), Nwer (2006).
ISLE	User friendly; based on FAO-SYS land evaluation model; results displayed as mapped colour coded land units.	Does not support wide range of issues in land evaluation.	Tsoumakas & Vlahavas (1999), Elsheikh *et al*., (2013).
LEIGIS	Advanced computer skills not required; based on FAO methodology; designed to evaluate physical land capabilities producing outputs in economic values for different agricultural land uses.	Application limited to wheat, barley, maize, seed cotton and sugar beet crops only; does not include climate data in analysis.	Kalogirou (2002), Elsheikh *et al*., (2013).
ALSE	ArcGIS based; based on FAO-SYS framework; includes soil, climate and topography spatial data in analysis; employs multi-criteria decision analysis (MCDA) to efficiently make land suitability maps.	Custom made model not publicly available.	Elsheikh *et al*., (2013).
ALUES	Open source freeware; includes soil, climate and topography spatial data in analysis; employs fuzzy logic in "R" scripting language to efficiently make crop suitability maps.	R scripting expertise required.	Salvacion & Asaad (2016).

3.4.4.1 Land evaluation methods in GIS

Since the 1990's GIS has become an increasingly used tool in land evaluation and suitability analysis. Land-use suitability analysis in a GIS environment aims to recognize the best fitting spatial pattern given the requirements and preferences of a given land-use (Collins *et al*., 2001). Methods used for land use suitability analysis can be divided into three groups: artificial Intelligence (AI), multi-criteria decision making (MCDM) and computer assisted overlay mapping. Regarding land evaluation, MCDM methods are the most appropriate (Malczewski, 2004) henceforth are discussed.

3.4.4.2 Multi-criteria decision making

Integration of MCDM into GIS is a significant advancement from the standard overlay analysis method relating to land suitability analysis (Carver, 1991). Multi-criteria decision making applied as a land evaluation framework within GIS is appropriate as multiple natural resource attributes e.g. topography, climate and soil properties can be processed Massawe (2015). Examples methods of MCDM include Boolean logic, fuzzy logic and weighted linear combination.

(A) Boolean logic theory

George Boole introduced Boolean logic where attributes can be one of two integers being 1 (True) or 0 (False) with the boundaries between the classes clearly defined, Figure 3.1:

0	0	0	1	1
0	0	0	1	1
0	0	1	1	1
0	1	1	1	1
1	1	1	1	1

Figure 3:1: Cells representing Boolean classes. Adapted from Elaalem (2010).

Boolean logic operators include Intersection (AND), Union (OR) and Complement (NOT). The operators use the cell integers (True or False) as input data used in cell by cell analysis. Boolean logic functions are available for use in ArcGIS (Elaalem, 2010).

(B) Fuzzy logic theory

MCDM methods can incorporate fuzzy logic techniques to work with imprecision, inaccuracy and ambiguity in datasets (Malczewski, 2004). Fuzzy logic is where the concept of membership function with which a given element is represented numerically by the degree to which it belongs to a set (Burrough, 1989). Thus, a value within a criterion can have degrees of membership between unsuitable (0) and suitable (1) (Gross, 2014). Fuzzy logic is in contrast to Boolean logic where boundaries are distinct. However, in fuzzy logic boundaries have a transition zone where cells have a lower membership grade related to the other (Elaalem, 2010, Figure 3.2).

0	0	0	0.6	1
0	0	0.6	0.8	1
0	0.4	0.8	1	1
0.4	0.6	0.9	1	1
0.8	0.9	1	1	1

Figure 3:2: Cells representing fuzzy logic classes. Adapted from Elalem (2010).

Due to the landscape being spatially variable (e.g. well drained hillslopes transitioning to poorly drained flood plains), Burrough & McDonnell (1998) proposed that fuzzy membership better captures the boundaries between land suitability classes than binary or categorical methods.

(C) Weighted linear combination (WLC)

Weighted linear combination (WLC) is considered the most extensive technique for solving spatial multi-attribute decision making problems. In WLC attributes are multiplied or changed to predetermined weights to normalise attribute values. This is repeated for multiple attributes then for each pixel values from all attributes are summed. Areas with maximum values are identified as highly suitable (Elaalem, 2010). WLC methodology is expressed in Equation 3.15:

$$S_i = \sum_{j=1}^{n} w_j \quad x_{i,j} \text{ where } \sum_{j=1}^{n} w_j = 1 \qquad (3.15)$$

Where S_i is the suitability rating for site i, w_j is the weight of criteria j, x_{ij} is the value of location I udder attribute j, and n is the number of attributes.

New Zealand examples of WLC include Griffiths (2003) and Grose (2013). In the work of Grose (2013) areas with annual rainfall between 600 – 900mm were considered well suited towards viticulture land use (Table 3.7). This was reflected in the weighting by giving it a weighting factor of 2 where all pixels with annual rainfall between 600 – 900mm were reclassified with the value 2. Pixels with annual rainfall between 500 – 600mm and 900 – 1000mm (considered suitable) were reclassed with values of 1; areas with annual rainfall of less than 500mm but greater than 1000mm (not suitable) were given values of 0. Grose (2013) repeated this method of reclassifying spatial data for slope, aspect, temperature and elevation attributes. Pixels within the study area then had each of their reclassified attribute values summed with high scoring pixels indicating areas with the most potential towards viticultural land use.

Table 3:7: Annual rainfall values reclassified according to viticultural suitability. Adapted from Grose (2013).

Annual rainfall (mm)	**Re-classified weighting value**	**Suitability Class**
<500	0	Not suitable
500 - 600	1	Suitable
600 – 900	2	Very suitable
900 – 1000	1	Suitable
>1000	0	Not suitable

WLC is considered an advancement on Boolean methods (Jiang & Eastman, 2000) and is suitable for weighting and combining raster data to produce land suitability maps (Eastman, 1993).

Table 3:8: Crop growth requirements for Golden Kiwifruit

Crop: Kiwifruit (*Actinidia chinensis* var. *chinensis* 'Zesy002' Gold3)		**Suitability range**			
Crop growth parameter		**Well suited**	**Suitable**	**Moderately suited**	**Unsuitable**
Soil characteristics:	**Depth (cm)**	>150	100 – 150	50 – 100	<50
	pH	<5; >7.5	5-5.5; 7-7.5	5.5-6; 7-7.5	<5; >7.5
	Drainage class	5	4	3	2 -1
Topography:	**Slope (°)**	0 – 3	3 – 7	7 - 11	>11
Climate:	**Chill hours (Apr - Aug; base 7°C)**	0 – 600	600 – 650	650 – 700	700
	Growing season rainfall (mm)	450 - 650	400 – 450; 650 - 700	350 – 400; 700 – 750	0 – 50; >750
References:	Wall *et al.,* (2008) Salinger & Kenny (1995) http://ecocrop.fao.org/ecocrop/srv/en/cropFindForm				

3.4.5 Summary & conclusion

This review supports the decision to employ weighted linear combination within GIS to identify areas with potential for a range of horticultural crops in the Wairoa District.

Chapter 4

Climate Mapping

4.1 Introduction:

Climate is one of the main limitations to the types of crops that can be grown in an area. The objective of the climate mapping was to develop local scale maps of Wairoa District for the following climate variables:

- October frost risk
- Chill hours
- Growing degree days

4.2 Methods

4.2.1 Introduction

Methods employed included using the long and short-term climate station records, installation of iButton temperature loggers and investigating satellite temperature data.

4.2.2 Downloading of existing temperature data

Daily minimum/maximum and hourly temperatures datasets for each of the long and short term climate stations (Tables 4.1, 4.2, Figure 4.1) were either downloaded from the cliflo website (NIWA, 2009) or requested from the Hawkes Bay Regional Council and Metservice. For each climate station an excel spreadsheet was created for both daily minimum/maximum and hourly temperatures. Within each climate station dataset, days and hours with missing temperature data were filled in by 2nd order polynomial regression with another long term operating climate station (Table 4.1, 4.2).

Table 4:1: Long term climate stations used in this study

Long-term climate stations	Daily min/max data period used in this study	Hourly temperature data period used in this study	R^2 with nearest long term climate station
Wairoa North Clyde EWS	1/1/1992 - 31/12/2017	1/1/1999 - 31/12/2017	0.81; Mahia AWS
Mahia Aws	1//1/1992 - 31/12/2017	1/1/1999 - 31/12/2017	0.81; Wairoa North Clyde EWS
Gisborne AWS	1/1/1991 - 31/12/2017	1/1/1992 - 31/12/2012	0.83; Mahia AWS
Taupo AWS	1/1/1991 - 31/12/2017	1/1/1995 - 31/12/2012	0.79; Turangi
Whakatu EWS	1/1/1998 - 31/12/2017	1/1/1992 - 31/12/2017	0.83; Napier AWS
Cricklewood	1/1/2001 - 31/12/2017	1/1/2001 - 31/12/2017	0.83; Wairoa North Clyde EWS

Table 4:2: Short term climate stations used in this study

Short term climate stations	Climate Station operating period	R^2 with nearest long term climate station
Wairoa Aero AWS	17/09/2012 - 31/12/2017	0.98, Wairoa North Clyde EWS
Ruakituri	1/03/2013 - 31/12/2017	0.92, Wairoa North Clyde EWS
Pukeorapa	14/10/2014 - 31/12/2017	0.78, Wairoa North Clyde EWS
Kotemaori	1/11/2014 - 31/12/2017	0.97, Cricklewood
Tuai	28/2/2012 - 1/3/2017	0.96, Cricklewood
Tarapounamu EWS	10/8/2006 - 31/12/2017	0.83, Cricklewood
Tutira CWS	1/11/2012 - 31/12/2017	0.93, Cricklewood
Galatea AWS	7/10/2009 - 31/12/2017	0.86, Taupo AWS
Gisborne EWS	29/12/2012 - 31/12/2017	0.83, Mahia AWS

Using the relationship between each short-term (3-11 years old) climate station and its nearest long term (17 -26 years old) climate station with its highest R^2, a long term daily minimum/maximum and hourly dataset was created for each short-term climate station.

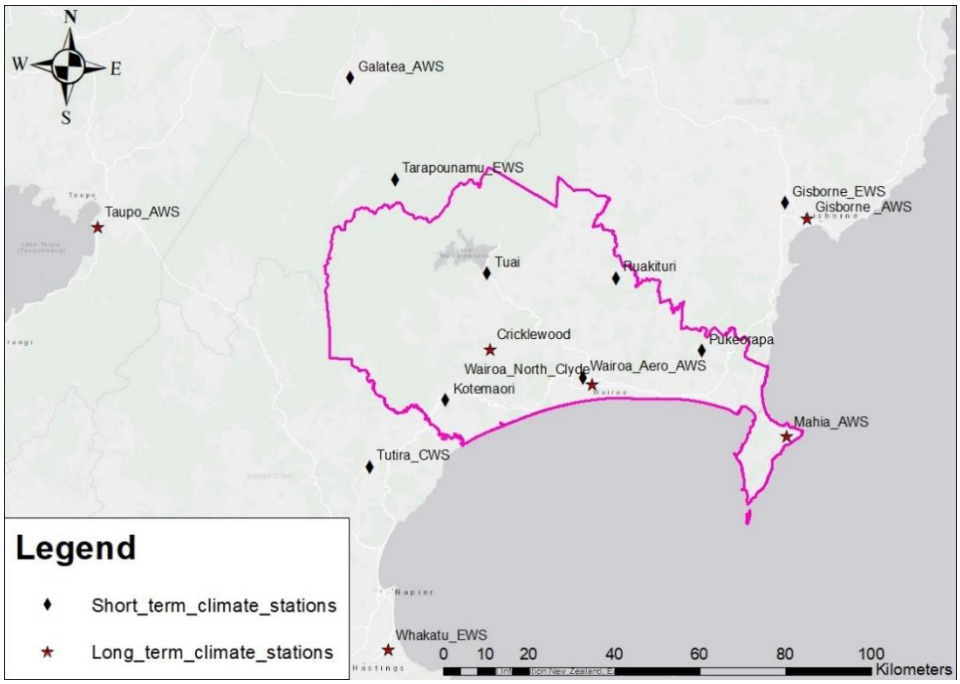

Figure 4:1: Location of long and short term climate stations.

4.2.3 Downloading of rainfall and evapotranspiration data

Climate data used to estimate crop irrigation in Chapter 5 included daily rainfall and potential evapotranspiration. Measured daily rainfall was available at only one site – Wairoa Airport. Evapotranspiration measurements were not available at any of the four selected sites. Instead NIWA's virtual climate station network (VCSN) was employed to estimate daily rainfall and potential evapotranspiration. VCSN estimates have been compared with measured climate variables to show good agreement between the two (Cichota *et al.,* 2008). Twenty-one years (1 September 1997 – 31 May 2018) of VCSN estimated daily rainfall and Penman evapotranspiration data per site was then downloaded.

As one of the soils (Awamate silt loam) was within 25m of the Wairoa Airport Climate Station, five years of daily rainfall (1 September 2013 – May 2018) was also downloaded. This allowed an opportunity to evaluate the daily rainfall estimates downloaded from the virtual climate station network which is discussed in Chapter 5.

4.2.4 Collection of local scale temperature data

IButton deployment sites were selected from land-blocks within Land Use Capability Classes 1-3 (Fig 2.8, Table 4.3) on open, level, areas away from roads, buildings, and large trees, but with good airflow and above short grass (Overton, 2007).

At 45 sites (Figure 4.2, Table 4.3) S1921G-F5 iButtons (Maxim Integrated Products; Dallas Semiconductor Inc., Sunnyvale, CA, USA) were deployed in duplicate, giving 90 iButtons in total. The iButtons were programmed to record hourly temperature. One disadvantage of the iButtons is not knowing when the battery life will expire and stop recording temperature data. It is unlikely that two iButtons, started together would both expire in the same operating period. For this reason, iButtons were deployed in duplicate per site.

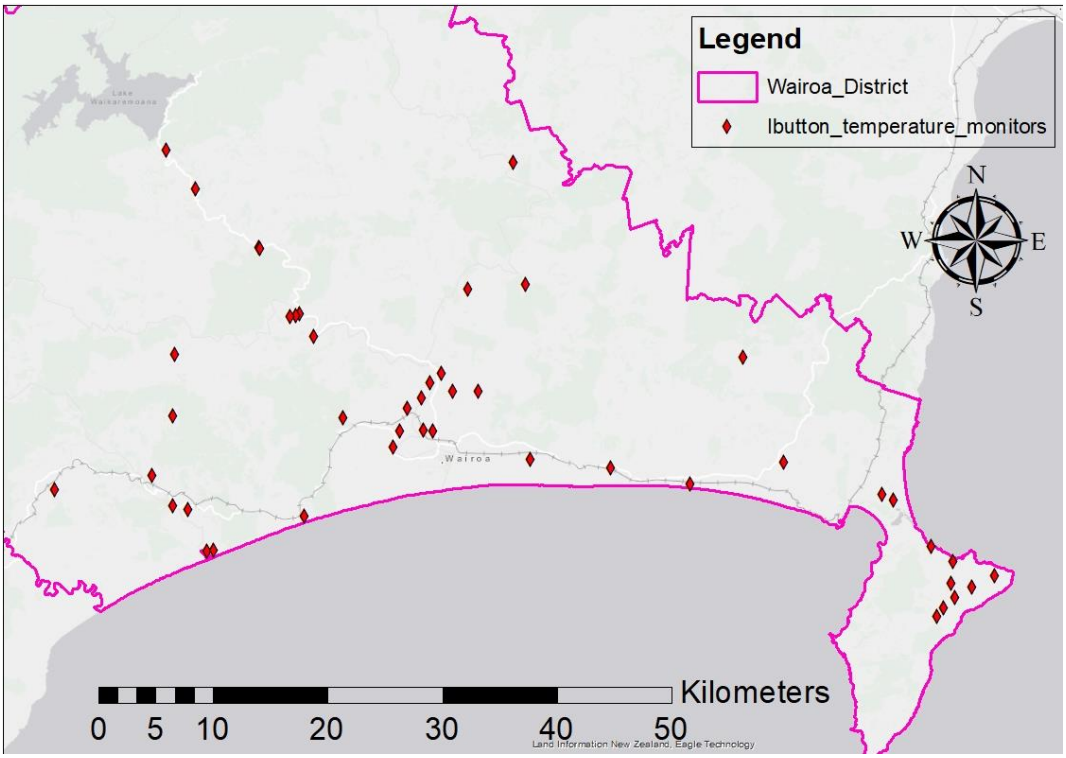

Figure 4:2: Location of 45 pairs of iButton temperature monitors from which hourly temperature was recorded for between 1 April – 31 October 2017.

IButtons (Figure 4.3a) are robust devices being resistant to environmental stressors e.g. soil, moisture and shock (Maxim Integrated Products; Dallas Semiconductor Inc., Sunnyvale, CA, USA). The iButtons were housed within cut 9 X 15cm lengths of PVC pipe (Figure 4.3b, 4.3c) which protected them against wildlife, stock, and direct solar radiation. The standard height to measure air

temperature is at 1.2m above ground level (Turner & Fitzharris, 1986, Purdie *et al.,* 1999; Webb *et al.,* 2016). Each PVC pipe/radiation shield was attached to a fence post approximately 1.2m above ground using removable staples and cable ties. The radiation shields were orientated north-south using a compass to minimise the chance of the daily east-west moving sun striking the iButtons and providing a false reading.

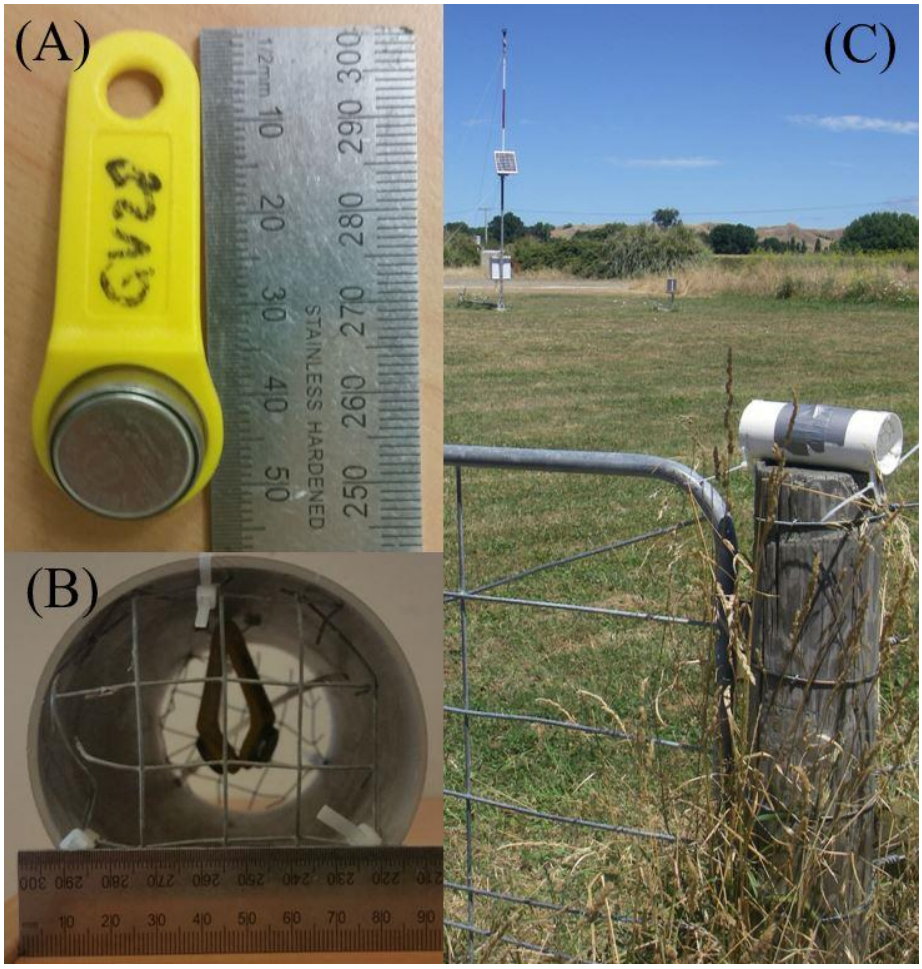

Figure 4:3 (a): IButton; (b) iButtons inside cut PVC pipe; (c) iButtons in PVC pipe 1.2m above ground on fencepost with Wairoa Airport Climate Station in background.

Each iButton can store up to 2048 continuous data entries within an operating temperature range of -40°C to +85°C in 0.5°C increments. Between -30°C to +70°C the iButtons are accurate to +/- 1°C, (Maxim Integrated Products; Dallas Semiconductor Inc., Sunnyvale, CA, USA). Each iButton was programmed to record hourly temperature. Data from each iButton was manually downloaded at least every 12 weeks (before limit of 2048 entries was met and data overwritten).

Table 4:3: Summary of sites where iButtons deployed.

ID No.	Latitude	Longitude	Elevation (m)	Landblock ref	Landscape unit
1A	-39.11905	177.19166	63	Allen	Mohaka River Terrace
1B	-39.11805	177.19828	66	Stockman	Mohaka River Terrace
2	-39.08500	177.15478	37	Adsett	Mohaka River Terrace
8	-39.08721	177.17053	88	Lambert	Mohaka River Terrace
10	-39.06164	177.13326	160	Putere Rd	Mohaka River Terrace
32	-39.08826	177.28801	17	Haynes	Te Kiwi Stream flood plain
3	-38.89817	177.49868	28	Koanga Inst	Mangapoike River Terrace
11	-38.98406	177.45639	20	Munroe	Valley floor
12	-38.98493	177.43088	11	Mill Rd	Valley floor
5	-39.00963	177.32154	27	Farr	Valley floor
6A	-38.87984	177.22963	86	Little lower	Waikaretaheke River Terrace
6B	-38.87572	177.22939	138	Little upper	Waikaretaheke River Terrace
34	-38.83582	177.16320	188	Kirikiri	Waikaretaheke River Terrace
9	-39.01490	177.15089	358	Gemmel	Rolling hill country
23A	-38.93001	177.27345	60	Quinn upper	Waiau River Terrace
23B	-38.93166	177.26971	63	Quinn mid	Waiau River Terrace
23C	-38.93286	177.26407	35	Quinn lower	Waiau River flood plain
19	-38.94728	177.28894	39	Moys	Waiau River Terrace
20	-39.03111	177.37378	13	Ruataniwha Rd	Wairoa River flood plain
7	-39.01785	177.37990	10	Paku	Wairoa River flood plain
21	-39.00029	177.38607	16	Charteris	Wairoa River Terrace
22	-38.97901	177.40734	14	Martin	Wairoa River Terrace
25	-38.97108	177.41797	20	Mangapoike Rd	Wairoa River Terrace
33	-38.99112	177.40014	12	Bell Rd	Wairoa River Terrace
13	-38.90472	177.44092	15	Beattie	Wairoa River Terrace
26	-39.03507	177.51177	2	Whakaki	Coasta flat
31	-39.04805	177.67306	4	Hutton	Coasta flat
18	-39.03905	177.59321	9	McEwan	Coasta flat
30	-39.05221	177.87798	4	Kamau	Tombolo
16	-39.04852	177.86712	11	Taumata	Tombolo
27	-39.08701	177.91920	60	Te Mahia School	Marine Terrace
24	-39.09818	177.94187	79	TeNahu	Marine Terrace
29	-39.14192	177.92830	133	Whanga	Marine Plateau
14	-39.13486	177.93493	150	O'Brien	Marine Plateau
15A	-39.12568	177.94566	133	Parker east	Marine Plateau
15B	-39.11472	177.94077	140	Parker west	Marine Plateau
17	-39.02705	177.76675	16	Smith	Nuhaka River flood plain
CS1	-38.94695	177.72035	533	Pukeorapa CS	Steeplands
CS2	-38.80369	177.47987	86	Ruakituri CS	Ruakituri River flood plain
CS3	-39.01627	177.40362	11	Wairoa Aero Aws	Wairoa River flood plain
CS4	-39.07690	177.03554	177	Kotemaori CS	Rolling hill country
CS5	-38.80707	177.13202	500	Tuai CS	Rolling hill country
CS6	-39.11735	177.96181	139	Mahia Aws	Marine plateau
CS7	-38.96635	177.15027	421	Cricklewood CS	Steeplands

4.2.5 Assessment of hourly iButton temperature data

IButtons were deployed at seven climate stations within the Wairoa District (CS1 – CS7, Table 4.3). The hourly climate station data, when plotted against the hourly iButton data, was used to assess the accuracy of the iButtons.

During hot days, the air within the PVC pipes appeared to heat up creating a mini "greenhouse effect" meaning the iButtons at such times recorded higher than actual temperatures. Figure 4.4 shows air temperature at the Wairoa Airport climate station plotted against the temperature of the nearby iButton for July 2017. The Figure shows 17 spikes where the iButton temperature peaks well above the climate station temperature.

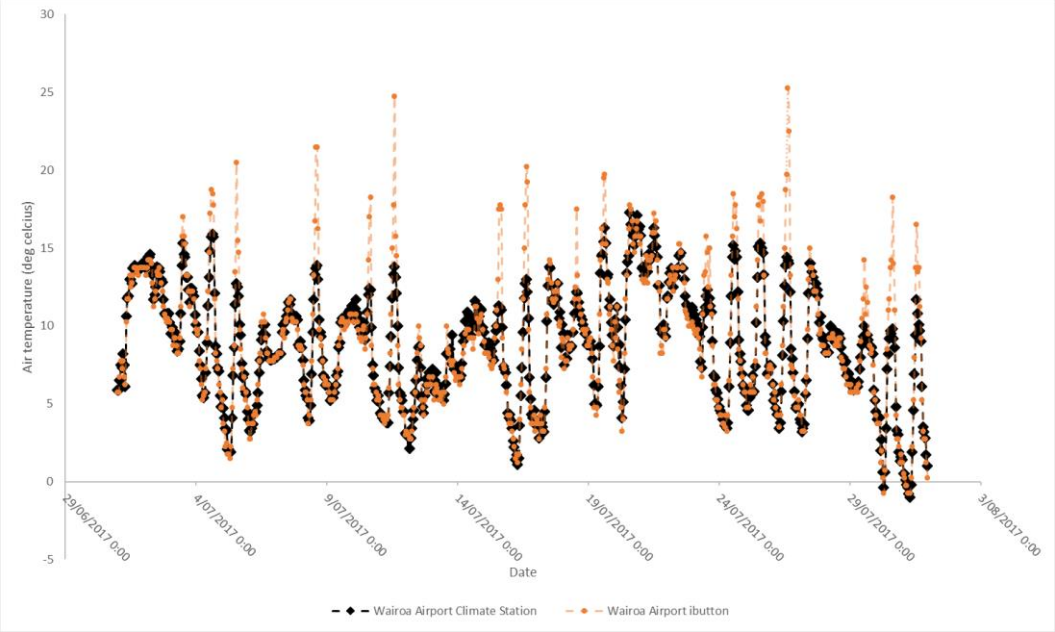

Figure 4:4: Time series plotting hourly Wairoa Airport climate station temperature vs hourly iButton temperature at Wairoa Airport for July 2017.

The daytime temperature spikes were removed within each iButton sites dataset by calculating the standard deviation of the difference between the iButton and nearest climate station temperatures. Cells with temperatures greater than two standard deviations between the hours of 10am and 4pm were subsequently removed. All the other data was left unchanged.

The problem of heightened daytime peaks in temperature monitors is not new and was observed by Lookingbill & Urban (2003), and Van Duivendijk (2015). Van Duivendijk (2015) developed a calibration method and applied 2nd order polynomial regression (rather than direct linear regression) between their iButton

dataset and the nearest climate station. The 2nd order polynomial approach was used in this study rather than direct linear regression.

As six to seven months (April – October 2017) is generally not long enough to derive a long-term dataset straight from a nearby long term (19 – 26 years) climate station, each iButton dataset (with outliers removed) was first plotted against a range of nearby short term climate stations corresponding hourly temperatures to identify which short term climate stations were highly correlated to the iButton site. After selecting a suitable short term climate station the resulting regression equation was then applied to the short-term climate station hourly dataset to derive a short term e.g. 5-year dataset for the iButton site. Alongside the same newly derived short term iButton dataset, for the corresponding period were also added datasets for each of the nearby long term climate stations of Wairoa North Clyde, Mahia, and Cricklewood. The new short term iButton dataset (e.g. 5 year) was plotted against the corresponding long term climate station datasets (also 5 year) using 2nd order polynomial regression to identify which long term climate stations were best correlated to the new short term iButton dataset. The resulting regression equation was then applied to the long-term stations temperature datasets to derive long term (19 - 26 years) daily minimum/maximum and (16 – 19 years) of hourly datasets for each iButton location.

4.2.6 Investigation of satellite images to aid in identification of frost prone areas.

MODIS Aqua satellite images were sourced to help identify areas prone to frost. The MODIS Aqua satellite has been in operation from July 2002 to present. The "R" package MODIStsp (Busetto, & Ranghetti, 2016) was used to download 15 years of MODIS Aqua images. ArcPy code was written (Appendix 1) and is summarised below:

- Each image re-projected to WGS1984 projection.
- For a 1 km^2 area surrounding each climate station the "ZonalStatisticsAsTable" function was used to extract land surface temperature (LST) and image reference time/date from each image.
- LST (in °Kelvin) converted to °C.

- "table_list_append(out_table)" function used to compile LST and image date/time from each image into a single database.

ArcGIS was then used to access the database file and copy station data over into an excel spreadsheet. The LST data was then organised as a time series. As most MODIS images were taken at approximately 0130 hrs these were regressed against corresponding climate station temperatures at 0200 hrs.

4.2.7 Calculation of climate variables

Using the derived long term dataset for each iButton/weather station, the following climate variables were calculated: Monthly frost risk, growing degree days and chilling hours.

4.2.7.1 Monthly frost risk:

Following the methods of Webb et al (2018) the number of frosts per month was calculated for each iButton/weather station (for the extended 19 – 26 year time period and then re-expressed as a proportion (Equation 4.1):

$$\mathrm{FR}_{\%} = \frac{\sum_{i=1}^{n} (Fr_i)}{n} \times 100 \qquad (4.1)$$

In which $FR_{\%}$ is the frost risk (%), n is the total number of years used in the analysis and Fr_i is explained in Equation 4.2:

$$Fr_i = \sum_{i=1}^{31} (T \le T_c) = \begin{cases} 1 \text{ if TRUE,} \\ 0 \text{ else.} \end{cases} \qquad (4.2)$$

Where Fr_i is a binary value (e.g. 1 representing a frost event) calculated for each year in n (Equation 2), i is each day in the considered month, T is the daily Tmin temperature value and T_c is the nominated temperature threshold value in this study as 0°C and -2.0°C. Equations 1 and 2 were automated in a pivot table to count days with temperature at or below 0°C and -2°C for each month. The count for each month was summed then divided by the number of years in the new dataset (e.g. 26 years if derived from the Wairoa North Clyde climate station dataset) to calculate the mean number of frosts per month. The monthly frost

count was then re-calculated as a proportion for both the 0°C and -2.0°C thresholds for September and October.

The frost risk for each iButton site was then classified into one of four categories as below then mapped (Figure 4.20).

- <1 frost every 5 years (frost occurs 0 – 20% of years).
- 1/5 to 1 frost every 2 years (frost occurs 20 – 50% of years).
- ½ to 1 frost every year (frost occurs 50 – 100% of years).
- >1 frost per year (frost occurs every year).

4.2.7.2 Growing degree days (GDD):

GDD is a measure of heat accumulation used to predict plant phenology. GDD are calculated per day by averaging the daily minimum and maximum temperatures then subtracting a nominated base temperature or Tbase (Equation 4.3; McMaster & Wilhelm, 1997).

$$\text{GDD} = \left(\frac{(Tmin+Tmax)}{2}\right) - Tbase \qquad (4.3)$$

From reviewed literature, the range of crops included in this study had a base of 10°C to calculate their optimal GDD. Therefore, a base temperature of 10°C was chosen to model GDD from October to April.

Daily minimum/maximum data were fed into another automated pivot table producing average monthly growing degree days.

4.2.7.3 Chill hours:

The minimum amount of time spent below a threshold air temperature to initiate dormancy for a given plant is called chill hours (Webb *et al.,* 2016). Occurring during late autumn to winter (typically April – August) chill hour accumulation is a significant growth phase for many plants and trees (Webb *et al.,* 2016). Inadequate chill hours can result in reduced fruit quality (Byrne & Bacon, 1992).

For each iButton/weather station chill hours were calculated as follows: at hour X if temperature >7°C and <0°C, chill hour (CH) = 0. At hour X if temperature <7°C but >0°C then CH = 1.

Each iButton site's derived long-term hourly dataset was fed into an automated pivot table which processed the data and produced average chill hours per month. A spreadsheet was compiled listing all the iButton sites, long and short term climate stations, their relative co-ordinates, and their corresponding chilling hours then repeated for growing degree days and frost days below 0°C and -2°C per month. These were then used as the basis for spatial interpolation of the climate variables constructing climate maps in ArcGIS.

4.2.8 Interpolation of climate variables by universal kriging.

Literature Review (Chapter 3) supported choosing the universal kriging technique to interpolate the climate variables of monthly frost risk, growing degree days (October – April) and chill hours (April – August). To assist the universal kriging, the NZDEM_SOS_V1.0 digital elevation model (DEM, spatial resolution 15m resampled to 30m) (Columbus *et al.,* 2011) was used as a basis on which the spatial modelling would occur. From the DEM, auxiliary datasets were derived as explanatory variables to help explain the quantitative relationships between the topography and climate variables. The software employed was ArcGIS (ArcGIS, E. S. R. I., 2018) with terrain derivatives given in Table 4.4.

Table 4:4: Terrain derivatives used to describe relationship between climate variables and topography.

Terrain derivative
Elevation (m)
Topographical wetness index
Slope (°)
Distance from coast (m)

4.3 Results

4.3.1 Established Climate Station data.

The climate data from the four long term stations (Table 4.6) are representative of the three main geographic areas within the Wairoa District. These are the warm

coastal areas (Mahia climate station), central Wairoa River floodplain and terraces (Wairoa North Clyde & Frasertown climate stations) and the steep hill country (Cricklewood Station) situated inland of Wairoa. Each area is distinct from each other possessing its own climate characteristics. The Mahia site was constantly 1 – 2 degrees warmer than the other sites and appears to be free of frosts year-round. The Mahia site, due to its warm temperatures, is also lower in chilling hours.

The Cricklewood site, with an elevation of 421m, has a moderately high number of chilling hours (approx. 1100 Apr – Aug) and low (<0.1) number of spring frosts. The steep topography likely supports cold air drainage downslope from the site while the elevation ensures temperatures remain cool. This is evidenced by Cricklewood having the lowest mean annual temperature (12.5°C) of the four climate stations.

The Wairoa North Clyde site is situated on an open flat flood plain approximately 3.7 km from the coast meaning temperatures are moderate year-round with moderately high growing degree days (>1400 Oct – Apr), no spring frosts (0.0) and moderate chill hours (600 – 800, Apr – Aug).

Table 4:5:Climate variables for long term climate stations in the Wairoa District.

Climate station Wairoa, North Clyde EWS	Time period	Jan	Feb	Mar	Apr	May	Jun	Jul	Aug	Sep	Oct	Nov	Dec	Annual
Mean daily minimum air temp (°C)	1991 - 2017	13.6	13.9	12.2	9.9	7.5	5.2	4.8	5.2	6.7	8.5	10.3	12.8	9.2
Mean daily maximum air temp (°C)	1991 - 2017	24.8	24.2	22.5	19.9	17.7	15.1	14.1	15.0	16.9	19.2	20.9	23.2	19.4
Daily mean air temp (°C)	1991 - 2017	19.2	19.1	17.4	14.9	12.7	10.2	9.5	10.1	11.8	13.8	15.7	18.0	14.3
Mean monthly GDD	1993 - 2016	283.1	254.3	226.2	147.4	NA	NA	NA	NA	NA	122.1	173.0	253.0	1459.1
Mean monthly chill hours	1994 - 2017	NA	NA	NA	22.5	88.2	164.7	209.7	181.9	NA	NA	NA	NA	667.0
Mean number of frosts	1992 - 2016	0.0	0.0	0.0	0.0	0.1	0.7	0.8	0.7	0.0	0.0	0.0	0.0	2.3
Mean monthly rain (mm)	1991 - 2017	96.4	93.7	104.0	134.7	104.9	120.3	136.0	99.6	85.8	96.0	81.6	75.9	1228.9
Mahia AWS, Wairoa District														
Mean daily minimum air temp (°C)	1991 - 2017	14.7	15.3	14.0	12.3	10.5	8.5	7.8	7.8	8.9	10.1	11.4	13.4	11.2
Mean daily maximum air temp (°C)	1991 - 2017	21.7	21.5	20.2	17.9	15.8	13.4	12.6	13.2	14.9	16.6	18.1	20.1	17.2
Daily mean air temp (°C)	1991 - 2017	18.2	18.4	17.1	15.1	13.2	11.0	10.2	10.5	11.9	13.4	14.7	16.8	14.2
Mean monthly GDD	1992 - 2017	254.9	238.7	219.4	154.2	NA	NA	NA	NA	NA	107.0	140.3	210.1	1324.6
Mean monthly chill hours	1991 - 2017	NA	NA	NA	1.2	5.3	35.8	49.5	57.7	NA	NA	NA	NA	149.5
Mean number of frosts	1991 - 2017	0	0	0	0	0	0	0	0	0	0	0	0	0.0
Mean monthly rain (mm)	1991 - 2017	57.2	75.5	89.0	112.3	101.1	127.3	140.5	102.5	71.3	70.4	77.5	64.8	1089.4
Cricklewood CS														
Mean daily minimum air temp (°C)	1997 - 2017	12.8	13.0	11.9	10.0	8.3	6.2	5.3	5.5	6.9	8.0	9.3	11.6	9.1
Mean daily maximum air temp (°C)	1997 - 2017	22.8	22.2	20.3	17.3	15.7	12.3	11.2	11.9	14.1	16.6	18.3	20.6	16.9
Daily mean air temp (°C)	1997 - 2017	17.3	17.0	15.5	12.9	11.7	8.9	7.9	8.3	10.0	11.9	13.4	15.6	12.5
Mean monthly GDD	1997 - 2016	242.0	214.0	190.7	107.3	NA	NA	NA	NA	NA	83.8	120.5	183.6	1141.9
Mean monthly chill hours	1997 - 2017	NA	NA	NA	56.1	144.6	270.2	390.9	316.3	NA	NA	NA	NA	1178.1
Mean number of frosts	1997 - 2017	0.0	0.0	0.0	0.1	0.0	0.1	0.4	0.9	0.0	0.1	0.1	0.0	1.6
Mean monthly rain (mm)	2011 - 2016	71.5	72.7	122.1	149.8	65.9	83.6	98.7	118.3	142.0	56.1	80.7	77.2	1138.6
Wairoa, Frasertown														
Mean daily minimum air temp (°C)	1964 - 1989	13.7	13.4	12.3	9.5	6.8	4.9	4.2	5.4	6.9	8.5	10.5	12.5	9.1
Mean daily maximum air temp (°C)	1965 - 1989	24.7	24.1	22.8	19.9	16.8	14.4	13.8	14.7	16.9	19.1	21.3	23.2	19.3
Daily mean air temp (°C)	1966 - 1989	19.2	18.8	17.5	14.7	11.8	9.7	9.0	10.0	11.9	13.7	15.9	17.8	14.2
Mean monthly GDD	1972 - 1989	286.6	247.6	232.9	143.5	NA	NA	NA	NA	NA	118.8	182.5	243.3	1455.1
Mean monthly chill hours	1973 - 1989	NA	NA	NA	6.5	56.1	155.9	189.2	143.0	NA	NA	NA	NA	550.7
Mean number of frosts	1963 - 1989	0.0	0.0	0.0	0.0	0.1	2.0	2.3	1.0	0.1	0.0	0.0	0.0	5.4
Mean monthly rain (mm)	1964 - 1989	82.5	130.1	127.9	142.9	139.2	135.7	125.8	139.4	104.2	85.3	76.5	110.3	1399.8

Table 4:6: Summary of climate data for climate stations in Wairoa District.

Climate Station	Latitude	Longitude	Elevation (m)	Location	Annual mean daily temperatures (°C)		Mean annual temperature (°C)	Mean GDD 10°C base (Oct - Apr)	Mean chill hours 7°C base (Apr - Aug)	Mean number of annual frosts	Mean annual rain (mm)
					Min	Max					
Wairoa, North Clyde EWS	-39.02906	177.42982	15	Central Wairoa	9.2	19.4	14.3	1459.1	667	3.2	1228.9
Mahia AWS	-39.11737	177.96182	136	Mahia Peninsula	11.2	17.2	14.2	1324.6	149.5	0	1089.4
Cricklewood C	-38.96630	177.15040	420	Inland hill country	9.1	16.9	12.5	1141.9	1178.1	1.6	1138.6
Wairoa, Frasertown	-39.00000	177.40500	8	Central Wairoa	9.1	19.3	14.2	1455.1	550.7	5.4	1399.8

4.3.2 Comparison of IButton data with Climate Station data

The hourly iButton temperature (°C) data was regressed against the hourly climate station air temperature (°C) (Figures 4.5 – 4.11, Table 4.7). The iButtons deployed at the seven climate stations within the Wairoa District all had high R^2 values (Table 4.5, 0.96-0.98) indicating that the recorded iButton temperature data were highly correlated with the air temperature measured at the nearest climate station. This allowed increased confidence in the iButton data for estimating long term temperature datasets and further modelling of growing degree days, chilling hours and frost risk (Table 4.6).

Table 4:7: Regression equations and R^2 values for correlations between Wairoa District Climate Stations and iButtons

Climate station	R^2 with iButton	Regression equation
Ruakituri	0.97	$y = 0.0034x^2 + 0.9574x + 0.0844$
Kotemaori	0.95	$y = 0.0026x^2 + 1.044x - 1.8231$
Pukeorapa	0.96	$y = 0.0035x^2 + 0.9763x - 0.0702$
Cricklewood	0.98	$y = 0.002x^2 + 0.9393x - 0.0777$
Wairoa Aero AWS	0.97	$y = 0.005x^2 + 0.942x - 0.1717$
Mahia AWS	0.97	$y = -0.0007x^2 + 1.065x - 0.9315$
Tuai	0.97	$y = 3E\text{-}05x^2 + 1.0452x - 1.0015$

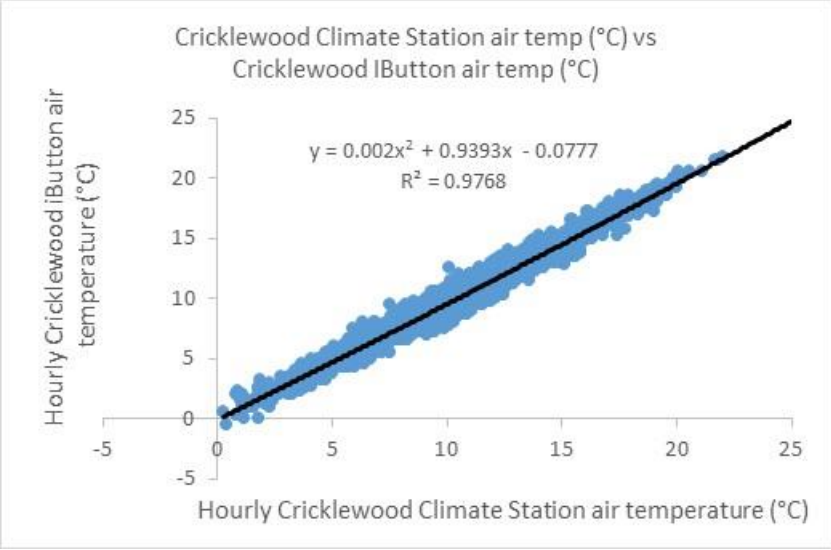

Figure 4:5: Scatterplot showing 2nd order polynomial regression of hourly Cricklewood Climate Station air temperature (°C) vs hourly Cricklewood iButton air temperature (°C) from July – October 2017.

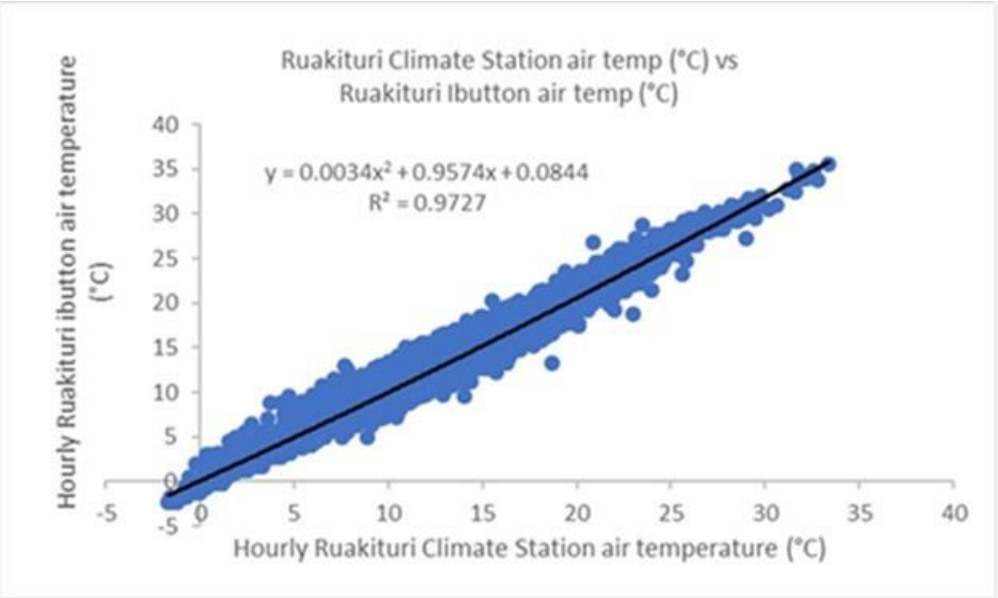

Figure 4:6: Scatterplot showing 2nd order polynomial regression of hourly Ruakituri Climate Station air temperature vs hourly Ruakituri iButton air temperature (°C) from February – October 2017.

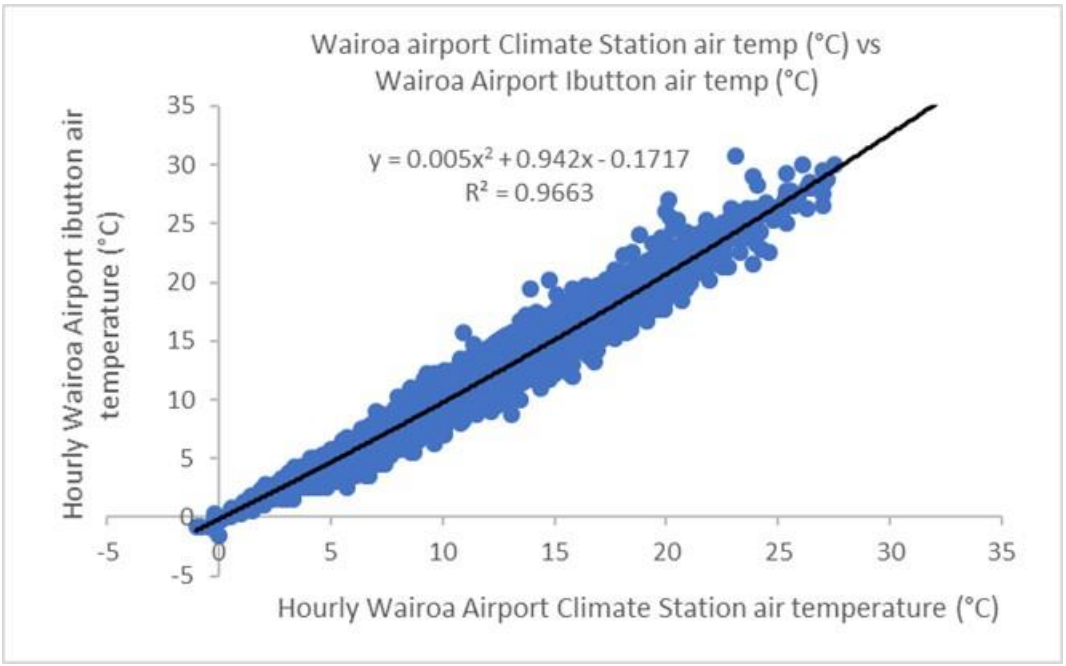

Figure 4:7: Scatterplot showing2nd order polynomial regression of hourly Wairoa Airport Climate Station air temperature (°C) vs hourly Wairoa Airport iButton air temperature (°C) from February – October 2017.

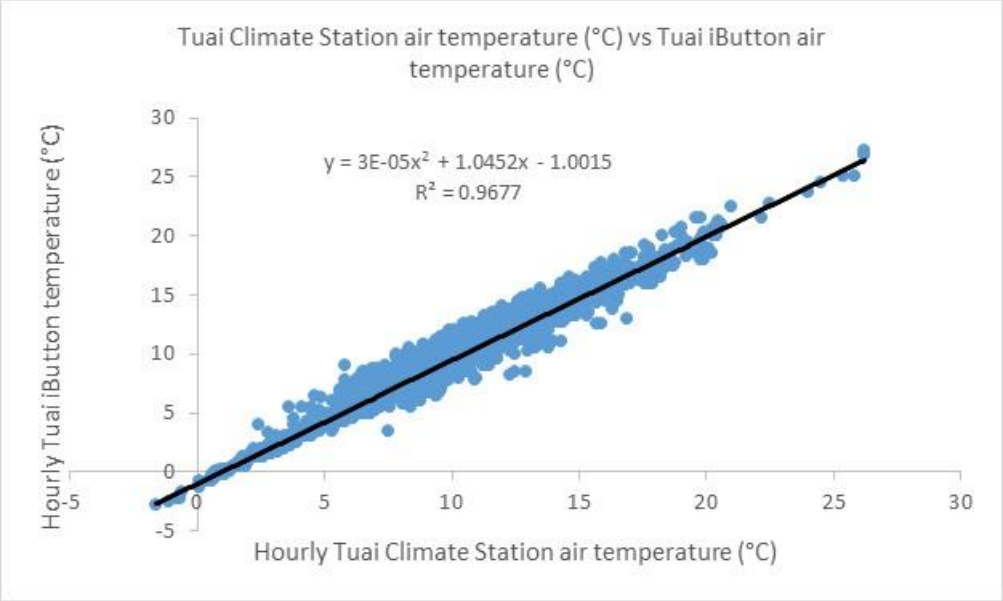

Figure 4:8: Scatterplot showing 2nd order polynomial regression of hourly Tuai-Kaitawa Climate Station air temperature (°C) vs hourly Tuai-Kaitawa iButton air temperature (°C) from February – October 2017.

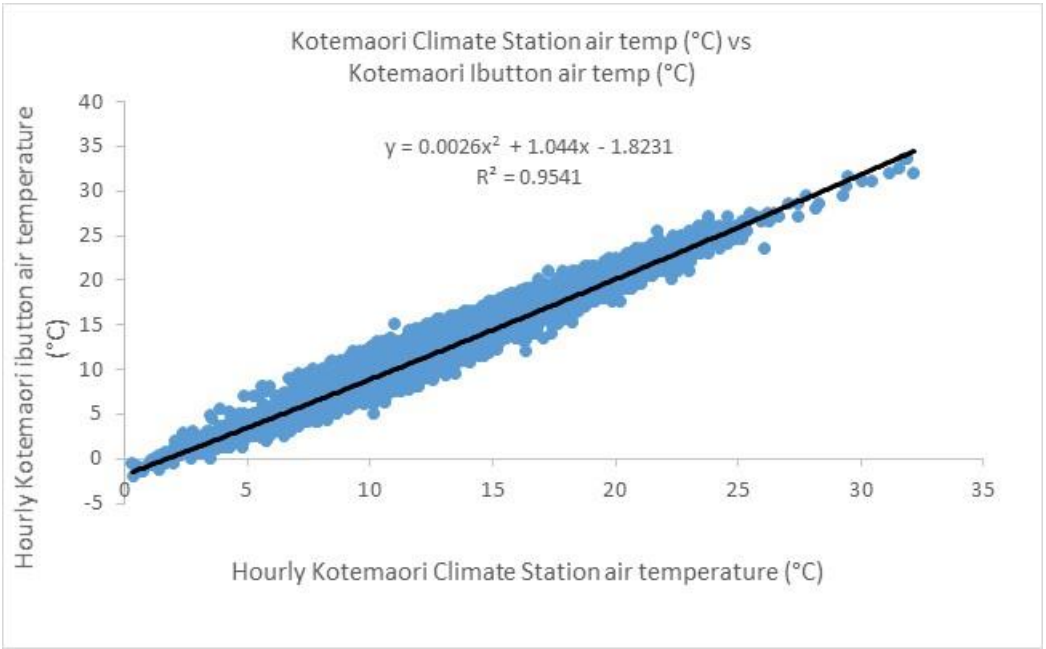

Figure 4:9: Scatterplot showing 2nd order polynomial regression of hourly Kotemaori Climate Station air temperature (°C) vs hourly Kotemaori iButton temperature (°C) from February – October 2017.

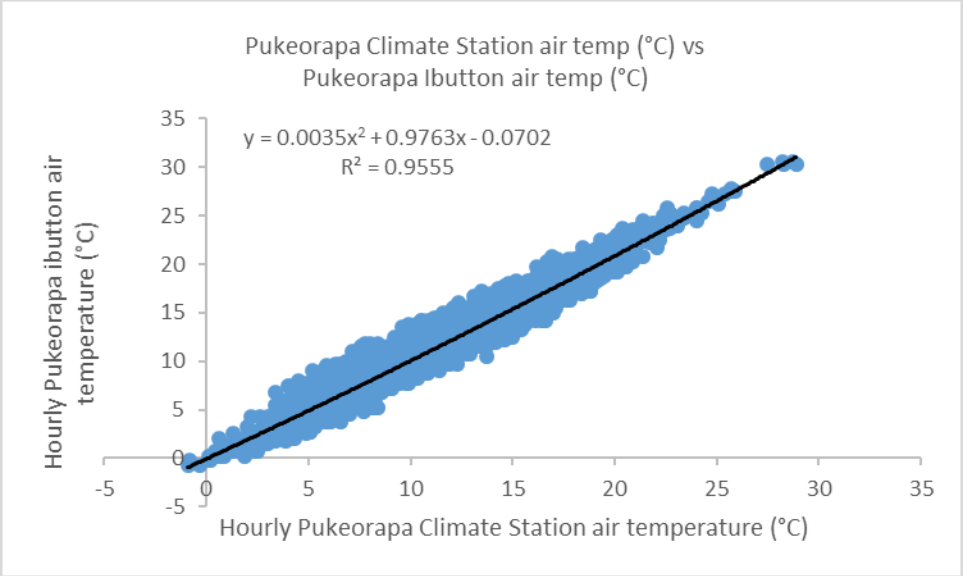

Figure 4:10: Scatterplot showing 2nd order polynomial regression of hourly Pukeorapa Climate Station air temperature (°C) vs hourly Pukeorapa iButton temperature (°C) from February – October 2017.

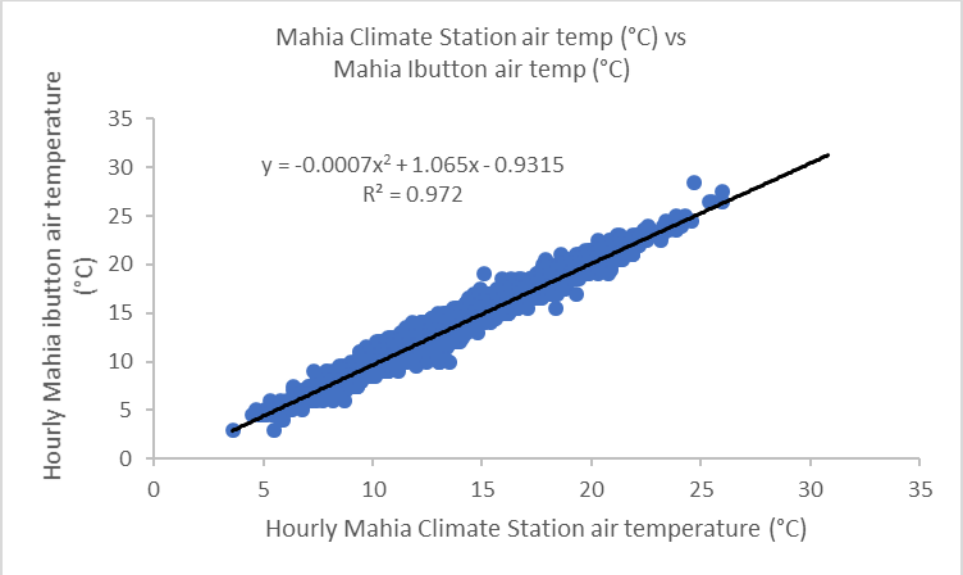

Figure 4:11: Scatterplot showing 2nd order polynomial regression of hourly Mahia Climate Station air temperature (°C) vs hourly Mahia iButton temperature (°C) from February – October 2017.

Table 4.8 shows that the long-term climate variables estimated from the iButton data are comparable with those from the long-term climate stations (Tables 4.5 and 4.6).

Table 4:8: Summary of estimated long term climate variables for iButton sites in Wairoa District.

Area iButton ID	Mean annual temps (°C) Min	 Max	Mean annual temp (°C)	Annual total GDD*	 CH*	 NFD*	GDD* Oct - Apr	CH* Apr - Aug	Oct frost risk (0°C, %)
Mohaka Valley									
1A	9.6	17.8	13.7	1435	584	0.7	1225	481	0
1B	8.4	15.3	11.8	1417	904	0	1209	**723**	**0**
2	8.6	18.6	13.6	1394	1014	4.5	1244	**801**	**4**
8	8.5	17.6	13	1278	1020	2.2	1133	**806**	**0**
10	8.4	17.4	12.9	1230	1022	1.8	1094	**808**	**0**
Inland River Terraces									
6A	7.6	18	12.8	1293	1379	16	1167	1051	27
6B	7.3	17.3	12.3	1133	1500	16	1034	1131	27
34	7.7	16.7	12.2	1061	1335	5.2	964	**1029**	**8**
23A	7.6	18.4	13	1364	1369	20.4	1228	1041	31
23B	7.5	17.6	12.6	1209	1421	14.8	1096	1079	27
23C	7.6	17.9	12.8	1278	1383	14.8	1152	1055	27
19	8.1	19.6	13.8	1612	1209	18.9	1427	932	31
13	8.5	19.2	13.9	1589	1098	9.2	1395	863	12
3	8.2	19	13.6	1525	1187	12.8	1350	922	27
Central Wairoa									
11	9	21.6	15.3	2078	969	18.9	1790	760	31
12	8.6	19.9	14.2	1722	1085	12.8	1506	**852**	**27**
5	8.5	19.3	13.9	1596	766	10.7	1403	621	19
20	9.5	20.4	14.9	1904	814	11.6	1624	655	23
7	8.9	20.2	14.6	1906	962	22.8	1645	**761**	**39**
21	9.2	18.8	14	1575	797	6.4	1357	644	12
22	8.9	19	13.9	1577	900	3.4	1370	**719**	**4**
25	8.4	18.2	13.3	1387	1111	5.2	1228	**875**	**8**
33	9.2	17.9	13.5	1402	748	0.2	1212	608	0
Coastal Wairoa									
32	8.7	17.2	12.9	1965	518	0.5	1628	429	0
26	10.7	18	14.3	1701	519	0.3	1453	415	0
31	11.8	20.2	16	2267	328	0.8	1884	267	0
18	11.2	19	15.1	1965	349	0.5	1654	283	0
Mahia Tombolo									
30	9.6	15.2	12.4	1566	311	0	1337	254	0
16	9.9	17.4	13.7	1391	420	0	1170	352	0

Table 4.8: Summary of estimated long term climate variables for iButton sites in Wairoa District (continued).

Area iButton ID	**Mean annual temps (°C)** **Min**	**Max**	**Mean annual temp (°C)**	**Annual total** **GDD***	**CH***	**NFD***	**GDD*** **Oct - Apr**	**CH*** **Apr - Aug**	**Oct frost risk (0°C, %)**
Mahia Peninsula									
27	10.1	15.3	12.7	1237	140	0	999	124	0
24	11.6	18.1	14.9	1823	130	0	1501	110	0
29	10.1	15.3	12.7	1099	292	0	956	240	0
14	10.6	16.3	13.4	1346	272	0	1149	224	0
15A	10.7	17.3	14	1566	349	0	1337	283	0
15B	10.1	14.8	12.5	1000	257	0	869	212	0
Nuhaka River Valley									
17	10.5	16.8	13.7	1450	328	0	1241	267	0
Climate Stations with iButtons									
Pukeorapa CS*	6.4	10.5	8.4	727	1386	0.2	675	1065	0
Ruakituri CS*	7.8	17.9	12.8	1459	1393	15.8	1296	1064	30
Wairoa Aero AWS*	8.2	18.3	13.3	1542	949	9.7	1352	753	20
Kotemaori CS	9.8	18.7	14.3	1878	1294	2.1	1590	964	17
Tuai CS*	8.5	16.4	12.4	1176	1506	2.8	1054	1110	23
Mahia AWS*	11.2	17.2	14.2	1587	121	0	1320	108	0
Cricklewood CS*	8.9	16.6	12.3	1247	1607	1.1	1106	1178	12
Climate Stations without iButtons									
Wairoa, North Clyde EWS*	9.3	19.4	14.4	1704	820	3.2	1464	660	0
Tarapounamu EWS*	7	15	11	945	2218	11.2	873	1565	82
Tutira CWS*	10.1	19.2	14.6	1842	972	2.1	1571	731	18
Taupo AWS*	6.9	16.8	11.9	1076	1104	43.9	1003	804	289
Whakatu EWS*	7.7	18.9	13.3	1411	1158	27.6	1228	863	70
Gisborne AWS*	9.6	19.4	14.5	1732	692	1.7	1484	557	0

**Where GDD = growing degree days; CH = chilling hours; NFD = number of frost days; EWS = electronic weather station; AWS = aero weather station; CWS = compact weather station; CS = Climate Station.*

4.3.3 MODIS satellite data

Following the downloading of the 15 years (2002 – 2017) of MODIS data, 12 images were selected and viewed in ArcGIS. To aid the selection the daily min/max databases of the long-term climate stations of Wairoa North Clyde, Mahia Aws and Cricklewood were filtered for days of minimum temperature less than 0°C. Figure 4.12 shows a MODIS image example for the morning of 30 July 2017 at 1:30am. The MODIS image extent extends out to North Sydney, Australia but is focused on the Central North Island, New Zealand. Figure 4.13 shows the same MODIS image but centred on the Wairoa District.

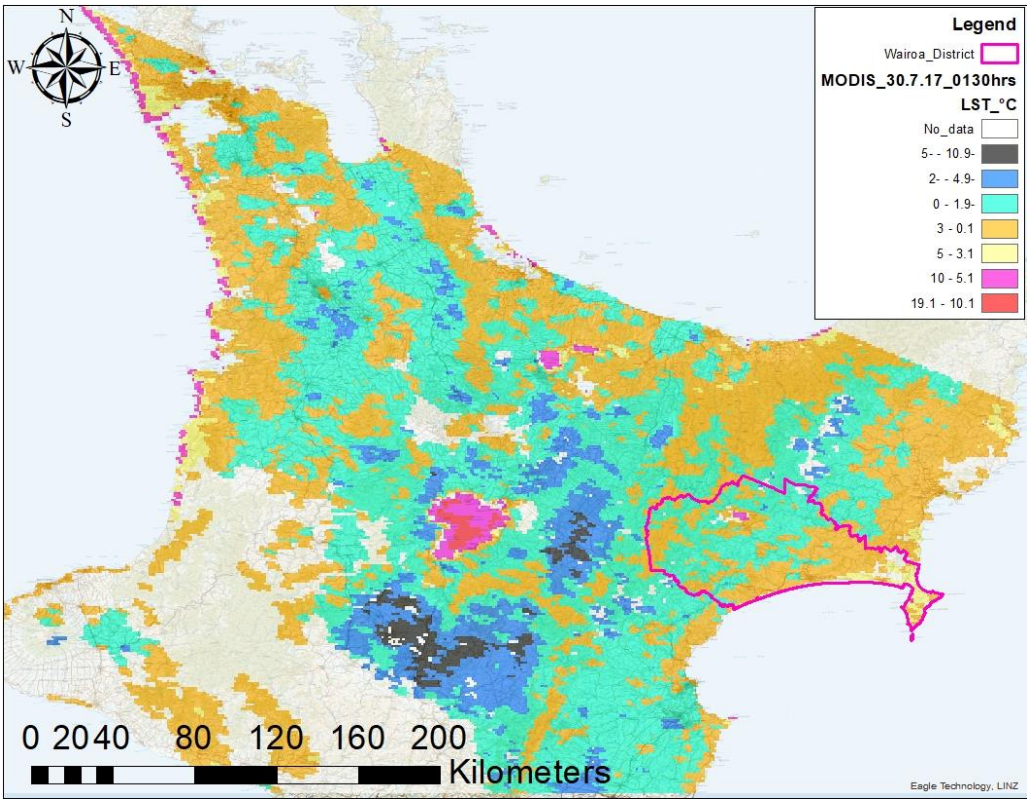

Figure 4:12: Example MODIS image showing land surface temperature (LST) as at 30 July 2017 1:30am over the Central North Island, New Zealand with Wairoa District.

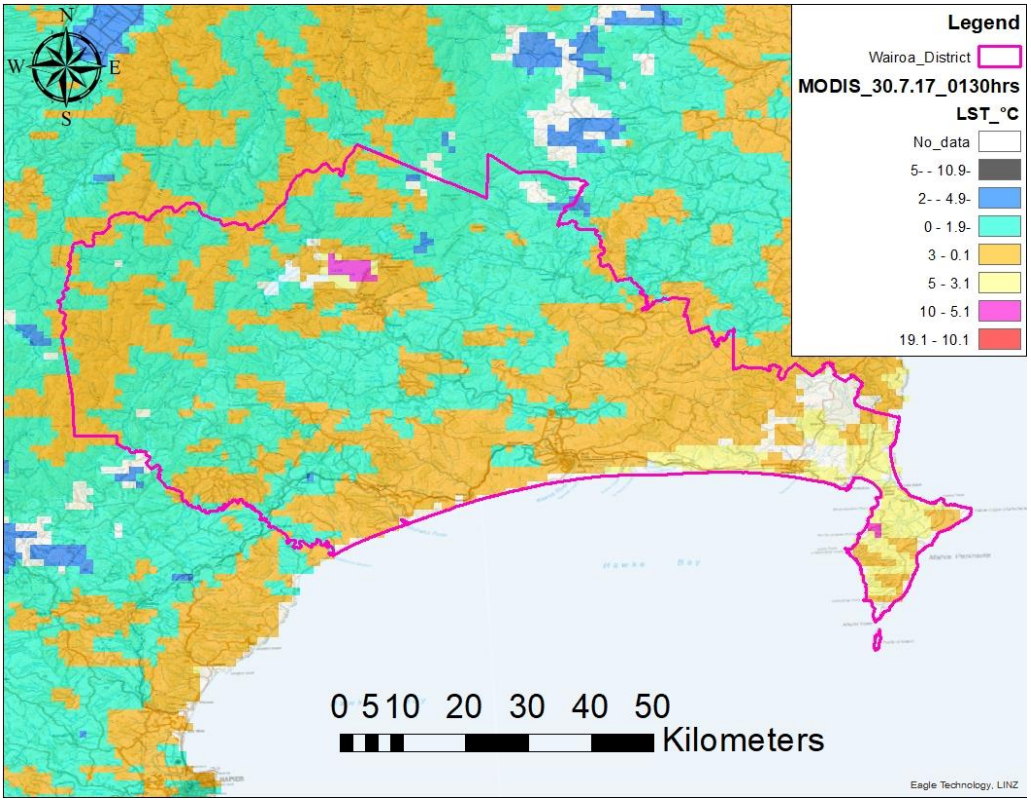

Figure 4:13: The same MODIS image in Figure 4.12 but centred on the Wairoa District.

The MODIS satellite data did not have a strong correlation with the measured air temperatures (Figures 4.10 to 4.23) for either the climate station data or the iButton data (Table 4.9).

Table 4:9: Summary table showing relationship between MODIS LST (°C) at 0130hrs and Climate Station daily minimum temperature (°C)

Climate Station /iButton site	Regression of MODIS LST (°C) at 0130hrs with CS temp (°C) at 0200hrs		Regression of MODIS LST (°C) at 0130hrs with CS daily Tmin (°C)	
	R^2	Regression equation	R^2	Regression equation
Wairoa North Clyde EWS	0.37	$y = 0.0036x^2 + 0.5488x + 1.1798$	0.39	$y = -0.0011x^2 + 0.6534x + 2.1635$
Cricklewood CS	0.48	$y = -0.0043x^2 + 0.7966x + 0.1632$	0.65	$y = 0.0039x^2 + 0.7914x + 0.5704$
Mahia AWS	0.64	$y = 0.0034x^2 + 0.8441x - 2.5032$	0.59	$y = 0.0095x^2 + 0.682x - 0.2159$
Wairoa AWS	0.36	$y = -0.001x^2 + 0.6361x + 1.1276$	0.41	$y = -0.0087x^2 + 0.7891x + 2.0974$
IButton site #7	0.32	$y = 0.3759x + 2.4253$	0.37	$y = 0 .7166x + 1.0764$

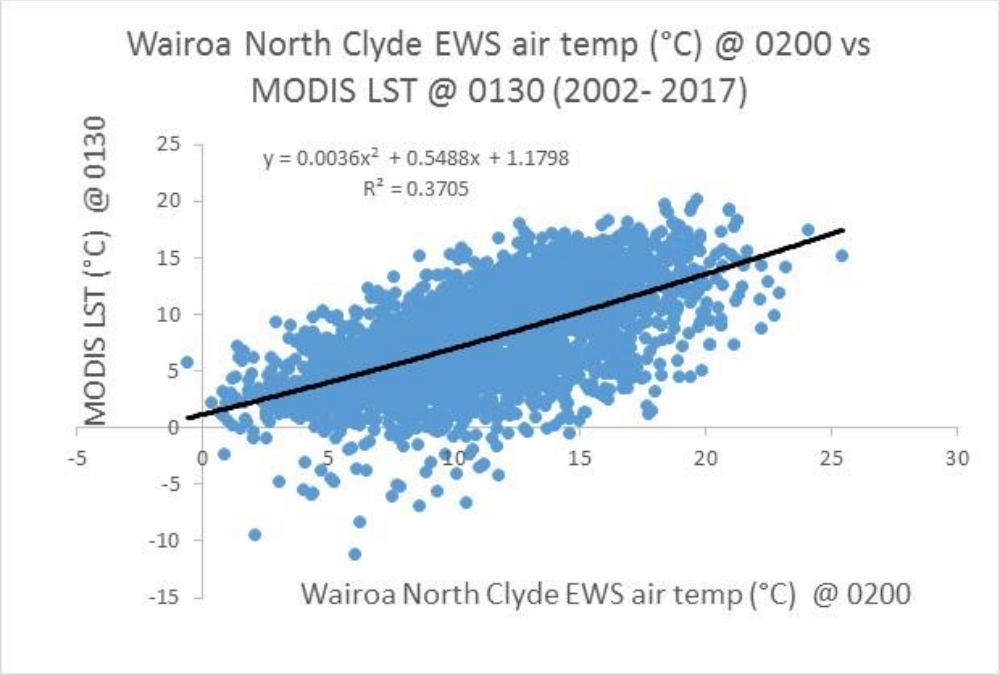

Figure 4:14: Scatterplot showing 2nd order polynomial regression of Wairoa North Clyde EWS air temperature (°C) at 0200hrs vs MODIS LST (°C) at 0130hrs between 2002 – 2017.

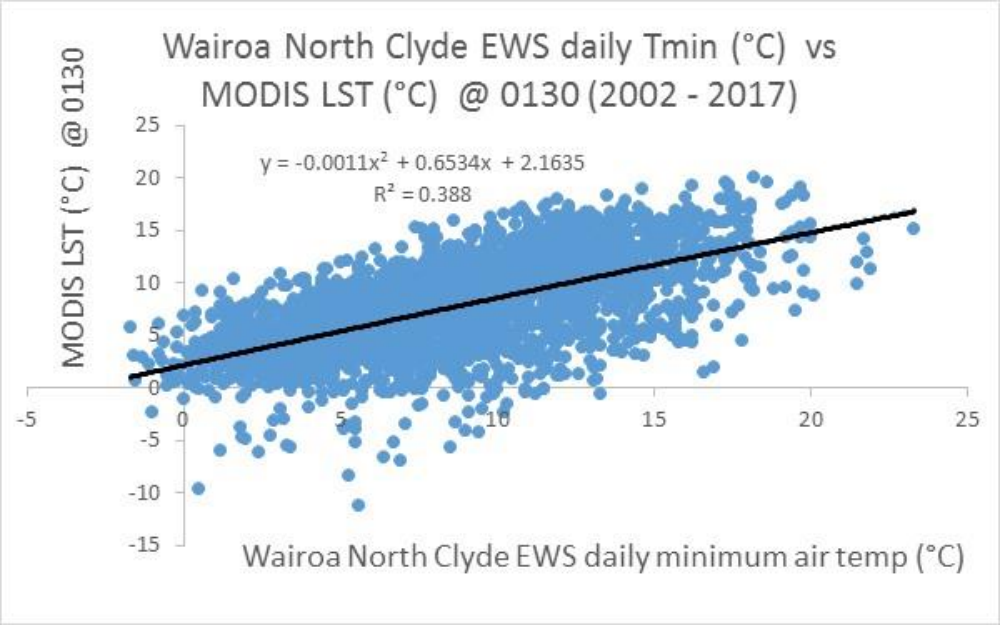

Figure 4:15: Scatterplot showing 2nd order polynomial regression of Wairoa North Clyde EWS daily minimum air temperature (°C) vs MODIS LST (°C) at 0130hrs between 2012 – 2017.

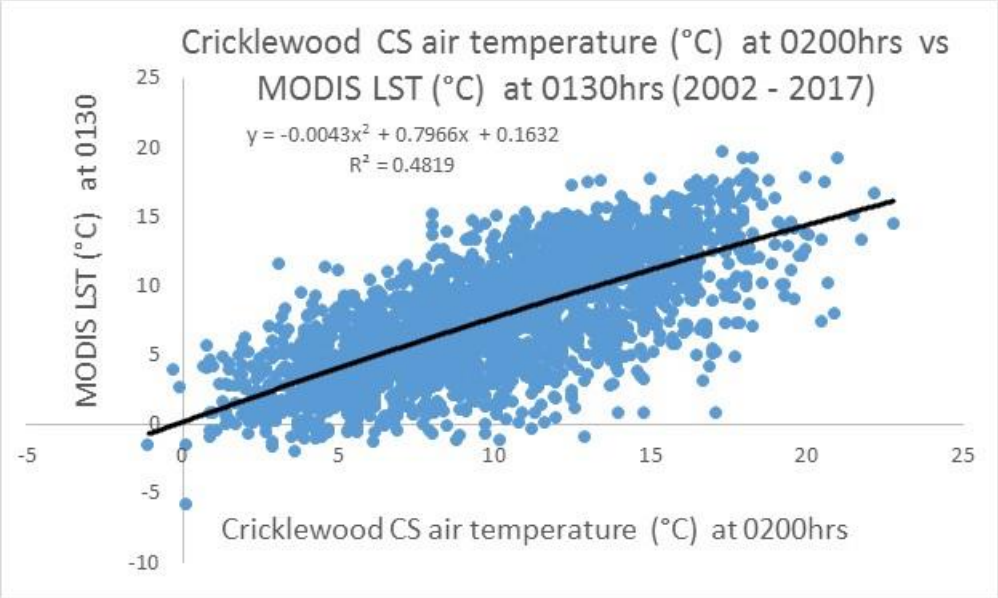

Figure 4:16: Scatterplot showing 2nd order polynomial regression of Cricklewood Climate Station air temperature (°C) at 0200hrs vs MODIS LST (°C) at 0130hrs between 2002 – 2017.

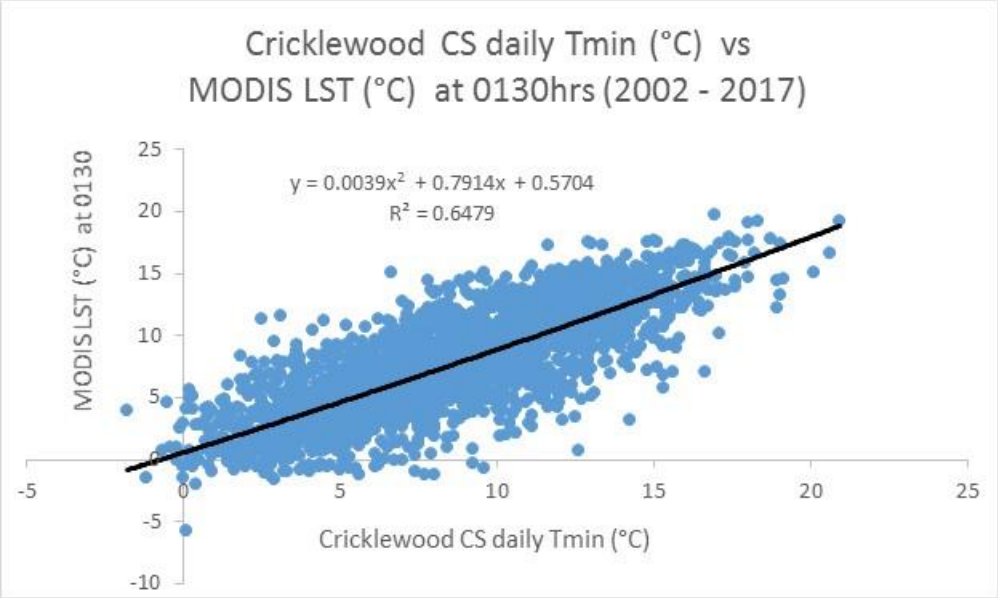

Figure 4:17: Scatterplot showing 2nd order polynomial regression of Cricklewood Climate Station daily minimum air temperature (°C) vs MODIS LST (°C) at 0130hrs between 2002 – 2017.

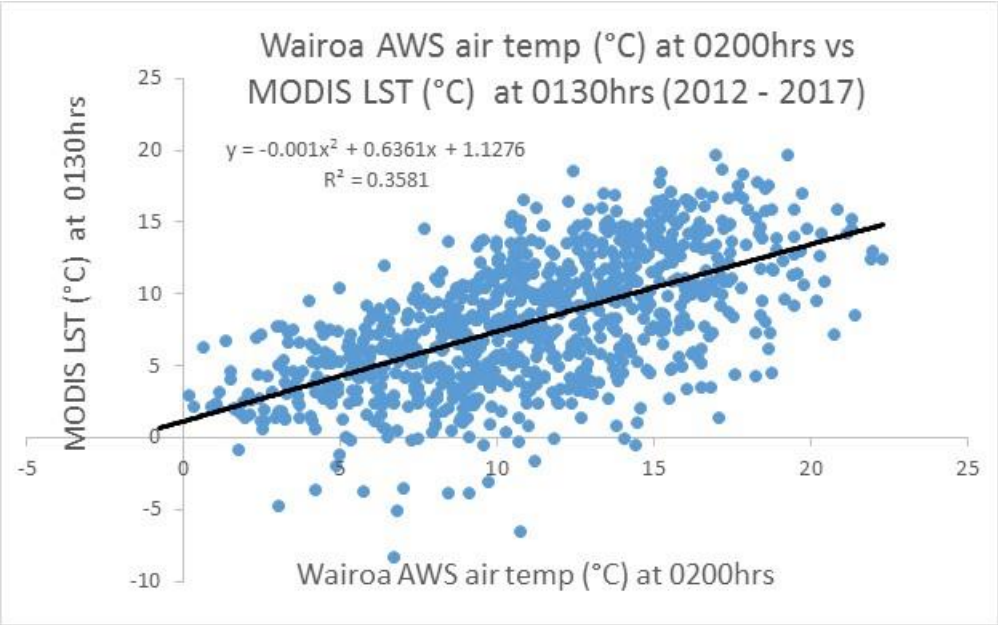

Figure 4:18: Scatterplot showing 2nd order polynomial regression of Wairoa AWS air temperature (°C) at 0200hrs vs MODIS LST (°C) at 0130hrs between 2012 – 2017.

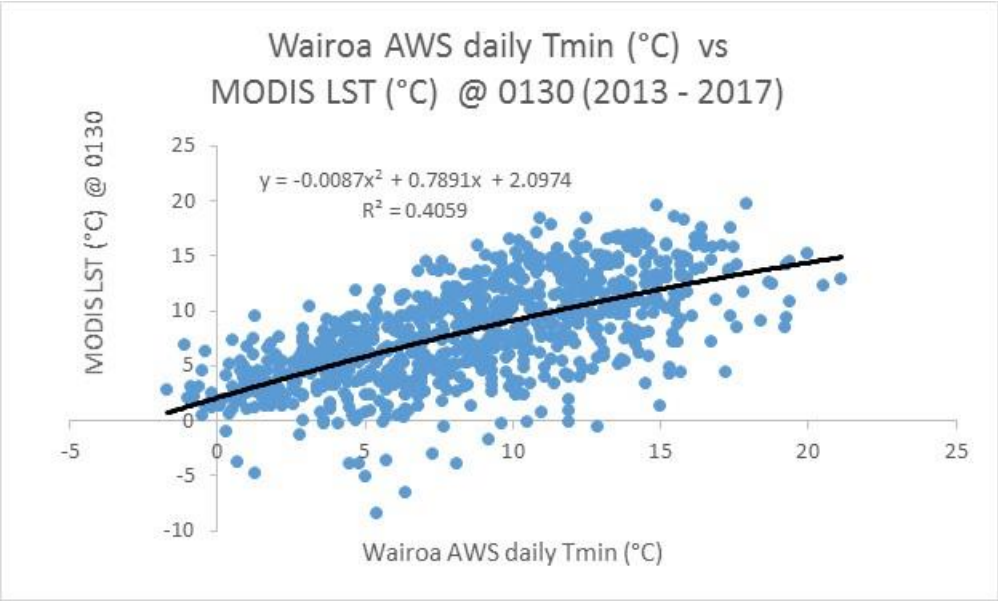

Figure 4:19: Scatterplot showing 2nd order polynomial regression of Wairoa Airport AWS daily minimum air temperature (°C) vs MODIS LST (°C) at 0130hrs between 2012 – 2017.

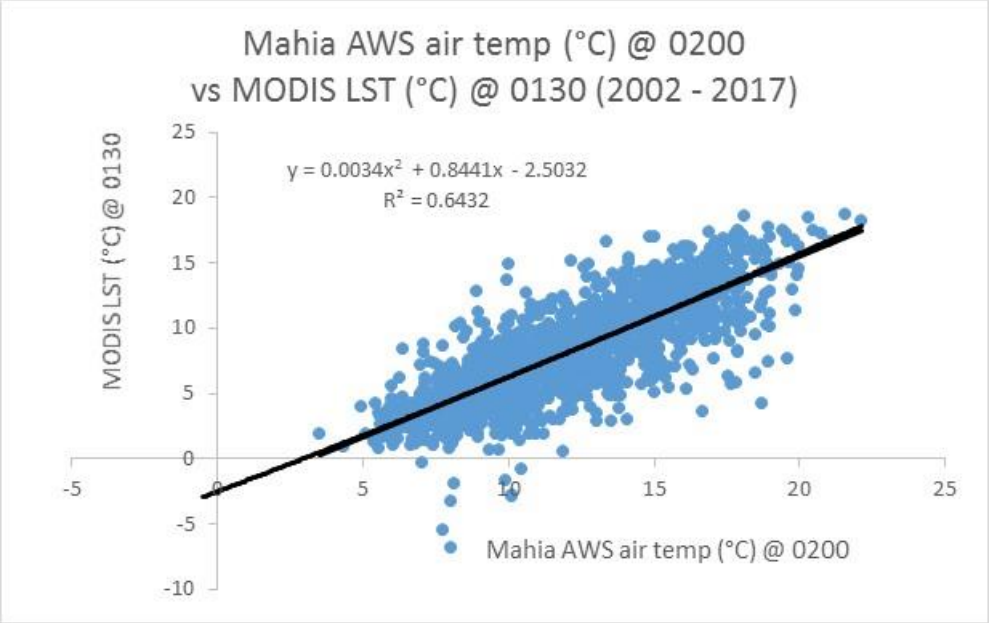

Figure 4:20: Scatterplot showing 2nd order polynomial regression of Mahia AWS air temperature (°C) at 0200hrs vs MODIS LST (°C) at 0130hrs between 2002 – 2013.

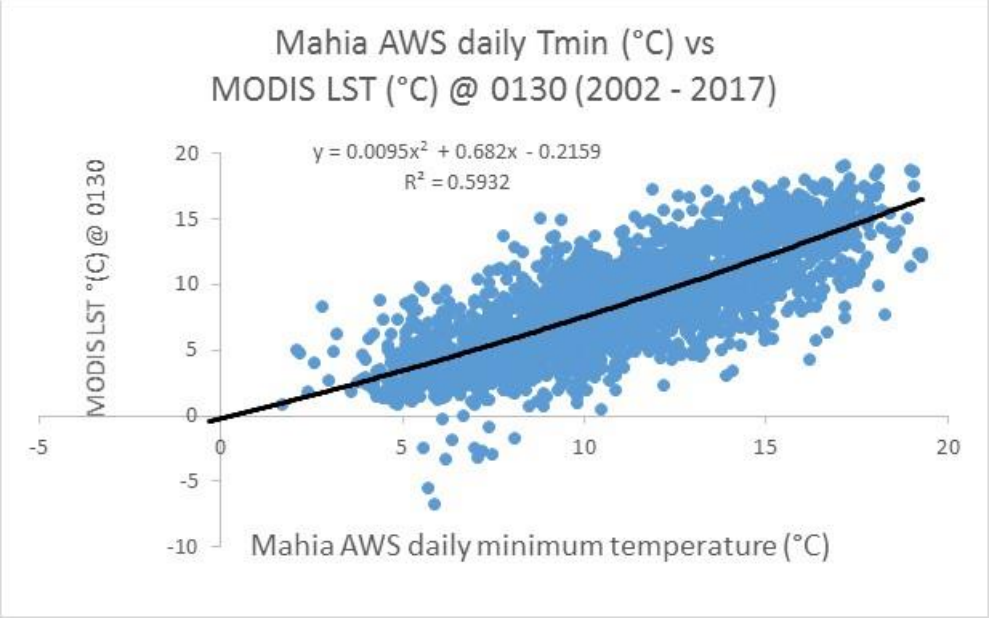

Figure 4:21: Scatterplot showing 2nd order polynomial regression of Mahia AWS daily minimum air temperature (°C) vs MODIS LST (°C) at 0130hrs between 2002 – 2017.

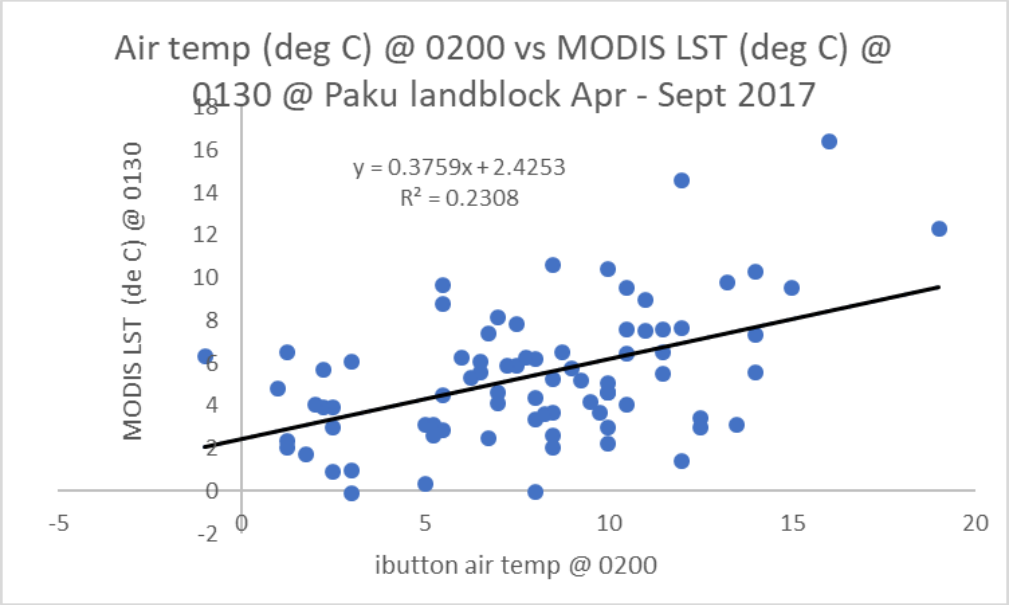

Figure 4:22: Scatterplot showing linear regression of Paku land block iButton air temperature (°C) at 0200hrs vs MODIS LST (°C) at 0130hrs between April – September 2017.

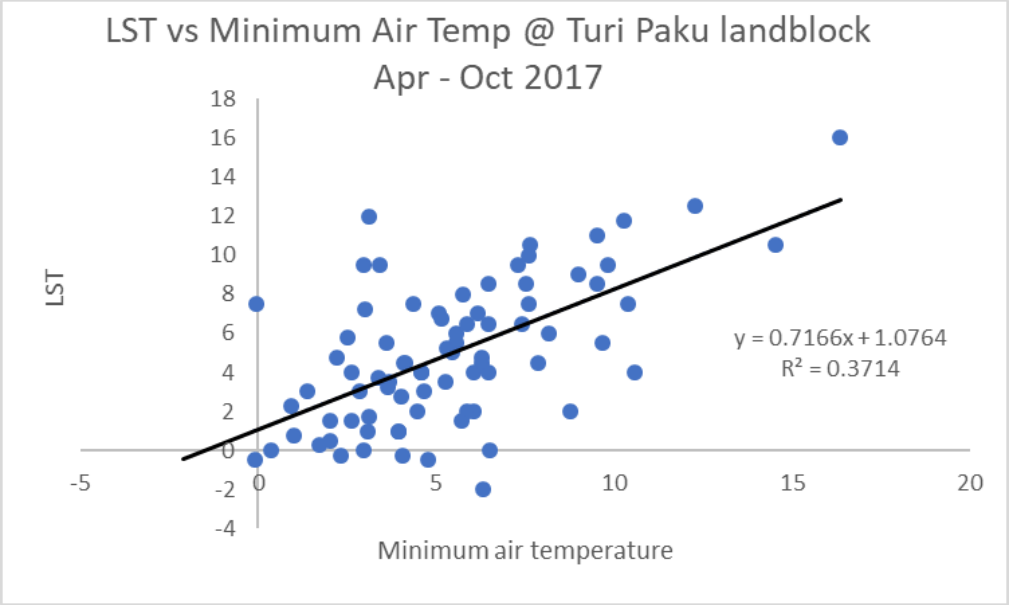

Figure 4:23: Scatterplot showing linear regression of Paku land block daily minimum iButton air temperature (°C) vs MODIS LST (°C) at 0130hrs between April – October 2017.

4.3.4 Climate maps

Mean monthly (October – April) growing degree days, mean monthly (April - August) chilling hours and October frost risk at 0°C calculated from each iButton's long term dataset, were fed into the universal kriging function in ArcGIS to construct the growing degree days, chilling hours and October frost risk maps for the Wairoa District (Figures 4.24, 4.25 and 4.26).

Figure 4.24 shows the central Wairoa area having the highest number of growing degree days (base 10°C, October – April) decreasing with distance from the coast inland. The Mohaka and Wairoa River Valleys appear to experience lower rates of growing degree days possibly due to their topography.

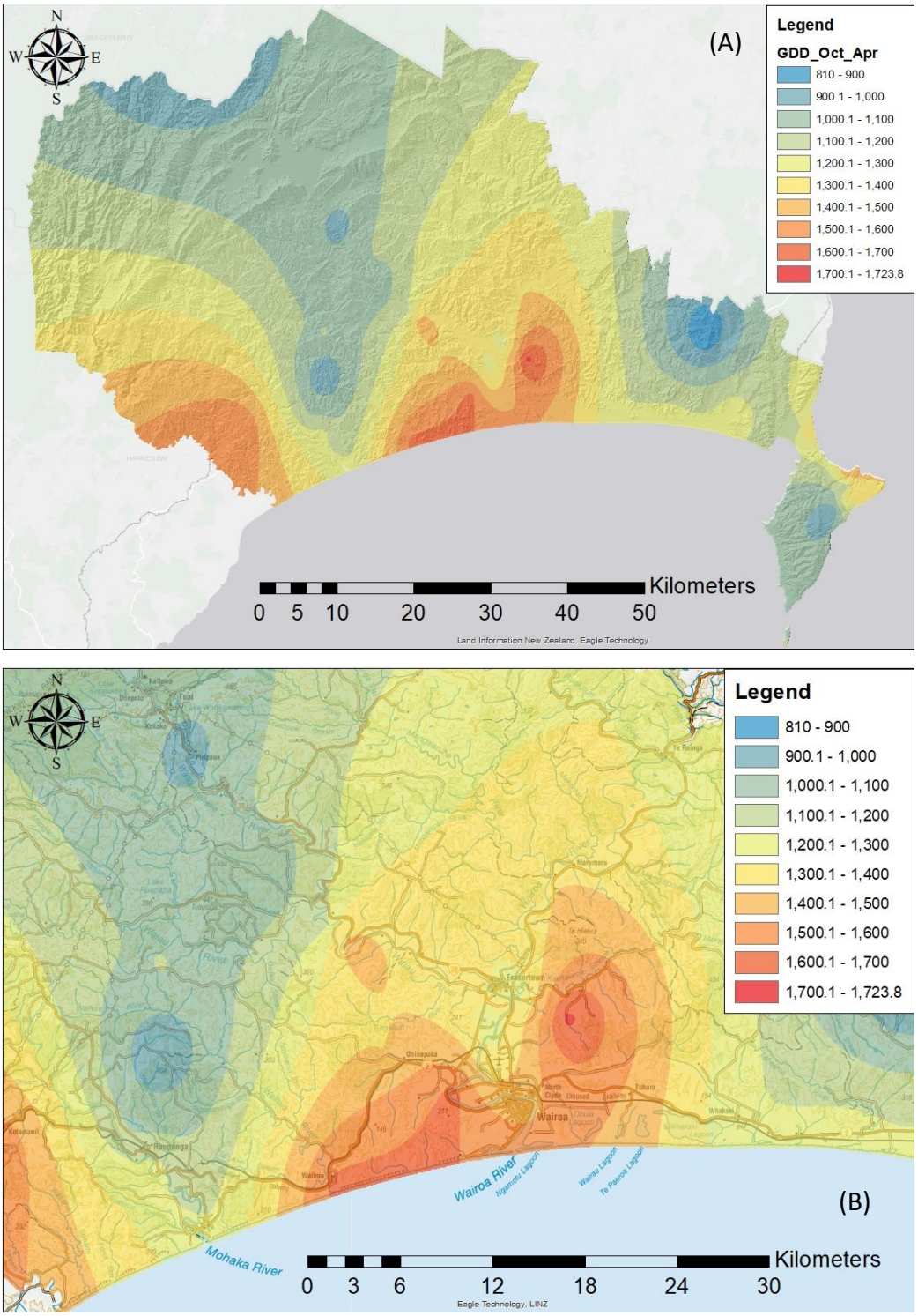

Figure 4:24: Map of growing degree days (base 10°C, October – April) for (A) Wairoa District, and (B) Central Wairoa township.

Figure 4.25 shows a general trend of areas near the coast having low chill hours – especially the Mahia Peninsula, to increase inland with distance from the coast. Frasertown and Raupunga appear to experience higher chill hours than other areas with equal distance from the coast. The lower Mohaka River valley although near the coast still experiences moderate chill hours. Many of the horticulture crops had a minimum chill requirement of 600 or more hours. For this reason the 600 – 700 chill hour category is coloured bright green.

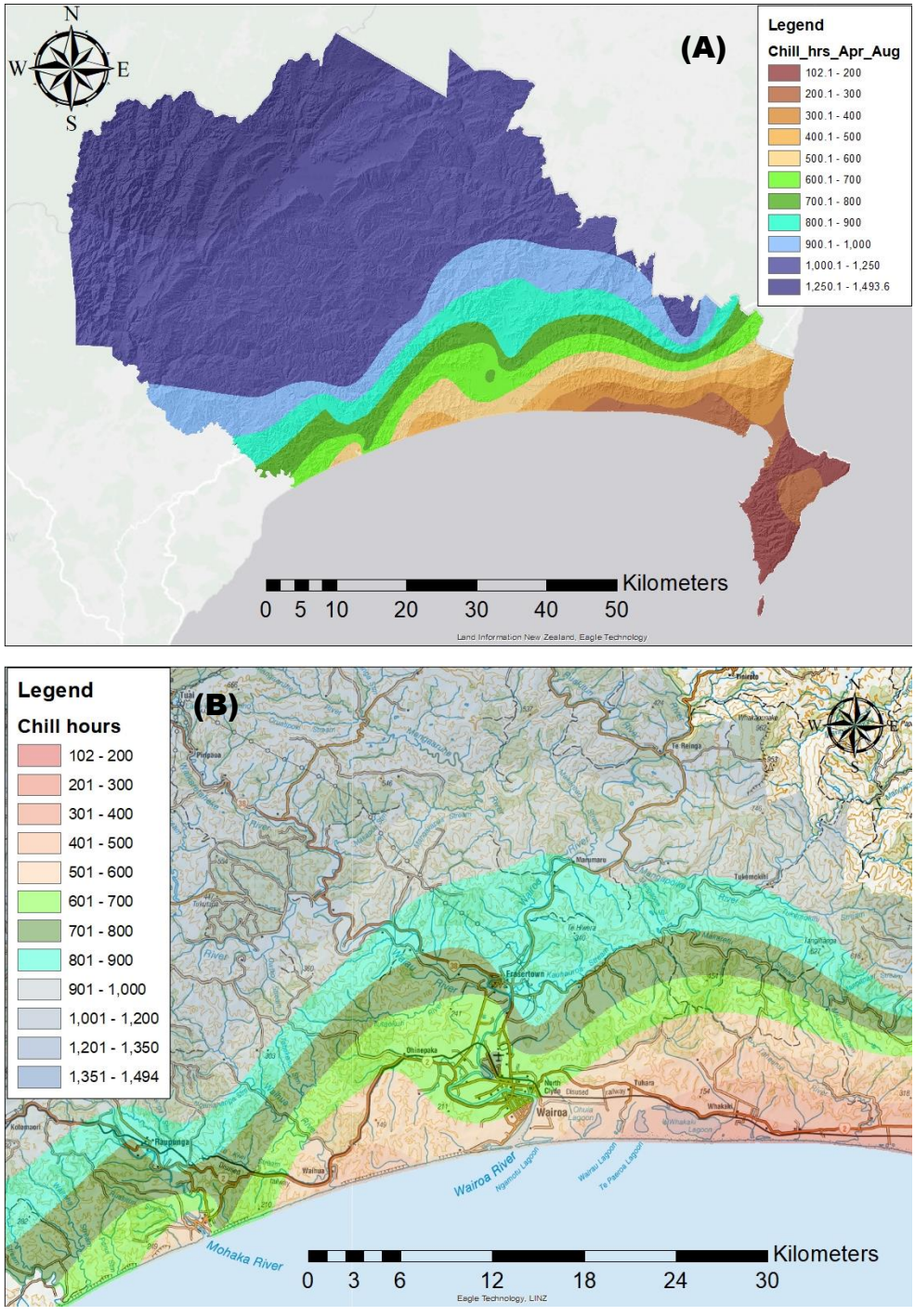

Figure 4:25: Map of chilling hours (base 7°C, April – August) for the (A) Wairoa District, and (B) Central Wairoa township.

Figure 4.26 shows areas near the coast to have an October frost risk of less than 10% (coloured red). This area includes much of the Mohaka valley and area from Frasertown to the coast.

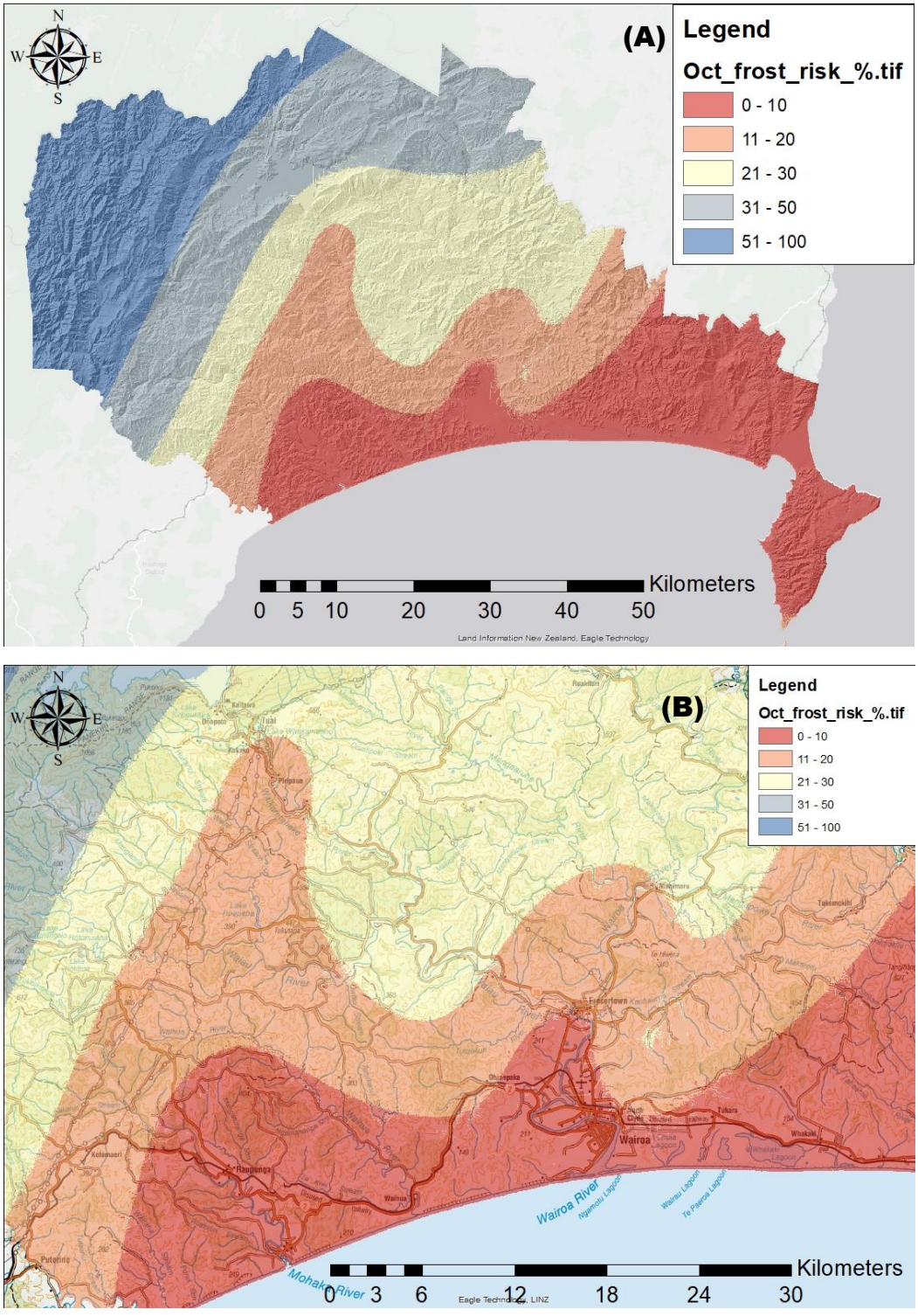

Figure 4:26: Map of October frost risk (%) at 0°C for (A) Wairoa District and Mohaka valley to Wairoa.

4.4 Discussion

Where temperature data from climate stations is sparse, or unavailable, the use of satellite images is justified (Pouteau, 2011; Zhu *et al.,* 2013). However, where air temperature data is available the inclusion of satellite images as explanatory co-variates may not be needed. Florio *et al*., (2004) and Cristobal (2006) both used satellite images as explanatory variables to aid the interpolation of temperature. Both authors proved the significance of using satellite data as predictors although improvement when compared to the geographical model (excluding satellite data) was modest. Cristobal (2006) reported an improvement of 0.1°C for modelling mean monthly air temperature while results by Florio *et al.,* (2004) showed a 0.06°C improvement for modelling mean daily air temperature. The results in Figures 4.14 to 4.23 show a poor agreement of climate station data and MODIS satellite data. This likely because although related the land surface temperature (near ground temperature) estimated by MODIS and the air temperature measured (approx. 2m above ground) by the climate stations are essentially two different aspects of temperature. Because of the poor correlation between the two, further use of the MODIS images in this study was rejected.

Figures 4.5 to 4.11 show excellent correlations between the iButtons deployed near the climate stations and that climate station. R^2 values for iButtons deployed further away from the climate stations also gave high correlations allowing confidence in estimated values for chill hour, growing degree days and October frost risk and the spatial interpolation of those values between iButton sites.

Table 4.8 reveals interesting climate characteristics for the individual iButton locations. IButton site #25 situated near Frasertown, on an elevated alluvial terrace. For within the central Wairoa area the site has the highest number of chill hours (875) yet one of the lowest October frost risk rates of only 8%. Growing degree days (October – April) are reasonable at 1228. The high chill hours, low frost risk rate can partly be explained by the locations surrounding topography. Being near Frasertown the site is further inland and is at the junction of the Waiau and Wairoa River valleys. This may ensure cold air drainage flows regularly through the site. The site is a paddock (approximately 4.5 Ha) featuring flat to gently undulating slopes and is elevated approximately 20m above an ephemeral stream

which borders the paddock. These features may afford it some drainage and protection against cold air wanting to settle on calm spring mornings.

IButton site #12 on Mill Rd receives chill hours of 852, growing degree days of 1506 and has an October frost risk of 27%. The locations topography is within the centre of a valley bordered by steep sides. Cold air would likely settle within the valley centre where the iButton was located explaining the moderately high chill hours and slightly elevated frost risk.

For the central Wairoa area iButton site #7 has the highest October frost risk of 39%. This can potentially be explained by its topography. The site lies on a flat to gently undulating alluvial plain west of the Wairoa River but east of Awamate Rd. The area upstream of the site is large including both the Wairoa and Waiau River catchments. Cold air draining from the catchment on calm spring mornings is likely to settle on flat topography such as that at iButton site #7. Knowing the risk of October frost can inform land owners plan future development.

IButton site #22, near Aranui Rd, Central Wairoa, has chill hours of 719, growing degree days of 1370 and a low October frost risk of 4%.

All other iButton locations within the central Wairoa feature chill hours ranging between 608 – 761, October frost risk between 0 – 31% and growing degree days (base 10°) between 1212 – 1790.

Of the Mohaka River Valley iButton sites only one site had an October frost risk greater than 0% - site #2 with 4% which is low indicating the Mohaka Valley to experience very little frosts in October. Chill hours for the Mohaka Valley ranged between 481 – 808 and growing degree days between 1094 – 1244.

IButton site #34 inland from Wairoa is situated on a gently sloping terrace above the Waikaretaheke River has an October frost risk of only 8%, chill hours of 1029 and growing degree days of 964. The low frost risk can partly be explained by its topography being elevated above the river valley providing good cold air drainage away from the site. Other iButton sites inland of Wairoa on river terraces experience moderately high chill hours between 863 – 1131, low to moderate October frost risk (12 -31%) and reasonable growing degree days (964 – 1427) as expected with an increase in elevation and distance from the coast.

IButton sites on coastal areas experience little to no October frosts (0% risk), low chill hours (110 – 429) and moderate to high growing degree days (1170 – 1884).

4.5 Conclusion

By deploying iButton temperature loggers throughout the Wairoa District the climate has been characterised. The Mohaka Valley appears to have low frost risk (0 - 4%) and moderate chill hours (481 – 808). This can be attributed towards its topography having elevated river terraces which slope gently towards the river to facilitate cold air drainage away from the terraces. In effect this may help create an area of quality climate amenable towards a range of crops.

The central Wairoa Valley has a greater area of flat to gently undulating alluvial floodplains. This appears to generate a moderate amount of chill hours, moderate to high growing degree days and moderate risk of October spring frost. Several of the sites appeared to have their own topoclimate. IButton site #25 (near Frasertown) results show high chill hours, moderate growing degree days and low frost risk. This can be explained by its surrounding topography influencing movement and drainage of cold air away from the site. IButton site #22 (near Aranui Rd) is surrounded by flat to gently sloping land and showed results of 719 chill hours, 1370 growing degree days and a low (4%) October frost risk. These locations represent areas of quality topoclimate conducive towards a range of crops. Other sites within the central Wairoa produced moderate chill hours (608 – 761), October frost risk between 0 – 31% and growing degree days between 1212 – 1790. The climate of the central Wairoa valley appears influenced by the cold mountain air draining into the valley producing moderate chill hours and on flat areas moderate risk of October frost risk. Growing degree days are moderate to high and will not likely limit crop growth.

The climate of the coastal areas is represented by low to nil October frost risk, moderate growing degree days and low chill hours.

The climate of the Wairoa District has been characterised showing variability in the variables studied. The data is further utilised in Chapter 6 to evaluate land for a range of horticultural crops.

Chapter 5

Soil Characterisation

5.1 Introduction

Quantifying crop irrigation requirements has several benefits including reducing agricultural demand on water resource use, increasing crop yield per unit of water consumed (Fereres *et al.,* 2003) and reduced expenditure to the landowner (Hedley *et al.,* 2010). The initial step towards effective water resource management needs an accurate estimate of the water needed for agricultural irrigation (Er-Raki *et al.,* 2010).

This chapter describes methods employed during field work (characterising the soils, estimating soil permeability) conducted between 4-8 July 2017 in the Wairoa District. The laboratory work (determining soil water holding capacity) completed between August – September 2017 at Landcare Research, Hamilton is also described. Results are presented then used, in conjunction with climate data (from Chapter 4), to estimate the irrigation needs for a range of potential horticultural crops.

5.2 Methods

5.2.1 Introduction

To model the soil water balance, data from three variables are needed: the soils "total available water holding capacity" (TAWHC), rainfall, and evapotranspiration (Horne & Scotter, 2016). This section details the field and lab methods used to describe the soil profiles, estimate soil permeability classes, measure soil water holding capacity and estimate irrigation needs for a range of crops. Soil profile descriptions allow soil potential rooting depth to be assessed as well as identifying any other potential soil limitations for crop growth.

5.2.2 Soil characterisation in field

5.2.2.1 Soil profile description

Between 4 – 8 July 2017, at four sites representative of the Wairoa District's main soil types (Figure 5.1), a profile pit was dug and the profile described following the methods of Milne *et al*, (1995). Soil properties described include colour, presence of mottles, consistence, pedality, texture, roots if any and parent material. Horizons were also tested for allophane using the NaF field test (Fieldes & Perrot, 1966). Horizon notation followed the methods of Milne *et al.,* (1995). Soil classification was undertaken following the methods of Hewitt (2010).

Within each soil profile pit, each horizon was sampled in triplicate by inserting numbered brass rings (each 68.6cm^{-3} in volume) into the levelled horizon centre. Using a sharp knife, excess soil surrounding each ring was carefully trimmed and a plastic disc was placed at each end to contain the sample then taped, with the three samples placed into a separate sealed bag labelled with the site and horizon names. Samples were then stored in a refrigerator at 4°C.

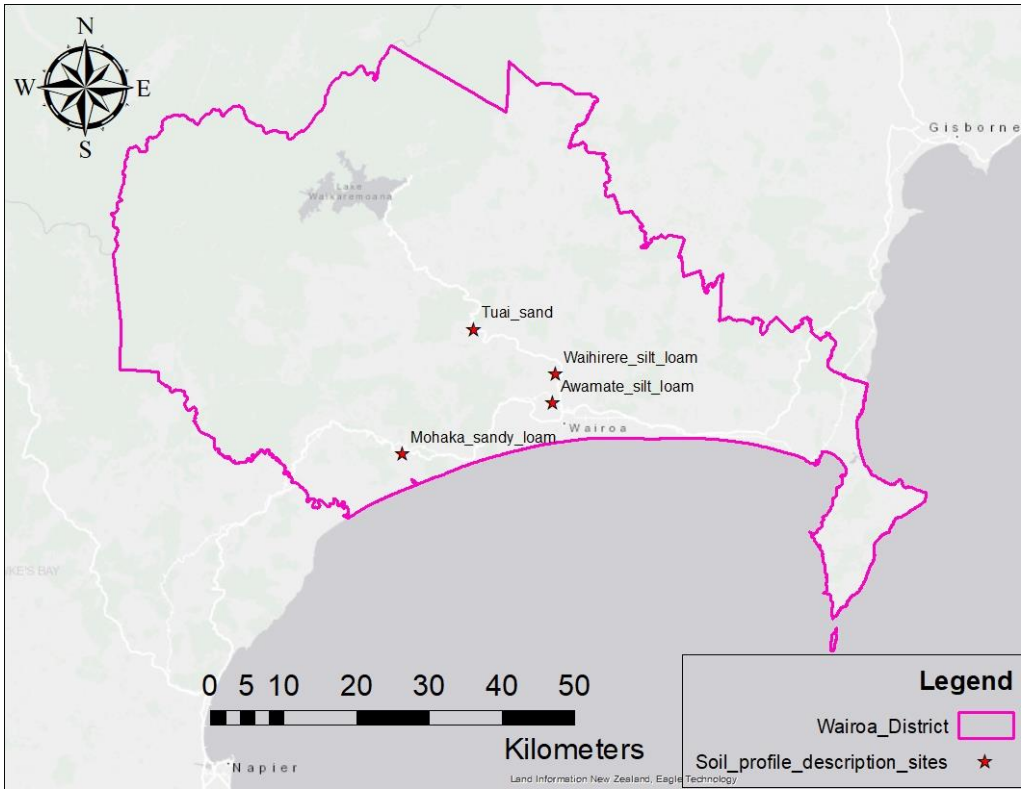

Figure 5:1: Location of four sampled soil sites for determining AWHC and bulk density.

5.2.2.2 Soil penetration resistance

Following the methods of Milne *et al.,* (1995), a hand-held penetrometer was used to measure penetration resistance for each soil horizon at each of the four sites. The penetrometer was pushed perpendicular into the soil horizon to 6mm depth then removed with the resistance reading recorded. 10 measurements were taken per horizon. The readings (in bar units) were then multiplied by the spring factor of 0.67, converted to kPa and classified according to Milne *et al.,* (1995) in Table 5.1.

Table 5:1: Penetration resistance classes. Adapted from Milne (1995).

Class	Penetration resistance (kPa)
Extremely low	0 – 500
Very low	500 – 1000
Low	1000 – 1500
Moderate	1500 – 2200
High	2200 – 3000
Very high	3100 – 4000
Extremely high	>4000

5.2.2.3 Soil degree of packing

Following the methods of Milne *et al.,* (1995) degree of packing for each soil horizon at each site was determined. A singleton blade (Figure 5.2(A)) was inserted into the soil horizon. A penetrometer was then used to push the blade until the soil ruptured (Figure 5.2(B)).

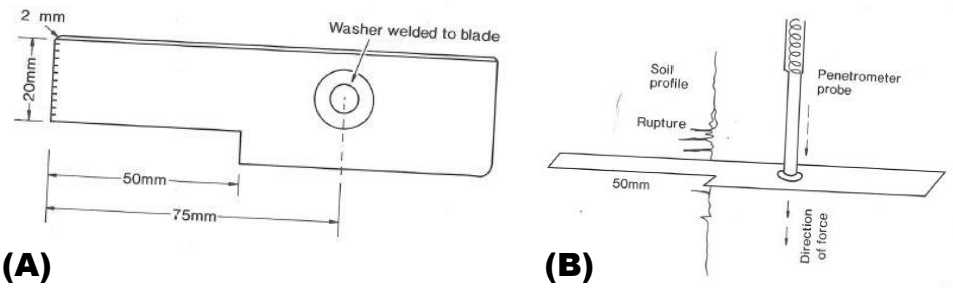

Figure 5:2: Singleton blade (A) pushed perpendicular into soil, with penetrometer forcing downwards pressure to assess degree of packing (B). Adapted from Milne et al., (1995).

The force required to do so was recorded (in bar units) and done so for 10 readings. Bar units were converted to kPa then reclassified according to Griffiths (1985) and Milne *et al.,* (1995) in Table 5.2.

Table 5:2: Degree of packing assessed by Singleton blade and penetrometer. Adapted from Griffiths (1985) and Milne et al., (1995).

Degree of packing	Bar (Griffiths, 1985)	kPa (Milne, 1995)
Very low	0 – 4	0 – 500
Low	5 – 9	500 – 1000
Moderate	10 – 22	1000 – 2200
High	23 – 30	2200 – 3000
Very high	31 – 40	3000 – 4000
Extremely high	>40	>4000

5.2.3 Laboratory determination of soil physical properties

Following field work laboratory work was completed at Landcare Research during August – September 2017. Methods by Claydon (1997) were followed for all laboratory work completed in sections 5.2.3.1 to 5.2.3.5.

5.2.3.1 Determination of gravimetric water content (Θg) at field moist state

Firstly, each soil sample within their numbered brass ring was weighed to 3 decimal places. With each ring pre-weighed meant the weight of each soil sample could be calculated. This is the soils "field moist state". Using the samples field moist (mass wet soil), the ring weight and the mass of dry soil each sample's gravimetric water content (Θg) at sampling could be calculated as the ratio of the mass of water to the soil's mass and given as a percentage (Equation 5.1, adapted from McCarty *et al.,* 2016):

$$\text{Gravimetric water content at sampling } (\Theta g) = \left(\left(\frac{(WS-L)-\text{DS})}{\text{DS}}\right) \text{ X } 100 \qquad (5.1)$$

Where WS = mass of wet soil; L = mass of ring; DS = mass of dry soil.

As drying out the soil to determine the dry soil weight damages the soil structure this was done after all the tensions from 5 kPa to 1500 kPa were done.

Upon applying the following tensions: 5 kPa, 10 kPa, 100 kPa and 1500 kPa with their soils re-weighed their respective gravimetric water contents could be calculated as per equation 5.1.

5.2.3.2 Gravimetric water content (θg) at 5 kPa tension

The 5kPa tension was determined using ceramic plates attached to a hanging water column (Figure 5.4). Samples within their rings were first saturated by placing on a permeable filter paper, capped with a plastic disc in a tray (Figure 5.3). Water was added to just below the liners upper surface. The samples were left overnight to ensure saturation.

Figure 5:3: Saturation of soil samples

Ceramic plates were saturated as follows: a large sink was filled with water. A 1.5 m x 5 mm plastic outlet tube was attached to the ceramic plates 5cm x 3 mm steel extraction tube. The plate was placed in the sink of water and fully submerged. To the free end of the outlet tube was attached a syringe which was used to withdraw water from the sink via the ceramic plate and outlet tube. With the syringe removed and water draining freely from the outlet tube into a drain or large tray below the sink and ceramic plates the system was left overnight to drain any air in the plates and become saturated.

The following morning, the filter papers, saturated samples, rings and discs were placed on the saturated ceramic plates and gently pressed down to ensure positive contact with the ceramic plate surface. To encourage drainage a syringe was used

to withdraw water from the outflow tube connected to the plates and samples. With each sample draining freely each tube was then placed in the collection vessel (Figure 5.4A, B) to collect all drained water. In the collection vessel was an incised exit hole (Figure 5.4B) from which surplus water could exit and collect in a secondary container. Using clamps holding the collection vessel, the exit hole was placed 50cm below the soil samples to create a 50cm hanging water column simulating 5 kPa tension (Figure 5.4A). Water was added to the collection vessel to the level of the exit hole. To minimise moisture loss by evaporation the soil samples on ceramic plates were covered in aluminium foil and a towel then left to drain for 3 – 5 days. When no further water was draining from the exit hole indicated the system was in equilibrium at 5 kPa. The samples were then carefully re-weighed.

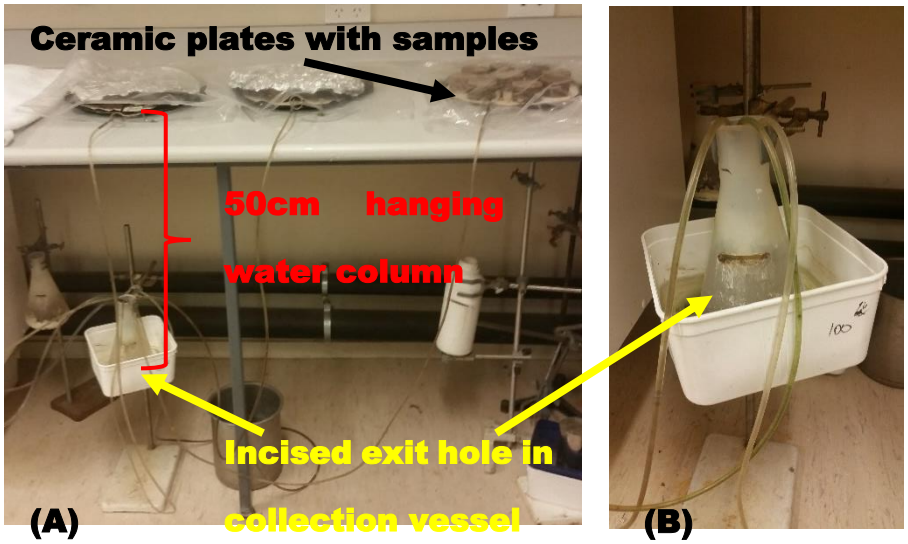

Figure 5:4 (A): Ceramic plates with samples above 50cm hanging water column to determine soil moisture content at 5 kPa tension; (B) collection vessel showing incised exit hole in collection vessel.

5.2.3.3 Gravimetric water content (Θg) at 10 kPa tension

The samples after being weighed at 5 kPa were then ready for the 10 kPa tension. For the 10 kPa tension a new set of pre-saturated ceramic plates (saturation method outlined in section 5.2.3.1.1.1) was used and the process used for the 5 kPa tension repeated but with a hanging water column height of 100cm. 100cm

drainage height is equivalent to applying 10 kPa tension to the soil samples. 5-7 days was used to drain the samples or until no more water was draining from the exit hole indicating the system was in equilibrium at 10 kPa. The soil samples were then re-weighed.

5.2.3.4 Gravimetric water content (θg) at 100 kPa tension

The samples after being weighed at 10 kPa were then ready for the 100 kPa tension.

5 bar pressure plate extractor (Soil Moisture, 2018) were used to determine soil moisture content at 100 kPa tension. First an open container of water was placed at the bottom of each pressure plate chamber to prevent the soil samples from drying out. Pre-saturated ceramic plates (saturation method outlined in section 5.2.3.1.1.1) were then placed inside a pressure plate chamber (Figure 5.5A) with the ceramic plate outflow tube connected to the pressure plate chamber outflow pipe. To prevent unwanted initial drainage the ceramic plate outflow tube was clamped. Soil samples were then placed on filter papers on the ceramic plates in the pressure plate chamber with up to three ceramic plates stored per chamber. The outflow tube was then un-clamped to allow drainage to begin with the lid put in place and screwed tight. A container was placed below the outflow pipe to collect water forced out of the system. Compressed air was gradually released into the chamber up to 100 kPa then left for a minimum of 7 days or until equilibrium was reached – when water stopped draining from the outflow pipe. When no more water was being drained into the collection tray indicated the chamber and soil samples were in equilibrium at 100 kPa. The compressed air was then shut off and the lid carefully removed. The soil samples were then weighed and recorded.

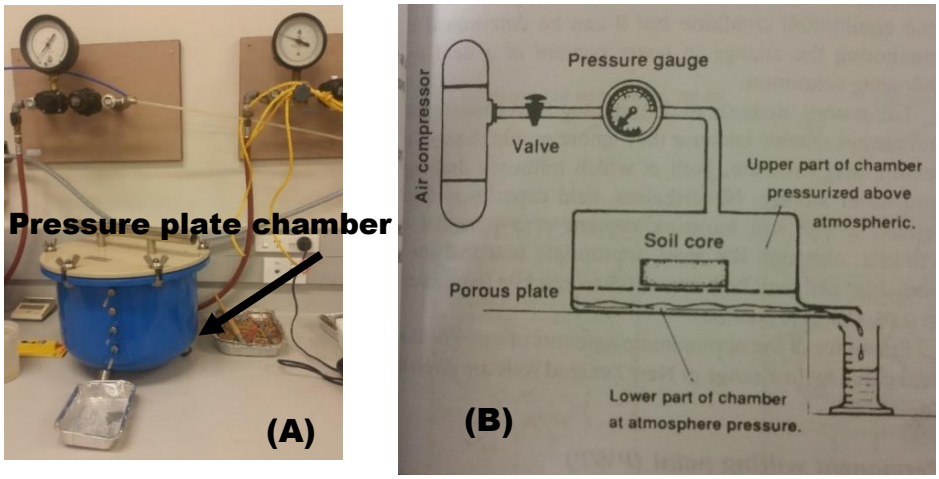

Figure 5:5: (A): Pressure plate chamber containing three ceramic plates at 100 kPa. (B) Schematic diagram outlining workflow of chamber pot (McLaren & Cameron, 1996).

5.2.3.5 Gravimetric water content (Θg) at 1500 kPa tension

To determine each sample's 1500 kPa tension intact soil samples are not needed. Instead loose samples collected during field work were used. This is because at 1500 kPa the soil's structure has less influence than at the lower pressures (Elrick & Tanner, 1955).

To begin two sheets of dry precut cellulose membrane were placed in a tray then covered with water for five minutes to soften. The cellulose once moistened becomes a permeable membrane. The cellulose sheets were then carefully placed separately onto the 1500 kPa pressure plates. Samples were done in duplicates with the first set starting near the air inlet then progressing clockwise around then inwards the plate centre. The second duplicate set was repeated but on another plate. To both plates a control sample of known gravimetric content at 1500 kPa was added. Record what sample is added first to each plate near the air inlet. This is important as it will help you identify which sample is which when you come to extract the samples for weighing and drying. Samples were added using a teaspoon which was cleaned between each sample. With all samples in place, using distilled water all samples were carefully saturated then left for 30 minutes to absorb the distilled water (Figure 5.6). Remaining soil samples were resealed and refrigerated.

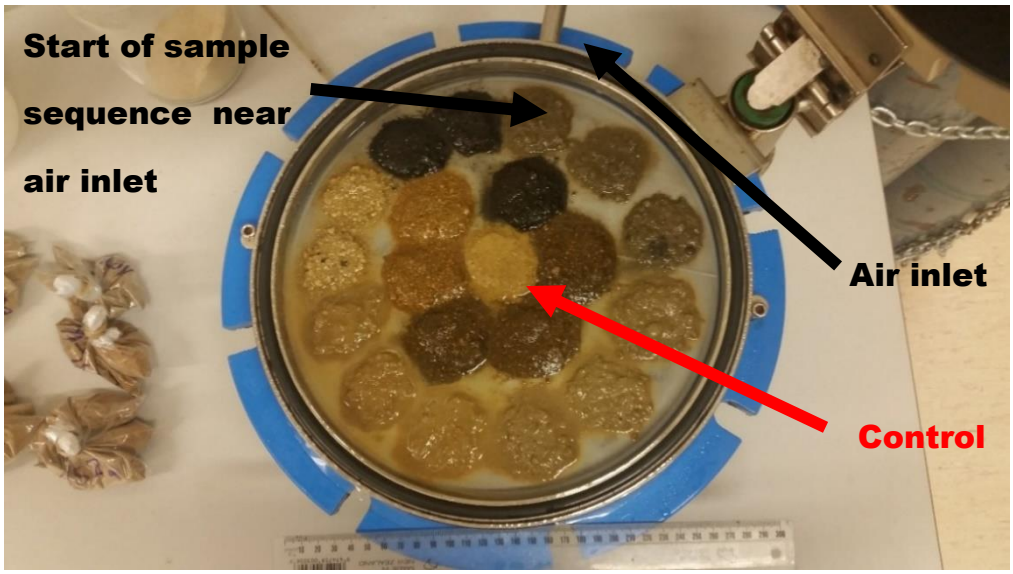

Figure 5:6: Pressure plate with saturated soil samples ready to be pressurised at 1500 kPa.

With all samples saturated the pressure extractor cover could be closed. The eight bolts were each tightened diagonally opposite each other initially to finger strength then tighter using a torque wrench to apply 20 Foot Pounds of pressure. Tightening the bolts using a cross over pattern (like tightening bolts on a car tire) ensures the cover is tightened evenly and will not be twisted or bent.

Because applying 1500 kPa pressure requires the use of compressed air extra care is advised for steps 1 – 9:

(1) Close the main outlet valve; (2) open the manometer valve; (3) the main regulator on the gas cylinder was opened; (4) slowly open the gas cylinder tap; (5) gradually turn the pressure regulator control on the gas cylinder clockwise until the main pressure gauge just registers a positive reading then immediately open the burette tap; (6) gradually increase the pressure inside the pressure extractor by turning the control regulator on the gas cylinder clockwise until the extractor manifold reads 14.0 Bar; (7) allow 30 minutes for the system time to settle with the burettes regularly drained of any water; (8) close the manometer isolation valve; (9) in small increments increase the pressure in the pressure extractor by turning the gas cylinder's pressure regulator clockwise until the manifold gauge reads exactly 15.0 Bar.

The samples were left to drain to equilibrium which is reached when the water level in the burette remained constant for minimum 24 hrs. Equilibrium was

reached within 48 hrs. During that time, the pressure gauge was checked thrice daily to read exactly 15 Bar or 1500 kPa. Upon reaching equilibrium the pressure was released by turning the gas cylinder's pressure regulator anti-clockwise until fully open. Next the air cylinder tap was closed then the manometer isolation valve opened. Slowly the main outlet valve was opened. When the main pressure gauge dropped to 9 Bar, the burette tap was closed to prevent water being drawn back into the samples. Next the cover bolts were removed with the extractor cover carefully raised making sure the soil did not adhere to the cover's underside.

Beginning with the sample nearest the air inlet i.e. the sample which was first added to the extractor plate of pre-recorded identity, a spatula was used to carefully remove a portion of each sample and placed in a labelled dish (Figure 5.7). This was repeated for each sample working in a clock wise direction towards the control in the centre. Each of the soil samples plus dishes was weighed accurate to three decimal places and recorded with "Mass of Dish + Wet Soil at 1500 KPa". Next the "wet soil" and dishes and dish lids were placed in an oven at 110°C with the dish lids left off, and dried overnight. The following morning the dishes were removed from the oven, dish lids replaced then when cool enough weighed to three decimal places and recorded with "Mass of Dish + Dry Soil at 1500 KPa".

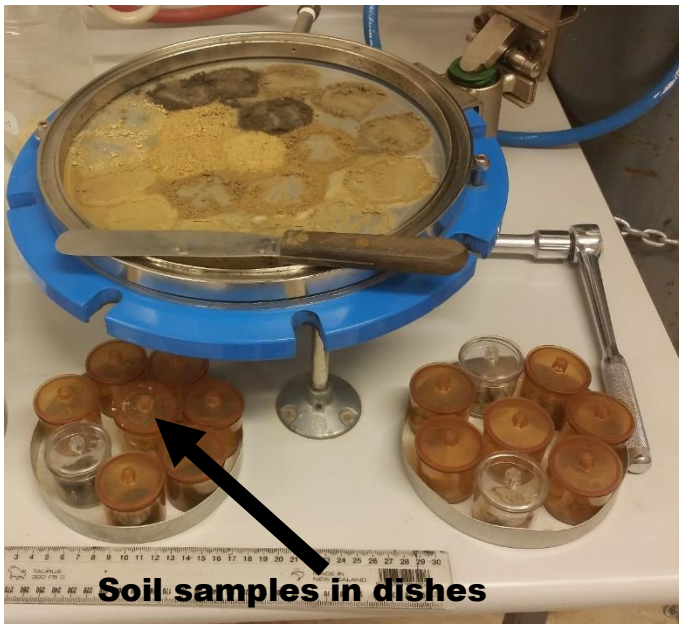

Figure 5:7: Soil samples at equilibrium from 1500 kPa in "wet soil" state ready to be weighed.

Gravimetric water content at 1500 kPa was calculated in Equation 5.2:

$$WC_{1500} = \left(\frac{(W1500-D1500)}{(D1500-T1500)}\right) X \left(\frac{(100)}{1}\right) \quad (5.2)$$

Where WC_{1500} = gravimetric water content at 1500kPa, W_{1500} = Mass of Dish + Wet soil, D_{1500} = Mass of Dish + Dry soil, T_{1500} = Mass of Dish. Dry soil mass was determined in Equation 5.5.

5.2.3.6 Determination of Soil Dry Bulk density (P_b)

Dry soil bulk density is the ratio of oven dried (105°C) soil mass to that soils volume, expressed in Equation 5.3 (McLaren & Cameron, 1996):

$$\text{Bulk density } (\rho b, g/cm^{-3}) = \frac{\text{Mass oven dried soil (g)}}{\text{Volume of soil (cm}-3)} \quad (5.3)$$

Samples for soil dry bulk density were collected by inserting metal rings (of known volume) into each horizon then using a sharp knife the rings and extra soil surrounding the ring were carefully extruded from the horizon. Each soil core in its brass ring was secured with plastic caps and duct tape then placed in a bag, labelled then stored at 4°C until ready for laboratory analysis.

Laboratory determination of dry soil bulk density was then carried out as per methods in Claydon (1997) as follows:

(1) Each soil sample had its duct tape and plastic caps removed then any excess soil carved off with a sharp craft knife blade.
(2) Each soil core and ring were weighed to three decimal places.
(3) Soil cores were extruded into an aluminium dish and weighed again to three decimal places recorded with "Mass of Dish + Wet Soil". This was repeated for each sample.
(4) Each soil sample and its water content dish placed in an oven at 105 - 110°C with lids open and left to dry overnight.
(5) The following morning lids, dishes and dried soil samples were removed then left to cool. Dishes and soil samples were then weighed to 3 decimal places and recorded as "Mass of Dish + Dry Soil".

Gravimetric water content at sampling is calculated in Equation 5.4:

$$WC_{sampling} = \left(\frac{(W-D)}{(D-T)}\right) X \left(\frac{(100)}{1}\right) \quad (5.4)$$

Where $WC_{sampling}$ = gravimetric water content at sampling, W = Mass of Dish + Wet Soil (g), D = Mass of Dish + Dry Soil (g), T = Mass of Dish (g).

Mass of dry soil was calculated in Equation 5.5:

$$\text{Dry soil} = \left(\frac{(\text{Wsampling}-\text{R})}{\left(1+\left(\frac{Wcsampling}{100}\right)\right)}\right) \quad (5.5)$$

Where DS = Mass dry soil (g), R = mass of ring, $W_{sampling}$ = Mass of Ring + soil at sampling.

Finally, dry bulk density was calculated in Equation 5.6:

$$\text{DBD} = \frac{\text{DS (g)}}{\text{Ring volume (cm}-3)} \quad (5.6)$$

Where DBD = dry bulk density, DS = dry soil mass. Brass core rings used in this study each had a volume of 68.6cm^{-3}.

5.2.3.7 Determination of volumetric water content (Θv)

Volumetric water content (Θv) for the 5 kPa, 10 kPa, 100 kPa and 1500 kPa tensions could be calculated as the ratio of volume of water to the total volume of soil.

With each sample's gravimetric water content calculated in section 5.2.3.1 and dry bulk density calculated in section 5.2.3.2 meant volumetric water content could be calculated as per Equation 5.7 (Claydon, 1995):

$$\text{Volumetric water content (Θv)} = \text{gravimetric water content (Θm) X dry bulk density } (P_b) \quad (5.7)$$

5.2.3.8 Determination of Particle density

Density is simply the ratio of mass to volume. Particle density is the ratio of the mass of dry solids to the volume occupied by those solids (Claydon, 1997). In this section mass of solids was determined by weighing. Volume was calculated from the mass (also density) of water displaced by the soil particles when placed in a density bottle of known volume. Laboratory determined particle density was determined as follows:

(1) Distilled water was de-aired and density bottles calibrated as per Claydon (1997).

(2) 10 – 15g of oven dried (105°C overnight) ground (by mortar & pestle) soil samples were placed into a clean dry 50ml density bottle then weighed to 3 decimal places. This was recorded with "Mass of Bottle + Soil".

(3) Distilled water was added to saturate the sample but not fill the bottle. The bottles and soil samples were then placed in a vacuum desiccator with the vacuum gradually increased. Extra caution advised as too much vacuum applied too early will cause the samples to bubble. Vigorous bubbling can lead to loss of samples. This can be avoided by regularly decreasing and increasing the vacuum in the desiccator.

(4) Gentle shaking of samples over the next 2 – 3 hours facilitated the de-airing of samples over which time small increments of distilled water were added, until each bottle was full to its marker at the base of its neck.

(5) When samples ceased to bubble, and having been under vacuum for an hour meant the samples were ready to be moved to a circulating water bath at 25°C and left to equilibrate for 30 minutes.

(6) Then each bottle had its matching stopper inserted, was dried thoroughly and weighed to 3 decimal places with the mass recorded with "Mass of Bottle + Water + Soil".

Particle density is calculated in Equation 5.8 (Claydon, 1997):

$$\text{Pd (t/m}^3\text{)} = \left(\frac{(0.99707 \text{ X } (\text{BS}-\text{B})}{(BW-(BWS-(\text{BS}-\text{B})))}\right) \quad (5.8)$$

Where Pd = particle density, BS = Mass of Bottle + Soil; B = Mass of Bottle; BW = Mass of Bottle + Water; BWS = Mass of Bottle + Water + Soil; 0.99707 = Density of water at 25°C.

5.2.3.9 Determination of Total Porosity, Macro porosity, Total Available Water Content, Readily Available Water Content, Field Capacity, Permanent Wilting Point

Following the calculation of dry bulk density, particle density and volumetric water content at the various tensions for each soil horizon meant the following could be calculated next:

Total porosity (%) = $$\left(1 - \left(\frac{\mathrm{BD}}{PD}\right)\right) X\ 100 \quad (5.9)$$

Where BD = Bulk Density; PD = Particle Density.

Macro porosity (%) = Total porosity – (Volumetric Water Content at 5kPa) (5.10)

TAWC (%) = $VWC_{10} - VWC_{1500}$ (5.11)

Where TAWC = Total Available Water Capacity; VWC_{10} = Volumetric Water Content at 10kPa; VWC_{1500} = Volumetric Water Content at 1500kPa.

RAWC (%) = $VWC_{10} - VWC_{100}$ (5.12)

Where RAWC = Readily Available Water Capacity (RAWC, %) = $VWC_{10} - VWC_{100}$
Where VWC_{10} = Volumetric Water Content at 10kPa; VWC_{100} = Volumetric Water Content at 100kPa.

FC VWC_{10} (5.13)

Where FC = Field capacity; VWC_{10} = Volumetric Water Content at 10 kPa.

PWP = VWC_{1500} (5.14)

Where PWP = Permanent Wilting Point; VWC_{1500} = Volumetric Metric Water at 1500 kPa.

5.2.4 Modelling of Crop Irrigation

Each site's soil laboratory determined TAWC, daily rainfall and Penman evapotranspiration estimates were fed into the Woodward *et al.,* (2001) model in an excel spreadsheet to calculate the soil water deficit (SWD) for pasture on relatively flat land. Other parameters used in the Woodward *et al.,* (2001) model include $TAWHC_s$, $TAWHC_{76}$, a scaling factor (β), AWHC, a water coefficient (α), an efficiency factor and a leaf area index – discussed in section 3.3.4. For use in this study changes made to the Woodward *et al.,* (2001) model include "Total Available Water Capacity" to Potential Rooting Depth (TAWC PRD) replacing "Available Water Holding Capacity (AWHC)", "Total Available Water Capacity" of topsoil

($TAWC_s$) replacing $AWHC_s$. These changes are discussed as follows. The soil AWHC data Woodward *et al.,* (2001) used were calculated using Equation 5.11 but used volumetric water content at 20 kPa instead of 10 kPa to calculate AWHC. As this study used 10 kPa to calculate AWHC or TAWC means a true comparison between the methods is not possible. From all the soil data used in the Woodward *et al.,* (2001) model none originated from the East Coast meaning such soils and their characteristics were not represented in the Woodward *et al.,* (2001) characterisation of their β factor. Woodward *et al.,* (2001) did not give a β factor for Recent soils meaning two soils in this study were incompatible with Woodward *et al.,* (2001) methods. These facts justify the means of rejecting Woodward *et al.,* (2001) use of their β factor to estimate soil profile AWHC. Instead the laboratory determined AWHC for each horizon for each soil are summed to provide an estimate of the profile AWHC to its potential rooting depth. For their "recharge zone" Woodward *et al.,* (2001) used a standard rate of 25mm. This is because for the original soil data, reliable estimates were not available. For this study because laboratory derived AWHC of each sites topsoil ($TAWC_s$) are available, these are used instead. Scotter & Horne (2016) noted that laboratory derived AWHC values used in a soil water balance model are adequate.

Additions to the Woodward et al., (2001) model include K_c and ET_c columns to calculate ET_c, addition of an "irrigation trigger" column and addition of a "rain plus irrigation" column. The working of this studies modified Woodward *et al.,* (2001) soil water balance model is summarised in Equations 5.15 – 5.22:

Each crop's growth season and K_c is subdivided into four stages being $K_{c\ ini}$ (season start), $K_{c\ dev}$ (crop development), $K_{c\ mid}$ (crop mid-season stage) and $K_{c\ end}$ (crop harvest date, Figure 5.8). $K_{c\ ini}$ and $K_{c\ mid}$ values are constant being equal to their crop growth stage being considered. However, during development stage and end season stage K_c varies linearly between K_c at the end of the previous stage and K_c at the beginning of the next stage. K_c for $K_{c\ dev}$ and $K_{c\ end}$ is calculated using Equation 5.15:

$$K_{c\ i} = K_{c\ prev} \left[\frac{i - \Sigma\ (Lprev)}{Lstage}\right] (K_{c\ next} - K_{c\ prev}) \qquad (5.15)$$

Where i is the day number within the growing season, $K_{c\ i}$ is the crop coefficient on day i, L_{stage} is the stage under consideration, $\mathbf{\Sigma}(L_{prev})$ is the sum of the lengths of all previous stages (days), $K_{c\ next}$ is the crop coefficient of the next stage, $K_{c\ prev}$ is

the crop coefficient of the previous stage. Alternatively, to Equation 5.15 because K_c increases linearly between $K_{c\ ini}$ and $K_{c\ mid}$ and decreases linearly between $K_{c\ mid}$ and $K_{c\ end}$, K_c in these stages can be plotted in excel using y = mx + c, where y = K_c, m = gradient, x = day of season and c = y intercept. An example crop coefficient curve is shown in Figure 5.8.

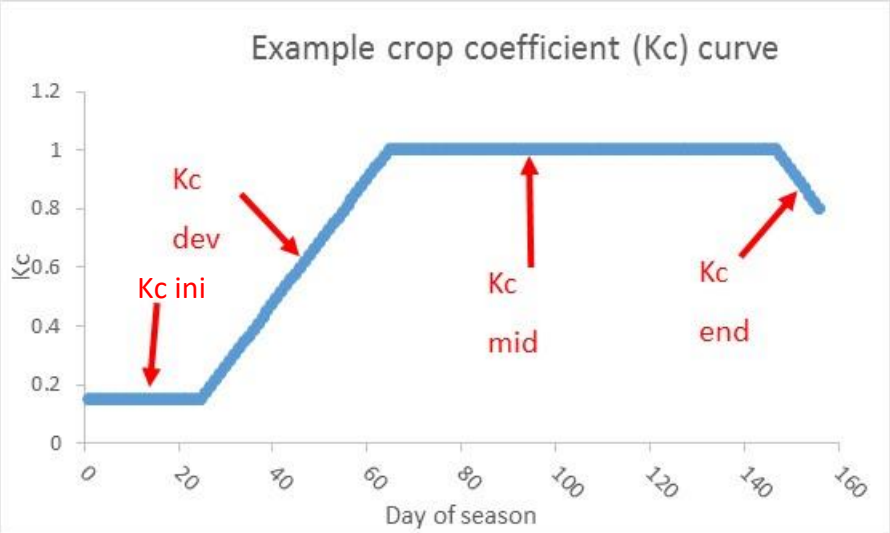

Figure 5:8: Crop coefficient curve for hypothetical crop with differing season growth stages.

With each K_c value determined for each day of the growth season allowed calculation of ET_c as per Equation 5.16.

$$ET_c = K_c * ET_o \quad (5.16)$$

Where ET_c = crop evapotranspiration (mm d^{-1}), K_c = crop coefficient (dimensionless), ET_o = reference crop evapotranspiration (mm d^{-1}). For this study reference crop evapotranspiration values used were Penman evapotranspiration estimates downloaded per site using NIWA's virtual climate station network.

Horne & Scotter (2016) modified the Woodward *et al.,* (2001) model. The changes made by Horne & Scotter (2016) with further additions are described in equations 5.17 – 5.24.

Equation 5.17 estimates the soil water deficit (SWD) for the soil profile at the end of day t:

$$SWD_{(t)} = MIN\ [0, SWD_{(t-1)} + P_{(t-1)} - AET_{(t-1)}] \quad (5.17)$$

Where MIN = function which sets $SWD_{(t)}$ to the lesser of the two values separated by the comma within the square brackets; $SWD_{(t-1)}$ is the soil water deficit from the day preceding day t, $P_{(t-1)}$ = rainfall plus irrigation (mm) preceding day t; $AET_{(t-1)}$ = actual evapotranspiration (mm) preceding day t. $SWD_{(t)}$ is always negative or zero.

Equation 5.18 estimates the soil water deficit for the top soil ($SWD_{s\,(t)}$) at the end of day t:

$$SWD_{s\,(t)} = MIN\,[0, SWD_{s\,(t-1)} + P_{(t)} - E_{s\,(t)}] \quad (5.18)$$

Where MIN = function which sets $SWD_{s\,(t)}$ to the lesser of the two values separated by the comma within the square brackets; $SWD_{s\,(t-1)}$ = the topsoil soil water deficit from the day preceding day t; $P_{(t)}$ = rainfall plus irrigation on day t; $E_{s\,(t)}$ = water extracted from the topsoil on day t.

$E_{s\,(t)}$ is calculated in equation 5.19:

$$E_{s\,(t)}) = MIN\,[ET_c, SWD_{s\,(tot)} + P_{(t)} + SWD_{s\,(t-1)}] \quad (5.19)$$

Where MIN is a function setting $Es_{\,(t)}$ to the lesser of the two values between the square brackets; $SWD_{s\,(tot)}$ = the available water holding capacity in the topsoil (mm).

Ex is calculated in Equation 5.20 to describe the maximum amount of water available from the soil profile for evapotranspiration:

$$Ex_{\,(t)} = MAX\,[E_{s\,(t)}, ET_c\,(TAWC + SWD_{(t-1)}) / (TAWC\text{-}RAW)] \quad (5.20)$$

Where MAX is a function setting $Ex_{\,(t)}$ to the greater of the two values between the square brackets; TAWC is the total available water holding capacity (mm) of the soil profile to potential rooting depth; RAW is the readily available water (mm) of the soil profile to potential rooting depth.

Once Equations 5.19 and 5.20 have been completed actual evapotranspiration on day t can be estimated using Equation 5.21:

$$AET_{(t)} = MIN\,[ET_{c,}, E_x] \quad (5.21)$$

Where MIN = function which sets $AET_{(t)}$ to the lesser of the two values separated by the comma within the square brackets.

Allen *et al.,* (1998) report that apples, cherries, pears, apricots, peaches, stone fruit and hops can extract 50% of Total Available Water (TAW) in the root zone (mm) before becoming stressed. Where TAW = (field capacity – permanent wilting point) * rooting depth. Rajanayayaka *et al.,* (2016) and McIndoe *et al.,* (2017) both used 50% TAW as a trigger point to initiate irrigation in a soil water balance model for a range of crops including horticultural crops. The maximum amount of irrigation modelled by McIndoe *et al.,* (2017) was 40% of TAW, that is when TAW dropped to 50%, 40% of TAW was added as irrigation. The 50% TAW trigger approach by McIndoe *et al.,* (2017) with 20% TAW modelled irrigation is adopted for use in this study with the remaining 30% left to account for any rainfall, minimise wastage and optimise efficiency.

The irrigation trigger with 20% TAW is given in Equation 5.22:

$$I_{(t)} = IF(SWD_{(t)} < (-TAWC/2), (-TAWC*0.2)) \quad (5.22)$$

The sum of all irrigation additions within each crop growing season, per year between 1 September 1998 and 31 May 2018 was done to calculate minimum, maximum and mean seasonal irrigation requirements per crop per soil type.

A rain + irrigation column (P) was added to the spreadsheet which calculated the sum of rainfall and irrigation given in Equation 5.23.

$$\text{Rainfall \& irrigation (P, mm)} = \text{rainfall (mm)} + \text{irrigation (mm)} \quad (5.23)$$

Lastly drainage is calculated in Equation 5.24:

$$\text{Drainage (mm)} = MAX\ [0, SWD_{(t-1)} + P_{(t)}) - AET_{(t)}] \quad (5.24)$$

Where $SWD_{(t)}$ is the soil water deficit on day t, $P_{(t)}$ is rainfall plus irrigation (mm) on day t, -efficiency is the negative efficiency factor (value -1), $AET_{(t)}$ is the actual evapotranspiration on day t. No matter how much rainfall occurs each day the model assumes excess water drains away before the start of the next day. Further the model assumes that all rainfall infiltrates the soil profile where it fell, that within a meter of the root zone there is no water table and the site being modelled is flat (Horne & Scotter, 2016).

The order in which the equations need to be completed are: 5.16, 5.19, 5.20, 5.21, 5.17, 5.18, 5.22, 5.23 and 5.24.

To calculate each horizon's total available water holding capacity Equation 5.25 was used then each horizons TAWC summed to provide a profile TAWC to its potential rooting depth.

Horizon TAWC (mm) = (Volumetric water at 10kPa (%) – volumetric water at 1500 kPa (%) / 100) * horizon thickness (mm) (5.25)

At the time of sampling in July 2017 for two soils (Tuai sand and Awamate silt loam, Tables 5.3, 5.4) a high-water table was present preventing the sampling of all horizons to 1 metre depth. To complete each soils AWHC estimate to 1 metre, horizon AWHC values from McLeod *et al.,* (1999) are used. Recognising that soil water storage values for the Gisborne-East Coast soils were scarce McLeod *et al.,* (1999) sampled 45 key soil profile layers for available water capacity, bulk density and % gravel. Available water capacity was calculated as per Equation 5.11 meaning values are comparable with this study. Because Wairoa District shares a similar physiography and parent material (rock type, tephra cover) to Gisborne-East Coast areas means the values published by McLeod *et al.,* (1999) are acceptable for use in this study. Table 5.17 shows the added values used from McCleod *et al.,* (1999) to complete the soil profile AWHC to 1 metre for Tuai sand and Awamate silt loam.

When choosing a start date for the soil water balance model Horne & Scotter (2016) give three options: (1) late winter or early spring or a few days after significant rainfall given as start date assuming the soil profile to be fully charged i.e. SWD = 0; (2) late summer or early autumn nominated as start date assuming all water available has been extracted i.e. SWD = -SWDtotal and SWDtopsoil = -SWDtopsoil.total; (3) start date nominated as date one year before period of interest assuming initial values do not matter. The start date used in this study is September 01, 1997. This date was chosen assuming the prior winter rainfall fully recharged the soil water content giving a soil water deficit of zero. The following summer of 1997-1998 saw extremely low rainfall. Including this period allows modelling irrigation requirements in a drought scenario.

5.3 Results

5.3.1 Soil profile descriptions

In the week prior to field work being undertaken in July 2017, 37 mm of rainfall fell at the Wairoa Airport Climate Station near the site for the Awamate silt loam site. The rainfall, along with low temperatures and low evaporation rates may have contributed to the high-water tables observed at all the sites.

The Tuai sand in Table 5.1 although classified as a Typic Impeded Allophanic (LIT) soil is similar to Typic Orthic Pumice (MOT) soils which constitutes 29% (70 km^2) of the soils in Land Use Capability (LUC) classes 1 – 3 found in the Wairoa District (Table 2.3). Tuai sand is thereby a soil which fairly represents a major portion of the versatile soils within the Wairoa District.

Awamate silt loam in (Table 5.2) this study is classified as a Mottled Orthic Recent soil (ROM) however the site is mapped as a similar but not distinct Mottled Fluvial Recent (RFM) (Pullar & Ayson, 1965) soil which comprises 68km^2 or 28% of LUC 1-3 (Table 2.3) in the Wairoa District. This means the Awamate silt loam is representative of one of the versatile soil types in Wairoa District.

The Waihirere silt loam (Table 5.3) in this study is classified as a Weathered Fluvial Recent (RFW) soil but is mapped as a similar Typic Fluvial Recent (RFT) (Pullar & Ayson, 1965). With Typic Fluvial Recent soils accounting for 35km^2 or 15% of LUC 1-3 (Table 2.3) in the Wairoa District this means the Waihirere silt loam is also representative of one of the versatile soils in the Wairoa District.

Mohaka sandy loam (Table 5.4) is classified as a Typic Perch-gley Allophanic (LPT) and is similar to Typic Orthic Pumice (MOT) soils making up 29% (70km^2) of the soils in LUC classes 1 – 3 found in the Wairoa District (Table 2.3). As such the Mohaka sandy loam is a soil which is representative of one of the more versatile soils in the Wairoa District.

Table 5:3: Soil profile description for Tuai sand on Waiau River terrace.

Soil name	Series: Tuai Type: Tuai sand (Rijkse, 1980)
NZ Soil Classification:	Typic Impeded Allophanic (LIT)
Location:	2311 Lake Rd, Frasertown, Wairoa 4195. 40m west of Ardkeen District Hall, 13m south of fence line running W-E, 15mW of fence line running N-S.
Latitude	-38.93002
Longitude	177.27409
Mean annual rainfall:	1400mm
Mean annual daily air temp:	13°C
Geomorphic Position:	Gentle slope of 3 - 5°C inclining southwards on Waiau River Terrace
Elevation:	75 m a.m.s.l; 30m above and 250m SE from Waiau River.
Erosion:	When vegetated = nil, when ploughed potential for sheet & rill erosion
Vegetation:	Pasture grass
Parent Material:	Holocene and late Pleistocene rhyolitic volcanic ashes
Drainage:	Imperfect to moderately well drained, class 3-4.
Land use:	Sheep & beef

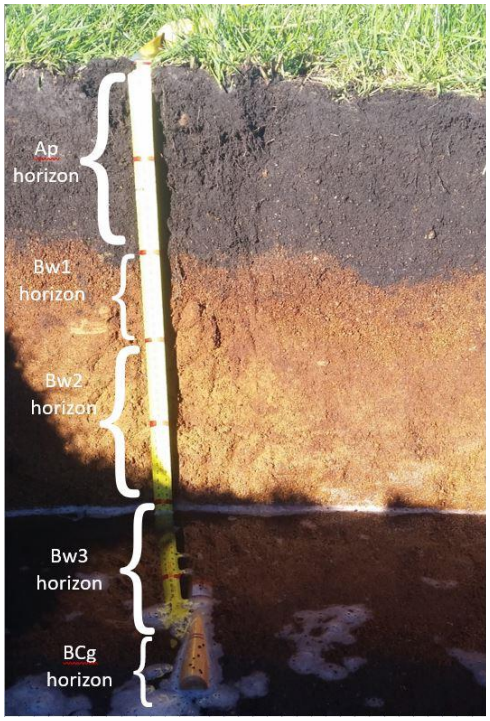

Horizon:	Depth (cm)	Description:
Ap	0-20	Black (7.5YR 2/1) sandy loam; friable; slightly sticky; blocky breaking to apedal earthy; many microfine roots; sharp wavy boundary. Taupo Pumice (Rijkse, 1980).
Bw1	20-30	Reddish yellow (7.5YR 6/8)) sand; very friable; non- sticky; non-plastic; apedal single grain; strongly allophanic; common microfine ubiquitous roots; distinct wavy boundary. Taupo Lapilli (Rijkse, 1980).
Bw2	30-50	Yellowish brown (10YR 5/8) sandy loam; brittle; non-sticky; non-plastic; strongly allophanic; few microfine ubiquitous roots; diffuse boundary; apedal earthy Waimihia Lapilli (Rijkse, 1980).
Bw3	50-70	Yellow (10YR 7/6) coarse sand; non-sticky; non-plastic; peds weak and very friable; strongly allophanic; no roots seen; distinct boundary; apedal single grain Waimihia Lapilli (Rijkse, 1980).
BCg	70-90	Pale brown (2.5Y 7/3) sandy loam, non- sticky; non-plastic; moderate pedality; weakly allophanic; no roots seen; smooth boundary.
2Cg	90-100	Light grey (2.5Y 7/2) clay loam; moderately sticky; moderately plastic; extremely fine polyhedral peds; allophanic; no roots; diffuse boundary.

Table 5:4: Soil profile description for Awamate silt loam on Wairoa River floodplain.

Soil name:		Series: Awamate Type: Awamate silt loam (Pullar & Ayson, 1965)
NZ Soil Classification:		Mottled Orthic Recent (ROM)
Location:		Wairoa Airport, Airport Rd, Wairoa. 25m NW of Airport Climate Station, 2m south of paddock fence line.
Latitude		-39.01638
Longitude		177.40336
Mean annual rainfall:		1400mm
Mean annual daily air temp:		13°C
Geomorphic Position:		Surrounding area flat to undulating on Wairoa River flood plain
Elevation:		35 m a.m.s.l; 15m above and 450m NE from Wairoa River.
Erosion:		When vegetated = nil, when ploughed potential for sheet & rill erosion
Vegetation:		Ryegrass pasture grass
Parent Material:		Alluvium derived from sedimentary rocks
Drainage:		Imperfectly drained, class 3.
Land use:		Airport, maize
Horizon:	Depth (cm)	Description:
Ap	0-15	Brownish black (10YR 2/3) silt loam; brittle; weak moderately sticky; very plastic; fine to coarse polyhedral breaking to apedal earthy; many microfine roots; abrupt boundary; many worms in top 5cm.
A/Bp	15-30	Brown (4YR 3/3) sandy clay loam; weak brittle; moderately sticky; very plastic; blocky breaking to apedal earthy; negatively allophanic; common microfine ubiquitous roots; indistinct wavy boundary.
B/Ag	30-40	Greyish brown (10YR 5/2) sandy clay loam; brittle; very sticky; very plastic; apedal earthy; negatively allophanic; microfine ubiquitous roots common; indistinct boundary.
Bg	40-70	Light brownish grey (10YR 6/2) sandy clay loam; very sticky; very plastic; slightly firm polyhedral peds; negatively allophanic; common microfine ubiquitous roots; indistinct boundary.
Br	70-100	Light grey (7.5YR 7/1) clay loam, very sticky; very plastic; apedal massive; weakly allophanic; no roots seen.

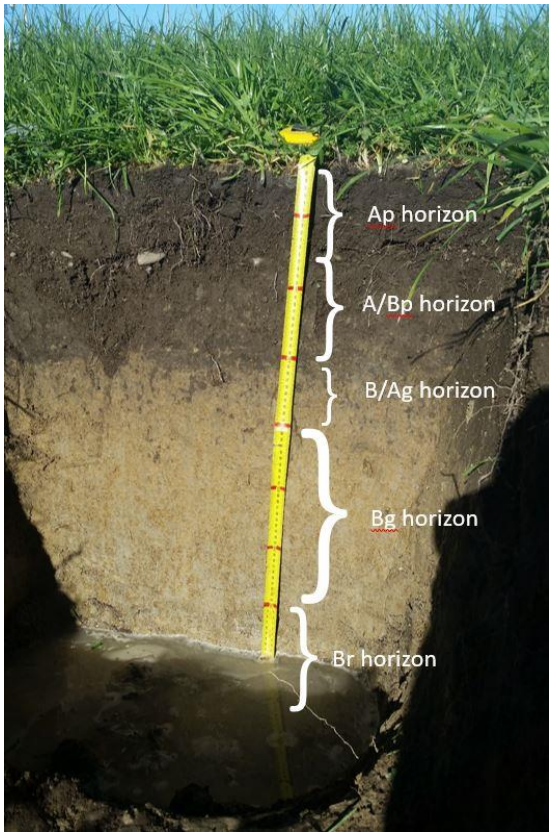

Table 5:5: Soil profile description for Waihirere silt loam on Wairoa River terrace.

Soil name:	Series*:* Waihirere Type: Waihirere silt loam
NZ Soil Classification*:*	Weathered Fluvial Recent (RFW)
Location:	Roscommon Farm, Aranui Rd, Wairoa. 75m SW from SW end of main house, 27m SE from fence line running SW-NE.
Latitude	-38.98006
Longitude	177.40677
Mean annual rainfall:	1400mm
Mean annual daily air temp:	14°C
Geomorphic Position:	Surrounding area flat to undulating, Wairoa River terrace.
Elevation:	20 m a.m.s.l; 8m above and 600m west of Wairoa River.
Erosion:	When vegetated = nil, when ploughed potential for sheet & rill erosion
Vegetation:	Ryegrass pasture
Parent Material:	Alluvium derived from sedimentary rocks and Holocene and late Pleistocene rhyolitic volcanic ashes.
Drainage:	Well drained, class 1.
Land use:	Sheep & beef.

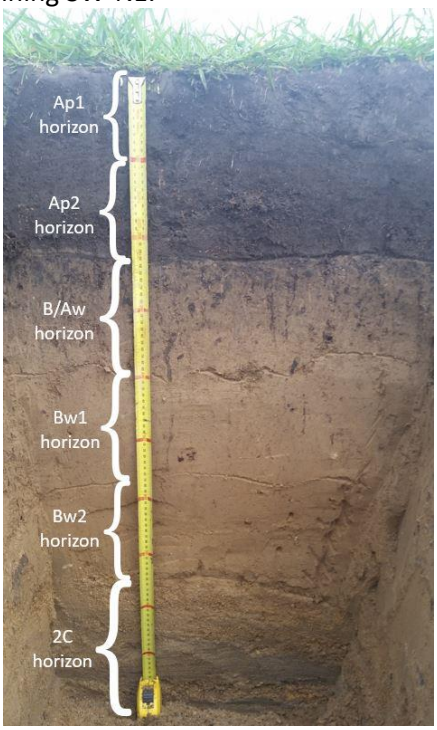

Horizon:	Depth (cm)	Description:
Ap1	0-10	Brownish black (10YR 2/2) silt loam; dense and compacted; slightly firm; moderately sticky very plastic; medium to extremely coarse blocky structure, strongly developed; negatively allophanic; many ultra-fine ubiquitous roots' smooth boundary. Compacted by stock and machinery.
Ap2	10-23	Brown (10YR 4/3) silt loam; brittle; moderately sticky; very plastic; very fine to coarse polyhedral breaking to apedal earthy; negatively allophanic; many microfine ubiquitous roots, distinct smooth boundary.
B/Aw	23-40	Yellowish brown (10YR 4/3) silt loam; brittle; moderately sticky; very plastic; medium to very coarse blocky peds; negatively allophanic; common microfine ubiquitous roots; indistinct wavy boundary.
Bw1	40–56	Yellowish brown (10YR 5/2) sandy clay loam; brittle; very sticky; very plastic; apedal earthy; negatively allophanic; microfine ubiquitous roots common; diffuse smooth boundary.
Bw2	56-75	Bright yellowish brown (10YR 6/2) silt loam; medium sticky; very plastic; slightly firm, brittle; medium to coarse polyhedral peds breaking to apedal earthy; negatively allophanic; common microfine ubiquitous roots; abrupt smooth boundary.
2C	75 - >110	Pale brown (10YR 6/3) sand; non-sticky; non- plastic; apedal massive single grain; positive allophanic; no roots seen.

Table 5:6: Soil profile description: Mohaka sandy loam on Mohaka River terrace.

Soil name:	Series*:* Mohaka Type: Mohaka sandy loam
NZ Soil Classification:	Vitric-acidic Orthic Allophanic (LOV)
Location:	Landblock behind 36 Mohaka Twp Rd, Wairoa 4189. 160m SE from water tank, 200m SW from Mohaka Twp Rd.
Latitude, Longitude	-39.08779, 177.16997
Mean annual rainfall:	1400mm
Mean annual daily air temp:	13°C
Geomorphic Position:	Surrounding area flat to undulating, Mohaka River terrace.
Elevation:	95 m a.m.s.l; 82m above and 530m east from Mohaka River.
Erosion:	When vegetated = nil, when ploughed potential for sheet & rill erosion
Vegetation:	Ryegrass pasture grass
Parent Material:	Holocene and late Pleistocene rhyolitic volcanic ashes.
Drainage:	Well drained, class 1.
Land use:	Beef, maize, neighbouring land block planted in apple tree lings for pulp.

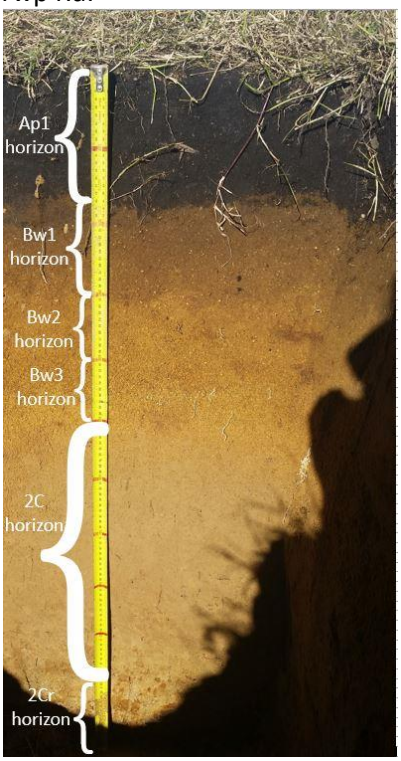

Horizon:	Depth (cm)	Description:
Ap1	0-20	Black (7.5YR 2.5/1) sandy loam; brittle; slightly sticky non-plastic; very fine to coarse polyhedral peds breaking to apedal earthy. Ubiquitous very fine fibrous and fleshy roots. Abrupt occluded boundary. Positive allophane test. Taupo Pumice (Rijkse, 1980).
Bw1	20-30	Dark yellowish brown (10YR 4/4) sandy loam; brittle, non-sticky, non-plastic, apedal single grain. Few ubiquitous very fine to large fibrous and fleshy roots. Abrupt wavy boundary. Taupo Lapilli (Rijkse, 1980).
Bw2	30-40	Yellowish brown (10YR 5/8) loamy sand; friable, non-sticky, non-plastic apedal earthy. Few ubiquitous very fine and fleshy roots. Distinct wavy boundary. Positive allophane test. Waimihia Lapilli (Rijkse, 1980).
Bw3	40-50	Yellowish brown (10YR 5/6) coarse sand. Friable non-sticky, non-plastic, apedal single grain. Few ubiquitous very fine to large fibrous and fleshy roots. Abrupt wavy boundary. Positive allophane test. Waimihia Lapilli (Rijkse, 1980).
2C	50-100	Light yellowish brown (10YR 6/4) sand. Very friable, non-sticky, non-plastic, apedal massive. Few ubiquitous ultra-fine to large fibrous roots. Abrupt occluded boundary. Negative allophane test.
2Cr	100 - >110	Pale brown (2.5Y 7/4) sandy clay loam. Very friable non-sticky, non-plastic. No roots. 50% abundance of 6-10mm fine, distinct yellowish brown (10YR 5/6) ubiquitous mottles. Negative allophane test.

5.3.2 Soil permeability

Table 5.7 shows the Awamate silt loam Ap horizon to have the lowest permeability (class 3, moderately slow) and infiltration rate (5 – 19 mm/hr). The Tuai sand had the highest permeability estimates (class 5 - 6, moderately rapid to rapid) and infiltration rates (65 – 25 mm/hr). All other soil horizons within the Waihirere silt loam, Mohaka sandy loam and remaining Awamate silt loam exhibited moderate to moderately rapid permeability and infiltration rates of mostly 20 – 64 mm/hr.

Table 5:7: Results summary for penetration class and degree of packing for four representative soil types in Wairoa District

Soil type	Horizon, base (cm)	Texture class	Penetration Class	Degree of Packing	Permeability Class, Infiltration Rates (mm/hr)
Tuai sand	Ap, 20	Sandy loam	Very low	Medium	6 -5, 65 – 250
	Bw1, 30	Coarse sand	Extremely low	Low	6, 130 - 250
	Bw2, 50	Sandy loam	Very low	Medium	6 -5, 65 – 250
Awamate silt loam	Ap, 15	Silt loam	Very low	High	3, 5 – 19
	A/Bp, 20	Sandy clay loam	Very low	Medium	4, 20 – 64
	B/Ag, 40	Sandy clay loam	Very low	Medium	4, 20 – 64
	Bg, 70	Sandy clay loam	Very low	Medium	4, 20 – 64
Waihirere silt loam	Ap1, 12	Silt loam	Very low	Medium	4, 20 – 64
	Ap2, 23	Silt loam	Low	Medium	4, 20 – 64
	B/Aw, 40	Silt loam	Moderate	High	4, 20 – 64
	Bw1, 56	Silt loam	Moderate	High	4, 20 – 64
	Bw2, 75	Silt loam	Moderate	Medium	4, 20 – 64
	2C, >110	Sand gravelly	Very low	Medium	5 - 6, 65 – 250
Mohaka sandy loam	Ap, 18	Sandy loam	Very low	Medium	4, 20 – 64
	Bw1, 30	Sandy loam	Low	Medium	4, 20 – 64
	Bw2, 38	Loamy sand	Low	Medium	4, 20 – 64
	Bw3, 50	Coarse sand	Very low	Low	5, 65 - 129
	2C, 100	Sand	Extremely low	Low	5, 65 - 129

5.3.3 Soil auger descriptions

Table 5:8: Soil auger description: Waihirere sandy loam

Soil name:		Series: Waihirere Type: Waihirere sandy loam
NZ Soil Classification:		Typic Fluvial Recent (RFT)
Latitude, Longitude:		-39.08463, 177.15567
Mean annual rainfall (mm):		1460
Mean annual daily air temperature (°C):		14.1
Geomorphic position:		Flat to gently undulating Mohaka River terrace
Elevation (m a.s.l):		38 m a.s.l; 20 m above and 570 m SE from Mohaka River.
Erosion:		When vegetated = nil, when ploughed potential for sheet & rill erosion
Vegetation:		Pasture, apple tree lings
Parent Material:		Alluvium derived from sedimentary rocks and Holocene and late Pleistocene rhyolitic volcanic ashes.
Drainage:		Well drained, class 5.
Land use:		Apple orchard for pulp
Horizon:	Depth (cm)	Description:
Ap	30	Black (10YR 2/1) fine sandy loam. Friable, grass roots down to 35cm.
Bw1	75	Olive yellow (2.5Y 6/6) fine sandy loam.

Figure 5:9: Photo depicting landscape near Waihirere sandy loam soil auger site.

Table 5:9: Soil profile description: Waihirere sandy loam

Soil name:		Series: Waihirere Type: Waihirere sandy loam
NZ Soil Classification:		Typic Fluvial Recent (RFT)
Latitude, Longitude:		-38.992194, 177.392928
Mean annual rainfall (mm):		1460
Mean annual air temperature (°C):		14.1
Geomorphic position:		Surrounding area flat to undulating, Wairoa River levee/terrace. Side cut into soil bank where compost stored.
Elevation (m a.s.l):		15 m a.s.l; <15 m above and 830 m west from Wairoa River.
Erosion:		When vegetated = nil, when ploughed potential for sheet & rill erosion
Vegetation:		Pasture
Parent Material:		Alluvium derived from sedimentary rocks and Holocene and late Pleistocene rhyolitic volcanic ashes.
Drainage:		Well drained, class 5.
Land use:		Sheep & beef
Horizon:	Depth (cm)	Description:
Ap	15	Very dark grey (10YR 3/1) sandy loam; friable, polyhedral structure.
Bw	90	Brownish yellow (10YR 6/8) fine sandy loam. Massive structure.
C	90 - 100	Pale brown (2.5Y 7/4) loamy sand. Loose structure.

Figure 5:10: Photo depicting landscape near Waihirere sandy loam soil auger site.

Table 5:10: Soil auger description: Mahia fine sandy loam

Soil name:		Series: Mahia Type: Mahia fine sandy loam
NZ Soil Classification:		Typic Orthic Pumice (MOT)
Latitude, Longitude:		-39.11750, 177.96172
Mean annual rainfall (mm):		1260
Mean annual daily air temperature (°C):		13.7
Geomorphic position:		Flat to gently undulating marine terrace
Elevation (m a.s.l):		140 m a.s.l
Erosion:		When vegetated = nil, when ploughed potential for sheet & rill erosion
Vegetation:		Pasture
Parent Material:		Holocene and late Pleistocene rhyolitic volcanic ashes.
Drainage:		Well drained, class 5.
Land use:		Sheep & beef
Horizon:	Depth (cm)	Description:
Ap	20	Dark yellowish brown (10YR 4/4) fine sandy loam. Friable.
1Bw	45	Yellowish brown (10YR 5/8) sandy loam.
2Bw	80	Yellowish brown (10YR 5/6) sandy clay loam.
C	>80	Light olive brown (2.5Y 5/4) clay loam. Firm.

Figure 5:11 : Photo depicting landscape near Mahia fine sandy loam soil auger site.

Table 5:11: Soil auger description: Tuai sand

Soil name:	Series: Tuai Type: Tuai sand
NZ Soil Classification:	Typic Impeded Allophanic (LIT)
Latitude, Longitude:	-38.93002, 177.27409
Mean annual rainfall (mm):	1400
Mean annual air temperature (°C):	13°C
Geomorphic position:	Gentle slope of 3 - 5°C inclining southwards on Waiau River Terrace
Elevation (m a.s.l):	75 m a.s.l; 30m above and 250m SE from Waiau River.
Erosion:	When vegetated = nil, when ploughed potential for sheet & rill erosion
Vegetation:	Pasture grass
Parent Material:	Holocene and late Pleistocene rhyolitic volcanic ashes
Drainage:	Imperfect to moderately well drained, class 3 – 4.
Land use:	Sheep & beef

Horizon:	Depth (cm)	Description:
Ap	0-20	Black (7.5YR 2/1) sandy loam, Taupo Pumice (Rijkse, 1980.
Bw1	20-30	Reddish yellow (7.5YR 6/8) sand, Taupo Lapilli (Rijkse, 1980).
Bw2	30-50	Yellowish brown (10YR 5/8) sandy loam, upper Waimihia Lapilli unit (Rijkse, 1980).
Bw3	50-70	Yellow (10YR 7/6) coarse sand, Wamihia Lapilli, lower unit (Rijkse, 1980).
BCg	70-80	Pale brown (2.5Y 7/3) sandy loam.
2Cg	90-100	Light grey (2.5Y 7/2) clay loam.

Figure 5:12 : Photo depicting terraced landscape near Tuai sand auger site.

Table 5:12: Soil auger description: Tuai sandy loam

Soil name:		Series: Tuai Type: Tuai sandy loam
NZ Soil Classification:		Typic Impeded Pumice (MIT)
Latitude, Longitude:		-38.80364, 177.47988
Mean annual rainfall (mm):		1600
Mean annual daily air temperature (°C):		13.5
Geomorphic position:		Flat to gently undulating terrace near Ruakituri River
Elevation (m a.s.l):		80 m a.s.l; <10m above and 100m SE from Ruakituri River.
Erosion:		When vegetated = nil, when ploughed potential for sheet & rill erosion
Vegetation:		Pasture
Parent Material:		Alluvium derived from sedimentary rocks and Holocene and late Pleistocene rhyolitic volcanic ashes.
Drainage:		Poorly drained, class 2.
Land use:		Sheep & beef
Horizon:	Depth (cm)	Description:
Ap	5	Dark brown (7.5YR 3/3) sandy loam.
Bw1	15	Brown (7.5YR 4/4) loamy sand.
Bw2	65	Olive brown (2.5Y 4/3) sandy loam. Water table between 55 – 65cm. Sloppy sand falling out of auger.
C	>65	Pale yellow (5Y 8/3) clay.

Figure 5:13: Photo depicting landscape near Tuai sandy loam soil auger site.

Table 5:13: Soil auger description: Tiniroto sandy loam

Soil name:		Series: Tiniroto Type: Tiniroto sandy loam
NZ Soil Classification:		Typic Orthic Pumice (MOT)
Latitude, Longitude:		-39.06169, 177.13367
Mean annual rainfall (mm):		1540
Mean annual daily air temperature (°C):		13.4
Geomorphic position:		Flat to gently undulating Mohaka River terrace
Elevation (m a.s.l):		160 m a.s.l
Erosion:		When vegetated = nil, when ploughed potential for sheet & rill erosion
Vegetation:		Pasture
Parent Material:		Holocene and late Pleistocene rhyolitic volcanic ashes
Drainage:		Imperfectly drained, class 3.
Land use:		Sheep & beef
Horizon:	Depth (cm)	Description:
Ap	20	Black (10YR 2/1) loamy sand. Friable, weak structure.
Bw	35	Dark yellowish brown (10YR 4/6) loamy sand. Weak polyhedral structure, fine to medium single grain – Taupo Pumice.
2Bw1	45	Yellowish brown (10YR 5/6) sand. Loose, weak medium to fine sand – Taupo Lapilli.
2Bw2	55	Brownish yellow (10YR 6/8) sand. Coarse, loose spheroidal single grain – upper Waimihia Lapilli unit (Rijkse, 1980).
2C	85	Pale brown (2.5Y 8/4) coarse spheroidal sand - lower Waimihia Lapilli unit (Rijkse, 1980).
3C	>85	Light grey (2.5Y 7/2) sandy clay loam.

Figure 5:14: Photo depicting landscape near Tiniroto sandy loam soil auger site.

Table 5:14: Soil auger description: Mohaka sandy loam

Soil name:		Series: Mohaka Type: Mohaka sandy loam
NZ Soil Classification:		Typic Orthic Pumice (MOT)
Latitude, Longitude:		-39.11843, 177.19824
Mean annual rainfall (mm):		1440
Mean annual daily air temperature (°C):		13.9
Geomorphic position:		Flat to gently undulating Mohaka River terrace
Elevation (m a.s.l):		64 m a.s.l
Erosion:		When vegetated = nil, when ploughed potential for sheet & rill erosion
Vegetation:		Pasture
Parent Material:		Holocene and late Pleistocene rhyolitic volcanic ashes.
Drainage:		Moderately well drained, class 4.
Land use:		Sheep & beef, lifestyle blocks.
Horizon:	Depth (cm)	Description:
Ap	30	Very dark grey (10YR 3/1) sandy loam.
Bw1	50	Yellowish brown (10YR 5/8) loamy sand. Many fine to coarse grains - upper Waimihia Lapilli unit (Rijkse, 1980).
Bw2	65	Yellowish brown (10YR 5/6) sand. Medium, loose grains – lower Waimihia Lapilli unit (Rijkse, 1980).
C	65 - 75	Brownish yellowish (10YR 6/8) sandy clay.

Figure 5:15: Photo depicting landscape near Mohaka sandy loam soil auger site.

Table 5:15: Soil auger description: Mohaka sandy loam

Soil name:		Series: Mohaka Type: Mohaka sandy loam
NZ Soil Classification:		Vitric-acidic Orthic Allophanic (LOV)
Latitude, Longitude:		-39.08780, 177.16988
Mean annual rainfall (mm):		1500
Mean annual daily air temperature (°C):		13.7
Geomorphic position:		Flat to gently undulating Mohaka River terrace
Elevation (m a.s.l):		96 m a.s.l
Erosion:		When vegetated = nil, when ploughed potential for sheet & rill erosion
Vegetation:		Pasture, apple tree lings
Parent Material:		Holocene and late Pleistocene rhyolitic volcanic ashes.
Drainage:		Moderately well drained, class 4.
Land use:		Sheep & beef; maize; apple tree lings for pulp
Horizon:	Depth (cm)	Description:
Ap	25	Very dark brown (10YR 2/2) sandy loam.
Bw1	37	Dark yellowish brown (10YR 4/6) sandy loam
Bw2	60	Yellowish brown (10YR 5/8) loamy sand. Many coarse sand grains - lower Waimihia Lapilli unit (Rijkse, 1980).
2C	>85	Light yellowish brown (10YR 6/4) sand.

Figure 5:16: Photo depicting landscape near Mohaka sandy loam soil auger site. Note the thick soils seeping water over a pale bedrock layer across river in background.

Table 5.16 is a comparison between the interpreted drainage classes for each of the four soil profile pits, seven augered soil descriptions plus three profile descriptions from Jessen (2002). The purpose of this is to ground truth the FSL drainage map layer which will then be edited in Chapter 6 and used for crop evaluation.

Table 5:16: Comparison of interpreted soil drainage to mapped Fundamental Soil Layer drainage class

Latitude, longitude	**Soil series**	**FSL mapped drainage**	**Interpreted drainage**
-38.93002, 177.27409	Tuai sand (Table 5.3)	Well drained, class 5.	Imperfect to moderately well drained, class 3-4.
-39.01638, 177.40336	Awamate silt loam (Table 5.4)	Imperfectly drained, class 3.	Imperfectly drained, class 3.
-38.98006 177.40677	Waihirere silt loam (Table 5.5)	Well drained, class 5.	Well drained, class 5
-39.08779, 177.16997	Mohaka sandy loam (Table 5.6)	Poorly drained, class 2.	Moderately well drained, class 4.
-39.08463, 177.15567	Waihirere sandy loam (Table 5.8)	Well drained, class 5.	Well drained, class 5.
-38.992194, 177.392928	Waihirere sandy loam (Table 5.9)	Well drained, class 5.	Well drained, class 5.
-39.11750, 177.96172	Mahia fine sandy loam (Table 5.10)	Well drained, class 5	Well drained, class 5
-38.80364, 177.47988	Tuai sandy loam (Table 5.12)	Moderately well drained, class 4	Poorly drained, class 2.
-39.06169, 177.13367	Tiniroto sandy loam (Table 5.13)	Well drained, class 5.	Imperfectly drained, class 3.
-39.11843, 177.19824	Mohaka sandy loam (Table 5.14)	Poorly drained, class 2.	Moderately well drained, class 4.
-39.08780, 177.16988	Mohaka sandy loam (Table 5.15)	Poorly drained, class 2.	Moderately well drained, class 4.
-38.952791, 177.424469	Waihirere silt loam (Jessen, 2002).	Well drained, class 5.	Well drained, class 5.
-38.965930, 177.421695	Awamate silt loam, (Jessen, 2002).	FSL mapped as Mahoenui sandy loam (ROT), class 4.	Poorly drained, class 2.
-38.953598, 177.431161	Mohaka sandy loam, (Jessen, 2002).	Poorly drained, class 2.	Poorly drained, class 2.

5.3.4 Soil water characteristics

The Ap1 horizon of the Waihirere silt loam had the highest water content at 1500 kPa (20.7% v,v) followed by the Ap2 horizon of the same soil (19.7% v,v). Also within the Waihirere silt loam the 2C horizon had the lowest water content at 1500 kPa (4.3% v,v). the horizon with the highest Total Available Water Capacity (TAWC) is the Ap horizon of the Tuai sand (31.7% v,v) closely followed by the Awamate silt loam Ap horizon (30.9% v,v) and Mohaka sandy loam Ap horizon (30.2% v,v). The Bw2 horizon of the Waihirere silt loam had the highest Readily Available Water (RAW, 19.2% v,v). When accounting for horizon thickness the horizon with the greatest TAWC is the 2C horizon of the Mohaka sandy loam (109.5 mm, 500 mm thick) followed by the Ap horizon of the Tuai sand (63.4 mm).

McCarty *et al.,* (2016) note that a water-retention capacity of between 120 – 250mm is desirable with 180mm ideal for plants to access water from within a soil profile. Hazelton & Murphy (2016) state that 1m soil profiles with 100 – 200m of AWHC are rated as medium and soils with AWHC greater than 200 are rated as high. The four soil profiles used in this study have available water holding capacities ranging between 206 – 234 mm (Table 5.17).

Gradwell & Rijkse (1988) noted that Gisborne Plains soils with topsoil's containing Taupo Pumice increased the soils ability to store water. This is given by the Taupo Pumice having low bulk density, high rates of hydraulic conductivity and large pores. Such properties increase their ability to store water making them favourable towards irrigation (Gradwell & Rijkse, 1988). Two soils in this study (Tuai sand and Mohaka sandy loam) were identified as having Taupo Pumice in their topsoil and Taupo and Waimihia Lapilli in their subsoils (Tables 5.3 & 5.6). Sampled horizons in both soils have low bulk densities (0.594 – 0.759 t/m3), medium to high macro porosities (14.2 – 53.5%, Table 5.17), high TAWC (30.2 – 31.7%) and high permeability rates (4 – 6, Table 5.7) which can be attributed towards the Taupo Pumice and Taupo and Waimihia Lapilli.

Table 5.7 shows the Waihirere silt loam to have a permeability class of 4 indicating a hydraulic conductivity rating of between 20 - 64 mm/hr. The soil profile description of Waihirere silt loam in Table 5.5 shows little to no mottling indicating

it is well drained. Table 5.17 shows the Waimihia silt loam to have a profile AWHC of 219 mm (high rating, Hazelton & Murphy, 2016).

The Awamate silt loam profile description in Table 5.4 shows a gleyed profile indicating poor drainage. This is represented by the low to medium macro porosity values (4.9 – 14.3%, Table 5.17).

5.3.5 Dry soil bulk density

The highest dry soil bulk density values come from the Awamate silt loam B/Ag horizon (1.386 t/m^3). Hazelton & Murphy (2016) note that for loams with a bulk density between 1.2 – 1.4 t/m^3 relates to a satisfactory soil condition. Loams and clay loams with dry soil bulk density values greater than 1.6 are considered too restrictive towards plant root penetration.

Table 5:17: Summary physical soil characteristic results for four soils in Wairoa District

Soil type	Horizon, base (cm)	Texture class	Dry Bulk Density (t/m3)	Particle Density (t/m3)	Total Porosity (%, v/v)	Macro Porosity (%, v/v)	Vol. WC 5kPa (%, v/v)	Vol. WC 10kPa (%, v/v)	Vol. WC 100kPa (%, v/v)	Vol. WC 1500kPa (%, v/v)	Readily available water (%, v/v)	Total available water (%, v/v)	Horizon AWHC (mm)	Profile AWHC (mm)
Tuai sand	Ap, 20	Sandy loam	0.759	2.22	65.8	14.2	51.7	46.7	32.2	15	14.5	**31.7**	63.4	
	Bw1, 30	Coarse sand	0.491	2.28	78.4	53.5	24.9	20.7	9.3	6.9	11.4	13.8	13.8	
	Bw2, 50	Sandy loam	0.673	2.31	70.9	28.8	42.1	36.2	18.5	13.2	17.7	23	46.0	
	Bw3, 70	Coarse sand	0.54*								11.8*	15.5*	31.0	
	BCg, 90	Sandy loam	0.65*								16.5*	22.4*	44.8	
	2Cg, 100	Clay loam	1.05*								15.1*	21.7*	21.7	221
Awamate silt loam	Ap, 15	Silt loam	1.052	2.49	57.7	4.9	52.7	49.8	40.2	18.9	9.6	30.9	46.4	
	A/Bp, 30	Sandy clay loam	1.251	2.58	51.5	10.8	40.6	37.8	26.8	15.2	10.9	22.6	33.9	
	B/Ag, 40	Sandy clay loam	1.386	2.63	47.2	14.3	32.9	30.4	18.6	14.6	11.8	15.7	15.7	
	Bg, 70	Sandy clay loam	1.358	2.59	47.6	12.9	34.6	32.2	20.1	15.8	12.1	16.4	49.2	
	Br, >100	Clay loam	1.41*								12.7*	20.2*	60.6	206
Waihirere silt loam	Ap1, 12	Silt loam	1.135	2.52	55	8.7	46.3	43.8	34.3	20.7	9.5	23.1	27.7	
	Ap2, 23	Silt loam	1.22	2.56	52.3	9.9	42.4	40.1	29.2	19.7	11	20.5	22.6	
	B/Aw, 40	Silt loam	1.274	2.56	50.3	11.6	38.6	36.7	24.6	15.8	12.1	21	35.7	
	Bw1, 56	Silt loam	1.323	2.6	49.1	9.8	39.3	37.7	26.3	17.3	11.4	20.4	32.6	
	Bw2, 75	Silt loam	0.998	2.52	60.5	17.3	43.2	38.4	19.2	12	19.2	26.5	50.4	
	2C, >100	Sand gravelly	0.468	2.18	78.6	48.5	30.1	24.3	11.8	4.3	12.5	19.9	49.8	218

Table 5.17: Summary physical soil characteristic results for four soils in Wairoa District (continued)

Soil type	Horizon, base (cm)	Texture class	Dry Bulk Density (t/m3)	Particle Density (t/m3)	Total Porosity (%, v/v)	Macro Porosity (%, v/v)	Vol. WC 5kPa (%, v/v)	Vol. WC 10kPa (%, v/v)	Vol. WC 100kPa (%, v/v)	Vol. WC 1500kPa (%, v/v)	Readily available water (%, v/v)	Total available water (%, v/v)	Horizon AWHC (mm)	Profile AWHC (mm/ 1000m)
Mohaka	Ap, 18	Sandy loam	0.72	2.25	68.1	17.6	50.5	44.6	30.8	14.4	13.8	30.2	54.4	
sandy	Bw1, 30	Sandy loam	0.737	2.31	68.2	22.6	45.6	39.6	20.9	14.2	18.7	25.3	30.4	
loam	Bw2, 38	Loamy sand	0.737	2.34	68.5	25.5	43	35.7	17.6	12.3	18	23.4	18.7	
	Bw3, 50	Coarse sand	0.594	2.32	74.4	42	32.4	28.1	13	10.4	15.1	17.7	21.2	
	2C, >100	Sand	0.913	2.48	63.2	27.7	35.5	31.1	14	9.1	17.1	21.9	109.5	234

*Values are those sourced from McLeod *et al.,* (1999).

5.3.1 Crop irrigation estimates

Table 5.18 summarises 5 years of daily measured rainfall from the Wairoa Airport Climate Station for the crop growing season between 1 September and 31 March compared against seasonal Virtual Climate Station Network rainfall estimates. The Table shows good agreement with the Virtual Climate Station Network estimates accounting for 94.5 – 101.4% of the measured seasonal rainfall values. This allows some confidence in using the estimated rainfall data for each site.

Table 5:18: Evaluation of seasonal Virtual Climate Station Network rainfall estimates at Awamate silt loam site

	Seasonal rainfall (September – March)		
Season end date	Wairoa Airport Climate Station measured rainfall (mm)	Awamate silt loam site estimated rainfall (mm)	%
31/03/2014	498.6	490	98.3
31/03/2015	463	469.5	101.4
30/03/2016	856.6	847.3	98.9
31/03/2017	766.2	740.1	96.6
31/03/2018	654.4	618.4	94.5

Using the modified Woodward *et al.,* (2001) model, 21 years of estimated daily rainfall and evapotranspiration, topsoil TAWC values, soil profile (1m) TAWC values and known crop coefficients were used to simulate seasonal irrigation requirements for a range of crops. These results are summarised in Table 5.19. To allow easy comparison with other studies, results are given in mm. To convert to litres per hectare multiply by 10,000.

Where possible local crop dates and irrigation practices were used to reflect local growing conditions. For example, Green *et al.,* (2017) states that Bay of Plenty kiwifruit growers stop irrigating in late February. This is done to reduce soil moisture to increase kiwifruit dry matter content before harvesting in March-April. Similarly, Hawkes Bay stone fruit orchardists stop irrigating approximately mid-December when harvesting commences until March/April.

Interestingly the Waihirere silt loam site for each crop, during the drought summer of 1997-1998 requires the least amount of irrigation. In contrast the Awamate silt loam site, for each crop in the drought year required the most water for irrigation.

Table 5:19: Irrigation summary for range of crops on profiled soils

Crop	Soil series	Seasonal irrigation (mm)		
		Mean (1998 - 2018)	Min (season)	Max (season)
Hops	Waihirere silt loam	200	0 (2004)	437 (1998)
	Mohaka sandy loam	210	0 (2004; 2012)	515 (1998)
	Tuai sand	216	0 (2004; 2012)	486 (1998)
	Awamate silt loam	245	0 (2004)	535 (1998)
Apples	Waihirere silt loam	304	88 (2000; 2004)	569 (1998)
	Mohaka sandy loam	324	47 (2004)	656 (1998)
	Tuai sand	326	88 (2004)	618 (1998)
	Awamate silt loam	359	82 (2004)	658 (1998)
Stone fruit	Waihirere silt loam	110	0 (1999)	219 (2008, 2017)
	Mohaka sandy loam	118	0 (2001, 2005)	234 (2008)
	Tuai sand	120	0 (2001; 2005)	221 (1997; 2008; 2012)
	Awamate silt loam	139	0 (2001)	247 (1998; 2008)
Kiwifruit	Waihirere silt loam	204	44 (2000; 2004)	394 (1998)
	Mohaka sandy loam	219	0 (2004)	469 (1998)
	Tuai sand	219	0 (2004)	441 (1998)
	Awamate silt loam	247	41 (2004)	494 (1998)

Table 5.20 compares the four soil sites seasonal rainfall and potential evapotranspiration estimates. Table 5.20 shows that the Waihirere silt loam site experiences higher estimated seasonal rainfall (mean 836mm) than the three other sites (774–785mm). Estimated seasonal estimated potential evapotranspiration rates are similar between the four sites.

Table 5:20: Comparison of seasonal rainfall and potential evapotranspiration estimates

	Mean seasonal estimates (Sept – March)		
Soil type	Rainfall (mm)	PET (mm)	Deficit
Waihirere silt loam	836.3	875.8	-39.5
Awamate silt loam	774.3	883.1	-108.8
Tuai sand	776.7	865.7	-88.9
Mohaka sandy loam	785.0	854.9	-69.9

Table 5.21 shows a comparison of data from the seasonal kiwifruit irrigation values from Bay of Plenty orchards in Green *et al.,* (2017) against the seasonal kiwifruit irrigation estimates from this study. Green *et al.,* (2017) in their study over seven kiwifruit orchards feature two soil types, both irrigated and non - irrigation practices and two kiwifruit varieties with the objective of modelling kiwifruit irrigation in a soil water balance to help better define irrigation limits.

The ETc values from Green *et al.,* (2017) in Table 5.21 compare well against those from this study indicating similar climate conditions for the modelled period. The BOP sites all had greater seasonal rainfall than the Wairoa District simulated sites. In turn the BOP sites had greater run off and drainage losses than Wairoa. Three of the BOP sites practice no irrigation and are rain fed only. Although the BOP sites all experienced run off the modified Woodward et al., (2001) model used in this study assumed a flat site with no run off. The seasonal irrigation estimates for all the Wairoa sites were higher than the Bay of Plenty sites possibly due to the estimated rainfall being less. Drainage losses at the Wairoa sites were less than the BOP sites. An additional column of "Deficit" was added calculating the difference between input of rainfall, irrigation and out puts of drainage, runoff and crop evapotranspiration. The Wairoa sites all have smaller deficits than the BOP sites potentially indicating greater efficiency of water use.

Table 5:21: Comparison of seasonal (1 Sept 2016 – 28 Feb 2017) irrigation estimates between BOP kiwifruit orchards and simulated Wairoa District kiwifruit growing sites in this study

Site	RF (mm)	IR (mm)	DR (mm)	RO (mm)	ETc (mm)	Deficit (mm)
P G3*	735	106	97	86	745	-87
A H*	1110	0	509	142	361	98
A H*	1125	0	438	214	655	-182
A-P H*	687	0	332	79	572	-296
P G3*	894	168	339	228	691	-196
P G3*	991	218	362	281	752	-186
P H*	868	155	323	243	657	-200
Waihirere silt loam	563	263	255	NA	665	-94
Awamate silt loam	572	370	257	NA	733	-48
Tuai sand	512	309	203	NA	714	-96
Mohaka sandy loam	515	328	206	NA	710	-73

*Data from Green *et al.,* (2017). A = Allophanic soil type; P = Pumice soil; G3 = A. chinensis var. chinensis 'Zesy002' Gold3; H = Actinidia chinensis var. deliciosa 'Hayward'; RF = rainfall; IR = irrigation; RD = drainage; RO = run off; ETc = crop evapotranspiration.

5.4 Discussion

Areas with the most potential for horticulture are the Recent soils on the alluvial plains and terraces (Pullar & Ayson, 1965; Rijkse, 1980). The most versatile soils are the Waihirere soils. Opportunities utilising Waihirere soils will likely see early and sustained development (Jessen, 2002). Pullar & Ayson (1965) noted that the Waihirere silt loam subsoil contained a moderate amount of Pleistocene volcanic ash allowing it to remain moist but not wet in winter. In summer the deep subsoil encourages moisture retention and with the water tables lower than 1 m allows absorption of large volumes of rainwater. Rijkse (1980) noted that the main limiting factor for Waihirere soils is fertility.

Table 5.7 shows the Awamate silt loam to be gleyed with mottles while Table 5.7 shows the Awamate silt loam Ap horizon to have the lowest permeability rating of 3. The Awamate silt loam B/Ag horizon gave the highest dry soil bulk density value of 1.386 t/m^3, lowest values for macro porosity (4.9%, Ap horizon) and lowest soil profile total water holding capacity (206mm/1000mm). these results indicate the Awamate silt loam to have poor drainage, potentially vulnerable towards soil compaction and with a limited ability to store water compared to the other soil types. Having identified such issues means areas of Awamate silt loam can be managed accordingly. Installing drainage is essential to improve soil aeration and encourage plant roots to grow at depth. Near Frasertown an orchard growing apples for pulp on Awamate silt loam has underground tile drainage installed. This means the alluvial plains becomes more capable of supporting alternative land uses including horticulture. The drainage allows tree roots to explore deeper soils for moisture and further anchor the growing tree. The site receives sufficient annual (>1200mm) and growing season rainfall meaning for most of the year's irrigation is not needed (J. McCullum, personal communication, 2018).

This study agrees with Jessen (2002) assessment of Awamate silt loam as a widespread soil which following drainage will yield sustainable productivity gains. Jessen (2002) and Rijkse (1980) for the Mohaka sandy loam both noted the presence of an underlying pan which caused development of a perched water table. Where the pan is present in shallow soils means the water table contributes towards poor drainage. Rijkse (1980) pan observation points are not known but

Jessen (2002) pan observations beneath Mohaka sandy loam soils were just north east of Frasertown and classed them as poorly drained. This study described Mohaka sandy loam on a high terrace above the Mohaka River in which mottles were observed just below a metre indicating well to moderate drainage. Table 5.7 gives Mohaka sandy loam a permeability class rating of 4 -5. The Fundamental Soil Layer currently maps the Mohaka sandy loam unit as poorly drained. Landscape picture (Figure 5.16) shows a thick layer of soil overlying pale siltstone. Jessen (2002) assessment of Mohaka sandy loam near Frasertown as a poorly drained soil is fair however due to the soil profile thickness varying throughout the district it seems unfair to characterise the entire Mohaka sandy loam soil unit as poorly drained. This study agrees with Jessen (2002) assessment that shallow soils overlying an impermeable pan can contribute towards poor drainage but disagrees with mapping the entire Mohaka sandy loam unit as poorly drained.

Table 5.3 shows the Tuai sand as an imperfect to moderately well drained soil but due to lying over an impermeable pan (Table 5.11, 2Cg horizon) means a perched water table can rise – at 50cm below surface in Table 5.3. the Fundamental Soil Layer mapped drainage class of well drained, class 5 is disagreed with in this study instead is re-classified as imperfect to moderately well drained, class 3-4. Drainage is recommended to improve soil aeration and encourage plant root growth at depth.

Laubscher (2014) noted that Will & Stone (1967) gave a dry soil bulk density value for a Taupo Tephra horizon of 0.76 g/cm3 with the bulk density of the underlying Taupo Lapilli horizons to range between 0.57 – 0.97 g/m3. Laubscher (2014) reported similar values of 0.78 g/m3 for Taupo Tephra and 0.58 g/m3 for Taupo Lapilli. These values correlate well to the dry soil bulk density values of the Tuai sand Ap horizon (0.759 t/m3, Taupo Pumice), Bw1 horizon (0.491 t/m3, Taupo Lapilli) and Mohaka sandy loam Ap horizon (0.72 t/m3, Taupo Pumice) and Bw1 horizon (0.737 g/m3, Taupo Lapili). Where 1 g/cm3 = 1t/m3 and Taupo Tephra = Taupo Pumice. McLeod *et al.,* (1999) reported for a horizon with Waimihia Lapilli dry soil bulk density value of 0.54 g/m3, RAW of 11.8% and TAW of 15.5%. this is similar to the Mohaka sandy loam Bw3 horizon of dry bulk density 0.59 t/m3, RAW of 15.1% and TAW of 17.7% to give further justification of the field identification of such horizons.

Because the Wairoa Airport Climate Station has only been operating for a short term (<5 years) it cannot be expected to be included in the Virtual Climate Station Network system which use long term climate stations to estimate rainfall. The nearest long term climate station is the Wairoa North Clyde Climate Station approx. 3.7 km from the Wairoa Airport Climate Station. Being such a short distance means it is expected that the rainfall estimates for the Wairoa Airport Climate Station site are of a reasonable accuracy.

Table 5.19 shows the Waihirere silt loam to "perform well" against the other three soil types in all crop scenarios during the drought summer of 1997 – 1998. The reason for this is when compared to the other three sites, the Waihirere silt loam site receives a greater amount of seasonal estimated rainfall as shown in Table 5.20. More rainfall means less irrigation is needed. Mason *et al.,* (2017) noted that the VCSN rainfall estimates for their study area were imprecisely estimated. Estimates produced from modelling are always a source of uncertainty. Further investigation of the level of uncertainty in this study however was not possible. Instead Table 5.21 shows good general agreement with another independent study of estimating irrigation needs for kiwifruit for the 2017 growing season. This indicates the kiwifruit results are generally acceptable. Other results are indicative only and likewise should be looked at for validation. This can be done by consulting local industry or conducting an intensive case study focusing on a particular crop for a given area and soil type.

5.5 Conclusion

Pullar & Ayson (1965) observation of Waihirere soils having a low water table, capable of absorbing large quantities of rainwater is agreed within this study.

The Waihirere silt loam is well drained (class 5), moderately permeable (class 4), has little to no restrictions to plant roots and has a high capacity to store water (219 mm per metre of soil profile). These properties make the Waihirere silt loam versatile as per Jessen (2002) assessment. Due to their scarcity, identification and mapping of Waihirere soils is essential to fully make use of their potential, maximise productivity and protect them against other land uses. Future developments on Waihirere soils should have chemical analysis conducted on the

soil to determine any fertility requirements. Land Use Capability class is LUC1c1 (Newsome et al, 2008).

Awamate silt loam is moderately permeable (class 3), has a high capacity to store water (206mm/1000m) but is restricted by its imperfect drainage (class 3), limited rooting depth due to localised high water tables and vulnerability to soil compaction. Installing drainage will improve potential productivity hence is recommended. Soil compaction can be reduced by standard soil management practices including not driving vehicles on soil when soil moisture is greater than field capacity, use of wide vehicle tires, avoiding oversized equipment and avoiding repeated wheel tracks. Although often sited on a flood plain, flood potential risk is low. As Awamate silt loam cover a large area within the Wairoa District, providing limitations can be managed, development of these soils will likely contribute to Wairoa Districts economic productivity. Land Use Capability class is LUC2w1 (Newsome et al, 2008).

All four soils used in this study can be considered to have physical properties suited towards storage of water for plant use. Providing drainage can be implemented where needed the Awamate silt loam, Tuai sand and Mohaka sandy loam can be considered favourable towards irrigation for crops. For a given site, intensive investigation of that crops potential for irrigation is recommended by researching the lands seasonal rainfall, evapotranspiration and soil profile water holding capacity. These can be used as inputs to a soil water balance model when calibrated to local crop conditions and dates, can produce reasonable irrigation estimates.

Local observations can help identify and re-classify areas with moderate to well drained soils. The Mohaka sandy loam soil unit of the Mohaka River valley for the purposes of this study is re-classified from poorly drained (class 2) to moderately to well drained (class 4 -5). Likewise, the Tuai sand unit near Ardkeen is reclassified from well drained (class 5) to imperfect to moderately well drained (class 3-4).

Chapter 6:

Evaluation of Land for Horticultural Potential

6.1 Introduction

When evaluating land for horticulture/alternative crops the aim is to identify an area's climate, soil and topographical resources then match those with a crop possessing similar growth requirements. The objective of this chapter is, for a range of crops (Table 1.1), to identify areas within the Wairoa District with the most potential for each crop. Chapter 3 supported the use of a Weighted Linear Combination (WLC) evaluation method to identify such areas. Crop growth characteristics used in the WLC method included chill hours, growing degree days or mean monthly growing season temperature, annual or growing season rainfall, October frost risk, slope angle, soil depth, soil pH, and soil drainage.

6.2 Methods

6.2.1 Introduction

Land suitability is "the fitness of a given type of land for a specified use" (Brink & Young, 1977). To evaluate the lands goodness of fit for a given crop requires information on the proposed crops ideal soil, climate and topographical growth requirements.

6.2.2 Geographical Information System (GIS) Mapping Crop Potential

Two digital elevation model's (Table 6.1) covering the Wairoa District were downloaded from the Koordinate's (Koordinates, 2018) website then combined and clipped to the Wairoa District boundary. To allow faster computer processing time the Digital Elevation Model was resampled from 15m to 30m resolution (still

at local scale). Using spatial analyst tools in ArcGIS (ArcGIS, E. S. R. I., 2018) slope map layers were produced from the Digital Elevation Model at 30m resolution.

For soil depth and drainage, the most recent spatial map layer being produced is Smap (Lilburne *et al.,* 2012). However, at present the coverage for Smap in the Hawkes Bay is unavailable. The alternative to Smap is the Fundamental Soil Layer (FSL) providing spatial data on drainage, potential rooting depth and pH (Newsome *et al.,* 2008). For the Wairoa District the FSL map data is composed of legacy soil bulletin map data from Pullar & Ayson (1965) and Rijkse (1979, 1980). The Pullar & Ayson (1965) map of central Wairoa is at a scale of 1:63,360. The scale of Smap is a nominal 1:50,000 (Lilburne *et al.,* 2004) meaning the soil spatial map data (Wairoa to Frasertown) from Pullar & Ayson (1965) is at a scale useful for this study. The North Island FSL map layer (Table 6.1) was downloaded from the LRIS website (LRIS, 2018). Spatial maps derived from the FSL map layer include soil drainage, pH and potential rooting depth. Using spatial analyst tools in ArcGIS (ArcGIS, E. S. R. I., 2018) these were then clipped to the Wairoa District boundary, converted from polygons to raster format then resampled to 30m resolution (Figure 6.1).

Mean monthly temperature maps are available from Leathwick *et al.,* (1998) with nation-wide coverage but not at local scale resolution. Similarly, chill hours, growing degree days and October frost risk spatial data are available from NIWA but not at local scale resolution. Instead chill hours, growing degree days and October frost risk and mean monthly daily average temperature maps (Table 6.1) were constructed in Chapter 4 at local scale to 30m resolution.

Table 6:1: Spatial datasets used as input layers for Weighted Linear Combination model

Input spatial layer	**Resolution**	**Reference**
Chill hours (base 7°C, April - August)	30 m	Chapter 4
Growing degree days (base 10°C, October - April)	30 m	Chapter 4
Growing season mean temperature (°C, October - April)	30 m	Chapter 4
October frost risk (%)	30 m	Chapter 4
Slope (°),	30 m	Columbus *et al.,* (2011)
Potential rooting depth (m), pH, drainage class	330 m	Willoughby *et al.*, (2008)
Annual rainfall (mm), growing season rainfall (mm)	100 m	Leathwick *et al.,* (1998)

With all the required input data available the crop growth requirements can then be evaluated against the land's soil, climate and topographical characteristics. The Weighted Linear Combination analysis involved reclassifying values within input layers into ranked categories based on their importance relevant to crop growth requirements. Spatial data values were reclassified as either 0 (unsuitable), 1 (moderately suited), 2 (suitable) or 3 (well suited) (Table 6.2) based on the spatial data values importance to crop growth requirements. Using the raster calculator function reclassified map layers were then combined to produce the crop potential maps (Figure 6.1). The software version used to implement the WLC model is ArcGIS 10.5 developed by ESRI (ArcGIS, E. S. R. I., 2018). The crop potential maps highlight areas in the Wairoa District worthy of further investigation for individual crops.

Table 6.2 demonstrates how spatial layers were reclassified using required annual rainfall (mm) for kiwifruit as an example.

Table 6:2: Reclassifying annual rainfall according to kiwifruit growth requirements

Spatial layer	Mapped values	Suitability rating	Reclassified value
Annual rainfall (mm)	900 - 1300	Well suited	3
	800 – 900; 1300 - 1400	Suitable	2
	700 – 800; 1400 – 1500	Moderately suited	1
	0 – 700; >1500	Unsuitable	0

The workflow in ArcGIS for how each crop potential map was produced is outlined in Figure 6.1. Green colour boxes represent data map layers, blue boxes represent ArcGIS functions used.

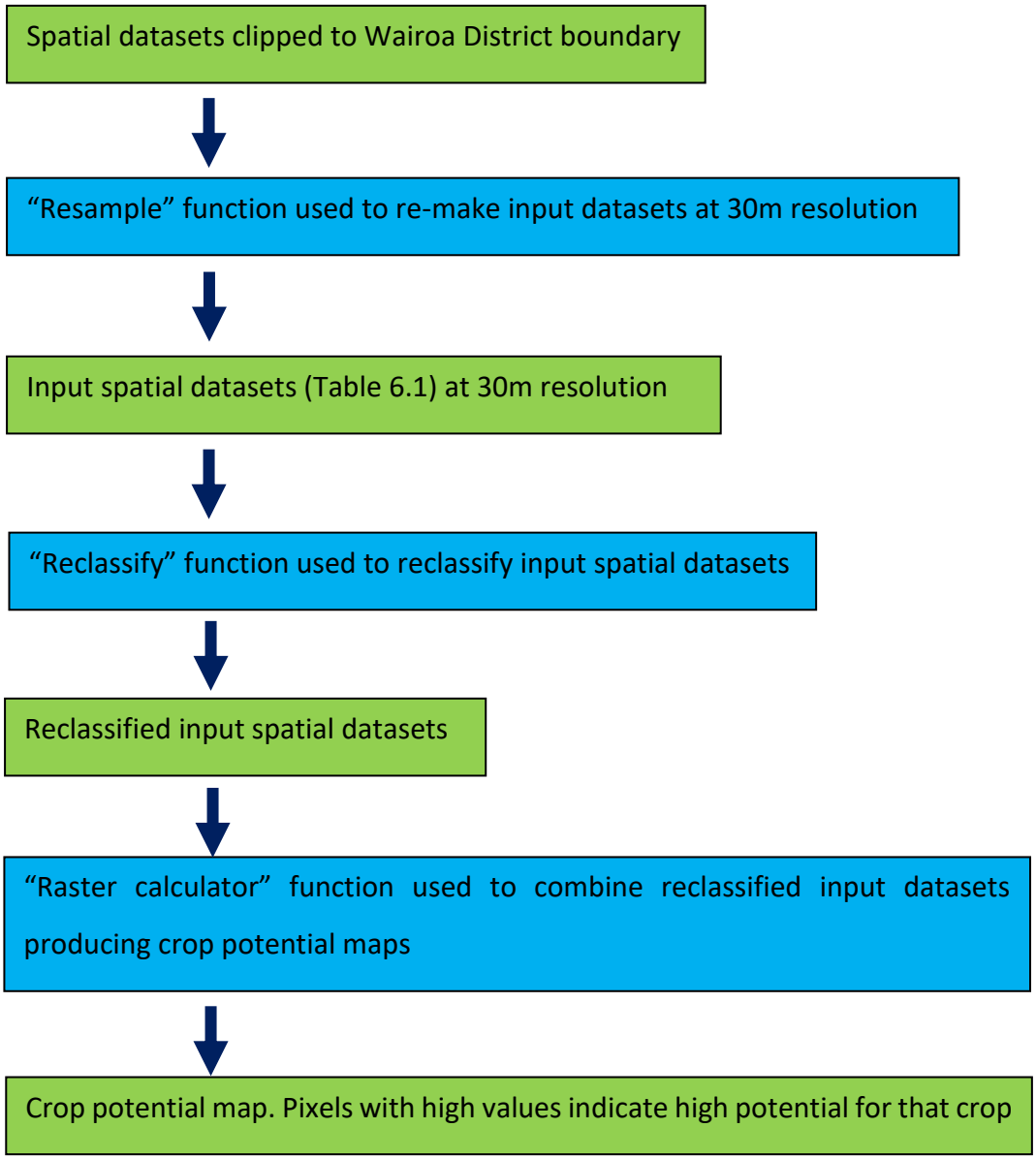

Figure 6:1: Workflow summarising WLC model applied to input data and crop rules to produce crop potential maps.

6.3 Results

6.3.1 Introduction

By production of local scale climate maps (Chapter 4), estimation of crop irrigation requirements (Chapter 5) and ArcGIS suitability mapping, areas with horticulture/alternative crop potential in Wairoa District have been identified (Figure 6.2 – 6.6). The Mohaka River Valley, Waikaretaheke River terraces, lower Waiau River, Marumaru to Frasertown, Frasertown to Wairoa, Coastal area from Wairoa to Nuhaka River valley, Mahia Tombolo and Mahia Peninsula have all been identified as areas with potential for horticulture/alternative crops.

6.3.2 Crop potential maps

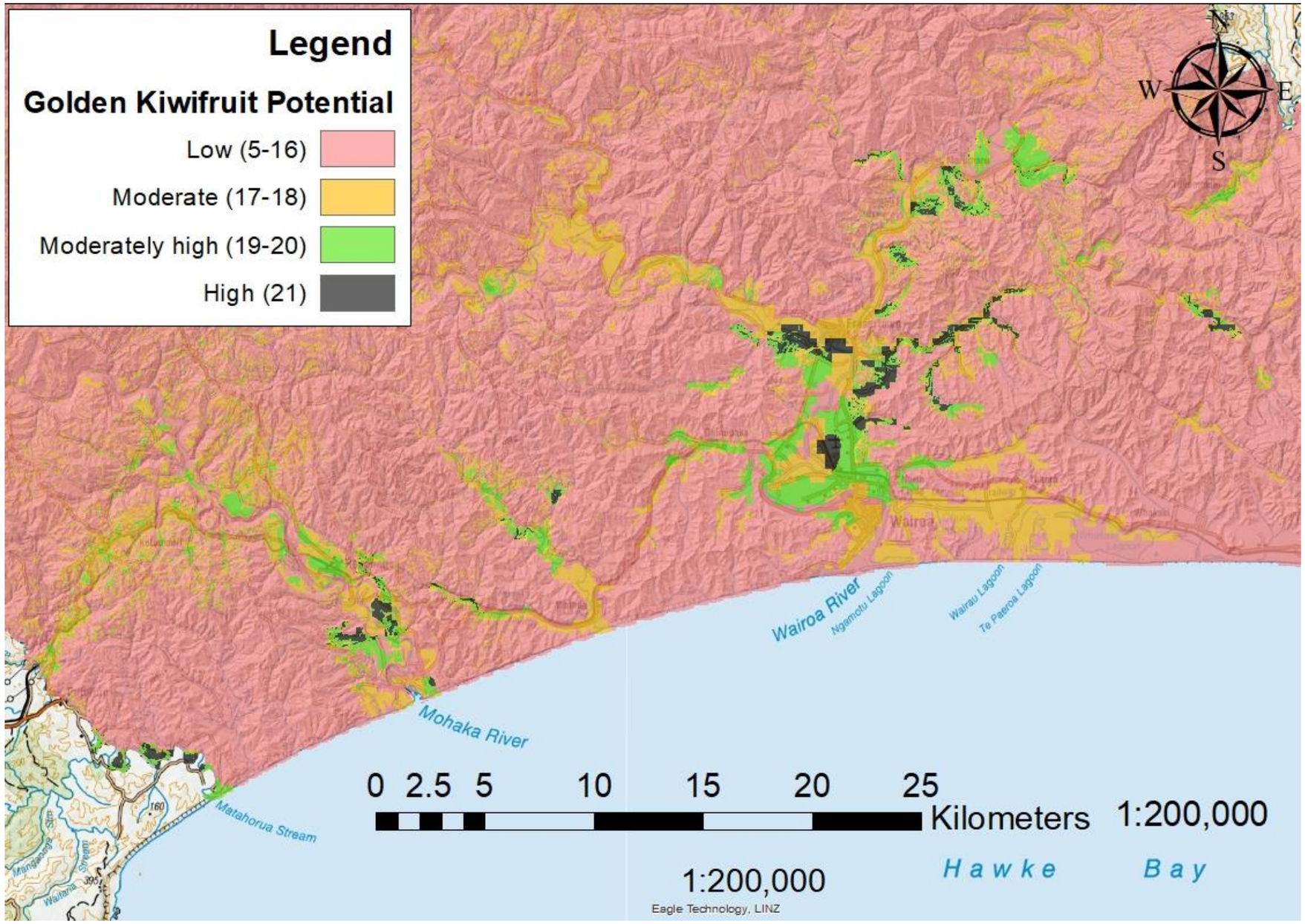

Figure 6:2: Crop potential map for kiwifruit var. Golden Sunshine (Actinidia chinensis), Wairoa District.

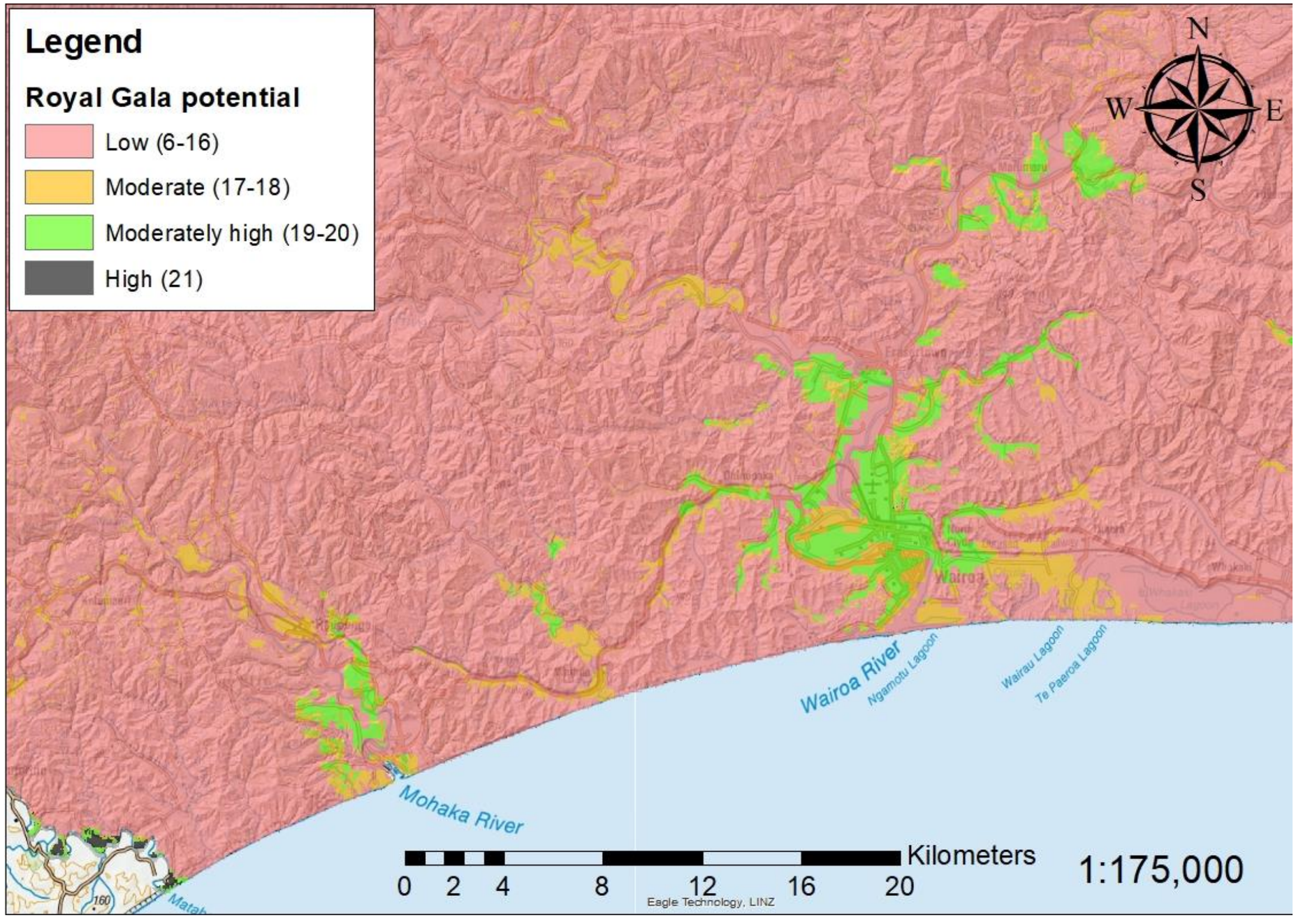

Figure 6:3: Crop potential map for apples var. Royal Gala (Malus domestica), Central Wairoa.

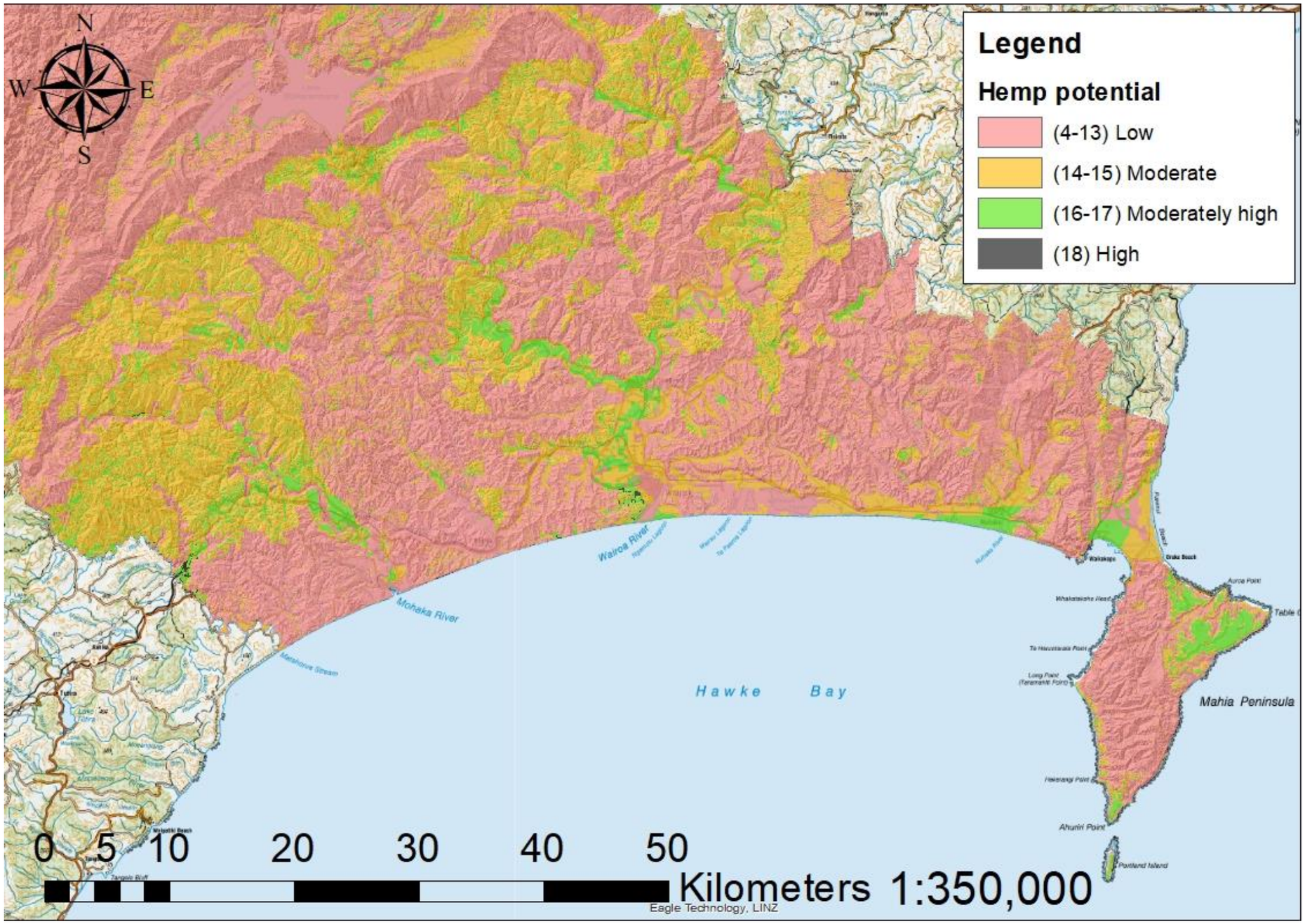

Figure 6:4: Crop potential map for Hemp (Cannabis sativa L.), Wairoa Valley.

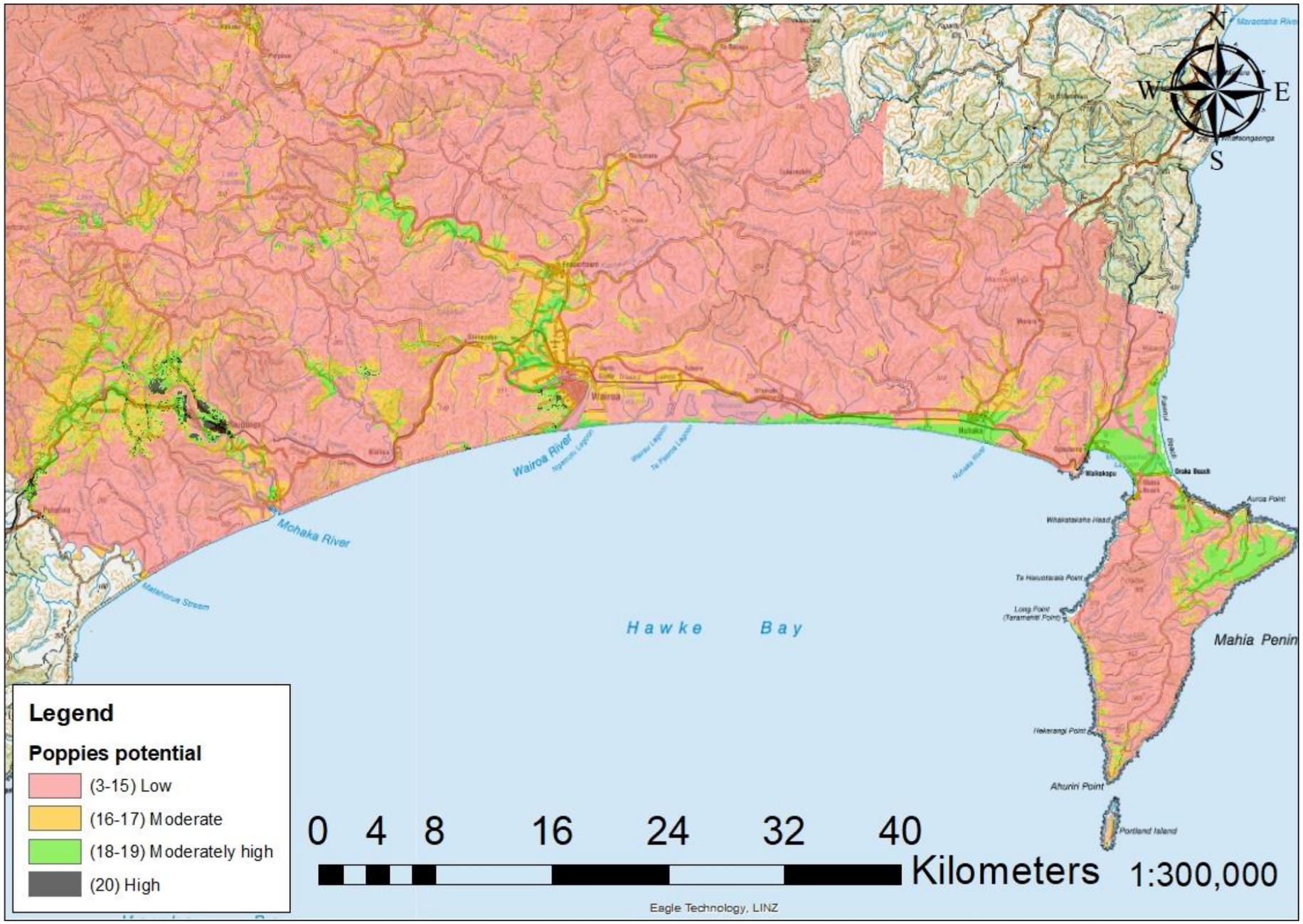

Figure 6:5: Crop potential map for Poppies (Papaver somniferum), Wairoa District.

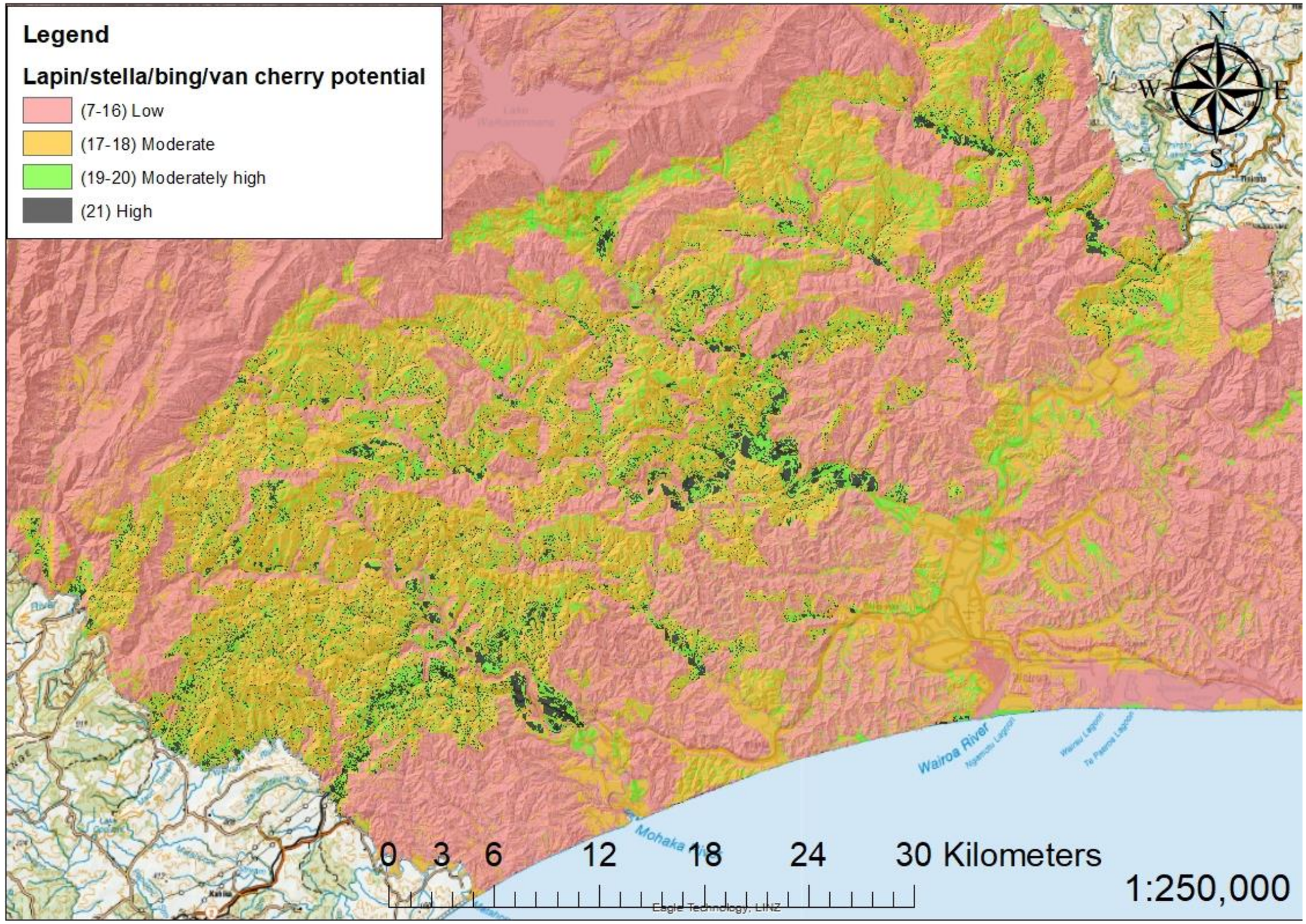

Figure 6:6: Crop potential map for Cherries (Prunus avium, var. Lapins, Stella, Bing & Van), Wairoa River Valley.

6.4 Discussion

6.4.1 Evaluating crop potential maps

With all GIS results and potential error sources, it becomes important to critique the data, methods used to produce the crop potential maps and finally the relevance of the crop potential maps. This is achieved by assessing limitations of the input data and assumptions made when ranking the categories in each climate, soil or topographical characteristic and how the final map was classified.

6.4.2 Data limitations

Limitations of the input data include resolution and accuracy which can affect the quality of the crop potential map produced. These are discussed herewith.

The Digital Elevation Model which formed the basis of the chill hour, growing degree day (GDD) and October frost risk (Chapter 4) and slope (Chapter 6) maps was made by Columbus et *al.,* (2011) at the National School of Surveying, University of Otago. Columbus et *al.,* (2011) compared their 15m resolution digital elevation model (DEM) against two other DEM's – one from Geographx Ltd (20m resolution) and another from Landcare Research (25m resolution). Columbus *et al.,* (2011) found an improvement in quality as expected in a higher resolution product. Therefore, we can have reasonable confidence in the DEM and derived slope map for accuracy.

The chill hours, growing degree days and October frost risk maps were made with high resolution spatial and temporal data with the DEM 15m changed to 30 m resolution (Chapter 4). Tobler's Law states that "everything is related to everything else, but near things are more related than distant things (Tobler, 1970). Therefore, we can be confident in the chill hours, GDD and October frost risk map estimates close to the iButton temperature deployment sites. Confidence in the climate map estimates decreases with increasing distance away from the iButton deployment sites. However, this may have been negated by the closeness of the deployed iButtons. Areas with poor iButton coverage included steep hill country which is unsuitable for horticulture. As such overall confidence in the resolution and accuracy of the chill hours, GDD and October frost risk climate maps is generally high.

The annual and monthly rainfall spatial data used in this study was sourced from Leathwick *et al.,* (1998). To construct the maps (resolution 100m) Leathwick *et al.,* (1998) used rainfall normals from 2202 climates stations throughout New Zealand between 1951 to 1980. For the analysis the resolution was changed from 100 m to 30 m. For the purposes of this study it is assumed that the monthly rainfall map estimates are of reasonable accuracy.

The soil drainage, pH and potential rooting depth spatial maps (resolution 330m) used in this study were derived from the Fundamental Soil Layer (Newsome *et al.,* 2008). Lilburne *et al.,* (2012) noted that New Zealand alluvial plains have considerable variability in their soil types and associated soil properties. Lilburne *et al.,* (2012) further noted that many of the soil reports and bulletins comprising the Fundamental Soil Layer do not capture much of the variability naturally inherent within New Zealand soils. Instead the mapped soil units are simplified and described being represented by a typical profile with no information given on soil variability (Lilburne *et al.,* 2012). Chapter 5 results compare interpreted soil auger drainage against FSL map values for the same location. For this Chapter where such values differ the FSL attribute values for that polygon were edited in ArcGIS to the interpreted drainage values. No pH tests were done so the FSL pH map was left unchanged. The values were changed to increase the soil drainage maps accuracy reflecting its natural variability. However, despite this there may still be many mapped soil areas of uncertainty.

Pullar & Ayson (1965) mapped the area from Wairoa to Frasertown using data obtained from intensive field work at a scale of 1: 63,360. Soil auger interpretations of drainage and potential rooting depth from Chapter 5 largely agree with the work of Pullar & Ayson (1965) therefore is considered reliable.

Rijkse (1979; 1980) mapped soils in the Mohaka and Tiniroto areas but did no field work instead relied on past field observations made in 1970, the work of Pullar & Ayson (1965), unpublished district soil surveys and interpretation of aerial photos. The work by Rijkse (1979; 1980) is of a high standard but is constrained by the limited amount of field work done. This may have led to some assumptions made. For example, Rijkse mapped the soils west of Whakaki Lagoon as an Acid Mesic Organic (OMA) soil. Hewitt (1998) describes Mesic Organic (OM) soils as occurring in very wet sites or sites with artificial drainage in which the peat materials are

moderately decomposed. Upon reconnaissance for Smap in 2017 Scott Fraser disagreed with Rijkse's assessment instead classified the soils west of Whakaki Lagoon as Raw Fluid and Recent Sandy soils (S. Fraser, personal communication, August, 2017). In this example, the soil west of Whakaki Lagoon classified as an Acid Mesic Organic soil is incorrect and corresponding pH, potential rooting depth and drainage estimates potentially incorrect also. This creates a degree of uncertainty in the Fundamental Soil Layer mapped values for drainage, pH and potential rooting depth within the Tiniroto, Mohaka and Mahia mapped areas making such areas potential sources of error in the final results.

6.4.3 Assumptions made when Ranking Categories in each Crop Growth Requirement

The crop growth requirements used in this study (Table 6.1) to produce the crop potential maps were split into four categories based on how important they were to each crop. The four categories used were high, moderately high, moderate and low. Values from each characteristic were split into the four categories as per knowledge from the existing literature and relevant industry. Two issues arise from categorising the input data. The first is that the boundaries given by the existing literature and industry may or may not be correct (Voogd, 1983). Secondly not all the required characteristics may have been included in the analysis (Eastman, 1997). The crop potential maps do not consider factors other than those used in the analysis. The list of crop factors used in this study is not complete as there may be more factors worthy of being included e.g. wind, soil salinity, humidity etc. Such factors may also be unavailable as GIS input layers.

In producing the crop potential maps, it is assumed that the existing literature and industry knowledge provides the best possible guidance for categorising the input data. Furthermore, it is assumed that the crop growth characteristics used represent the majority required to effectively identify areas with crop potential.

6.4.4 Classification of final crop potential maps

Combined scores within each crop potential map ranged between 5 – 18 or 21 depending on how many crop growth characteristic layers were used for each crop. For example, golden kiwifruit used seven input layers meaning the maximum

score an area could receive is 21 indicating such areas met all the growth requirements of golden kiwifruit and possess the highest potential for golden kiwifruit orchard development. These areas were given the category “high” in the kiwifruit potential map. Because slopes with areas greater than 11° are generally unfit for horticultural land use most such areas, regardless of their score were given the category “low”. For golden kiwifruit these were values 5 to 15. This left the categories of “moderate” and “moderately high”. The lower boundary of the moderately high category was two values below that of the highest value. For golden kiwifruit, this included the values between 19 – 20. This left the values 16 – 18 to be categorised as “moderate”. For transparency, the values used in each category were added to the crop potential map legend.

6.4.5 Validation of GIS results

Areas of moderately high to high crop potential are summarised in Table 6.3. Validation of GIS results is best achieved by site field work however due to time constraints this was not possible within the time frame of this study however is highly recommended. Methods of evaluating areas with high potential include gaining local knowledge from the landowner – past land use (any horticultural or which crops grows well) spring frost occurrence, monthly rainfall, soil drainage rates, soil depth, wind intensity/direction, coastal sea spray, susceptibility to flooding and any other factors already used in this study. On site evaluation methods include digging a soil profile pit to assess drainage; potential rooting depth; samples taken to determine soil pH; visual soil assessment (Shepard, 2009) to assess soil health and use of virtual climate station network to estimate growing season/annual rainfall.

Validation of GIS results by field work gives confidence in the results allowing landowners to make informed decisions regarding change in land use.

6.5 Conclusion

For predominantly the alluvial floodplains and terraces of the Wairoa District a range of horticultural/alternative crop opportunities have been identified. Crops that satisfied all the growth requirements (high potential) with reasonable land

coverage include Golden Kiwifruit; Lapin/Stella/Bing/Van Cherries; Royal Gala apples; Poppies and industrial hemp. Limitations to the results include the resolution and accuracy of the input data. The soil drainage, pH and potential rooting depth maps were the lowest resolution (330m) and probable least accurate maps used in this study. These are therefore a likely source of error. Once available it is expected that use of Smap drainage and depth spatial maps in place of the FSL drainage and potential rooting depth maps will improve the accuracy of the crop potential maps. Until then areas with high potential for horticulture/alternative crops should be assessed by field work to ground truth the results.

References

Ahmed, K., Shahid, S., & Harun, S. B. (2014). Spatial interpolation of climatic variables in a predominantly arid region with complex topography. *Environment Systems and Decisions*, *34*(4), 555-563.

Ahrens, R., Rice, T. J., & Eswaran, H. (2003). Soil classification: past and present. *Soil classification: a global desk reference*, 19-25.

Allen, R. G., Smith, M., Pereira, L. S., & Perrier, A. (1994). An update for the calculation of reference evapotranspiration. *ICID bulletin*, *43*(2), 35.

Allen, R. G., Pereira, L. S., Raes, D., & Smith, M. (1998). Crop evapotranspiration-Guidelines for computing crop water requirements-FAO Irrigation and drainage paper 56. *FAO, Rome*, *300*(9), D05109.

Allen, R. G., & Pereira, L. S. (2009). Estimating crop coefficients from fraction of ground cover and height. *Irrigation Science*, *28*(1), 17-34.

An, Y. (2010). *Evaluation of Evapotranspiration Estimation Methods and Their Impacts on Crop Yield Simulations* (Doctoral dissertation, Carleton University).

Anderson, M. C., Allen, R. G., Morse, A., & Kustas, W. P. (2012). Use of Landsat thermal imagery in monitoring evapotranspiration and managing water resources. *Remote Sensing of Environment*, *122*, 50-65.

Anthony, T. (2002). *A comparison of environmental risk models developed from NZLRI and Topoclimate South soil survey data: a thesis presented in partial fulfilment of the requirements for a Masters degree in Applied Science at Massey University* (Doctoral dissertation, Massey University).

ArcGIS, E. S. R. I. (2018). ArcGIS.(2018). *Retrieved January08*.

Attorre, F., Alfo, M., De Sanctis, M., Francesconi, F., & Bruno, F. (2007). Comparison of interpolation methods for mapping climatic and bioclimatic variables at regional scale. *International journal of climatology*, *27*(13), 1825-1843.

Baldocchi, D. (2008). 'Breathing'of the terrestrial biosphere: lessons learned from a global network of carbon dioxide flux measurement systems. *Australian Journal of Botany*, *56*(1), 1-26.

Barnes, F. (2011). Estimating Crop Water Requirements in Arizona and New Mexico.

Barnes, P. M., Nicol, A., & Harrison, T. (2002). Late Cenozoic evolution and earthquake potential of an active listric thrust complex above the Hikurangi subduction zone, New Zealand. *Geological Society of America Bulletin*, *114*(11), 1379-1405.

Bastiaanssen, W. G., Menenti, M., Feddes, R. A., & Holtslag, A. A. M. (1998). A remote sensing surface energy balance algorithm for land (SEBAL). 1. Formulation. *Journal of hydrology*, *212*, 198-212.

Baxter, P., & Jones, C. (1985). *Growing fruit and nuts in New Zealand*. Auckland, N.Z.: David Bateman.

Beek, K. J., de Bie, K., & Driessen, P. (1997, August). Land evaluation for sustainable land management. In *Introductory paper of the conference on Geoinformation for Sustainable Land Management, Enschede, Netherlands* (pp. 17-21).

Benavides, R., Montes, F., Rubio, A., & Osoro, K. (2007). Geostatistical modelling of air temperature in a mountainous region of Northern Spain. *Agricultural and Forest Meteorology*, *146*(3-4), 173-188.

Bhatti, G. H., & Patel, H. M. (2014). Methods for Estimation of Crop Evapotranspiration using Climate Data: A Review.

Bibby, J., & Mackney, D. (1969). *Land use capability classification* (Technical monograph (Soil Survey of England and Wales) ; no. 1). Harpenden (Herts.): Rothamsted Experimental Station

Blair, R., Fitzharris, B. B., & Richards, K. (2002, December). Interpolation of growing degree-days in non-homogeneous terrain. In *Proceedings 14th Annual Colloquium of the Spatial Information Research Centre* (pp. 3-5).

Bland, K. J., & Kamp, P. J. (2014). Hawke's Bay forearc basin (eastern North Island, New Zealand): Stratigraphy, biostratigraphy, chronology, geological maps and paleogeography.

Brink, R., & Young, A. (1977). *A framework for land evaluation* (No. 22). ILRI.

Burrough, P. A. (1989). Fuzzy mathematical methods for soil survey and land evaluation. *Journal of Soil Science*, *40*(3), 477-492.

Burrough, P. A., & McDonnell, R. A. (1998). Principles of GIS. *Oxford University Press: London, UK*.

Busetto, & Ranghetti. (2016). MODIStsp: An R package for automatic preprocessing of MODIS Land Products time series. *Computers and Geosciences, 97*, 40-48.

Caloiero, T. (2014). Analysis of daily rainfall concentration in New Zealand. *Natural hazards*, *72*(2), 389-404.

Chai, H., Cheng, W., Zhou, C., Chen, X., Ma, X., & Zhao, S. (2011). Analysis and comparison of spatial interpolation methods for temperature data in Xinjiang Uygur Autonomous Region, China. *Natural Science*, *3*(12), 999-1010.

Chappell, P., R. (2013). The climate and weather of the Hawke's Bay (3rd Ed). NIWA.

Childs, C. (2004). Interpolating surfaces in ArcGIS spatial analyst. *ArcUser, July-September*, *3235*, 569.

Cichota, R., Snow, V. O., & Tait, A. B. (2008). A functional evaluation of virtual climate station rainfall data. *New Zealand Journal of Agricultural Research*, *51*(3), 317-329.

Claydon, John., J. & Manaaki Whenua-Landcare Research New Zealand Ltd. (1997). Laboratory Methods for Water Release & Solid\Void Characterisation of Soils.

Clothier, B. E., Kerr, J. P., Talbot, J. S., & Scotter, D. R. (1982). Measured and estimated evapotranspiration from well-watered crops. *New Zealand journal of agricultural research*, *25*(3), 301-307.

Collins, F. C. (1995). *A comparison of spatial interpolation techniques in temperature estimation* (Doctoral dissertation, Virginia Tech).

Collins, M. G., Steiner, F. R., & Rushman, M. J. (2001). Land-use suitability analysis in the United States: historical development and promising technological achievements. *Environmental management*, *28*(5), 611-621.

Columbus, J., Sirguey, P., & Tenzer, R. (2011). A free fully assessed 15 metre digital elevation model for New Zealand. *Survey Quarterly*, *300*(66), 16

Cristóbal, J., Ninyerola, M., & Pons, X. (2008). Modeling air temperature through a combination of remote sensing and GIS data. *Journal of Geophysical Research: Atmospheres*, *113*(D13).

Daly, C., Gibson, W. P., Taylor, G. H., Johnson, G. L., & Pasteris, P. (2002). A knowledge-based approach to the statistical mapping of climate. *Climate research*, *22*(2), 99-113.

Davies, T. R., McSaveney, M. J., & Beetham, R. D. (2006). Rapid block glides: slide-surface fragmentation in New Zealand's Waikaremoana landslide. *Quarterly*

Drinnan, M. M. (2011). *Stratigraphy and sedimentology of Pliocene limestones in northern Hawke's Bay: the Opoiti, Whakapunake and Tahaenui Limestones* (Doctoral dissertation, University of Waikato).

Eastman, J. R. (1997). GIS and uncertainty management: new directions in software development. *Lurralde*, *20*, 53-66.

http://ecocrop.fao.org/ecocrop/srv/en/cropFindForm

Elaalem, M. (2010). *The Application of Land Evaluation Techniques in Jeffara Plain in Libya using Fuzzy Methods* (Doctoral dissertation, University of Leicester, United Kingdom).

Eldrandaly, K. A., & Abu-Zaid, M. S. (2011). Comparison of Six GIS-Based Spatial Interpolation Methods for Estimating Air Temperature in Western Saudi Arabia. *Journal of environmental Informatics*, *18*(1).

Elrick, D. E., & Tanner, C. B. (1955). Influence of Sample Pretreatment on Soil Moisture Retention 1. *Soil Science Society of America Journal*, *19*(3), 279-282.

Elsheikh, R., Shariff, A. R. B. M., Amiri, F., Ahmad, N. B., Balasundram, S. K., & Soom, M. A. M. (2013). Agriculture Land Suitability Evaluator (ALSE): A decision and planning support tool for tropical and subtropical crops. *Computers and electronics in agriculture*, *93*, 98-110.

Er-Raki, S., Chehbouni, A., Boulet, G., & Williams, D. G. (2010). Using the dual approach of FAO-56 for partitioning ET into soil and plant components for olive orchards in a semi-arid region. *Agricultural water management*, *97*(11), 1769-1778

Farooq, M., Wahid, A., Kobayashi, N., Fujita, D., & Basra, S. M. A. (2009). Plant drought stress: effects, mechanisms and management. In *Sustainable agriculture* (pp. 153-188). Springer Netherlands.

Fereres, E., Goldhamer, D. A., & Parsons, L. R. (2003). Irrigation water management of horticultural crops. *HortScience*, *38*(5), 1036-1042

Field, B. D., & Uruski, C. I. (1997). *Cretaceous-Cenozoic geology and petroleum systems of the East Coast region, New Zealand* (Vol. 1). Institute of Geological & Nuclear Sciences.

Fieldes, M., & Perrot, K. W. (1966). The nature of allophane in soils. I. Significance of randomness in pedogenesis. *New Zealand J. Sci*, *9*, 622-632.

Fitzharris, B. B. (1989). A Review of Topoclimatology in New Zealand. *Weather and Climate*, 7-13.

François, C., Bosseno, R., Vacher, J. J., & Seguin, B. (1999). Frost risk mapping derived from satellite and surface data over the Bolivian Altiplano. *Agricultural and forest meteorology*, *95*(2), 113-137.

Geiger, R., Aron, R. H., & Todhunter, P. (2009). *The climate near the ground*. Rowman & Littlefield.

Griffiths, E. (1985). *Interpretation of soil morphology for assessing moisture movement and storage*. Department of Scientific and Industrial Research.

Griffiths, G., Tait, A., Wratt, D., Jessen, M., McLeod, M., Reid, J., ... & Richardson, A. (2003). Use of Climate, Soil, and Crop Information for Identifying Potential

Land-Use Change in the Hokianga and Western Kaipara Region. *NIWA report prepared for the FNDC, Available from: http://www. fndc. govt. nz/about-the-district/soil-and-climate study/soilclimate. pdf, Accessed*, *20*(11), 2011.

Grose (2013). *Hill Slope Viability for Industrial Viticultural Development in the South Island of New Zealand* (Master's thesis, University of Canterbury, Christchurch, New Zealand). Retrieved from http://ir.canterbury.ac.nz/bitstream/handle/10092/7673/Thesis_Final.pdf?sequence=1&isAllowed=y

Gross, J. J. (2014). *Assessment of future agricultural land potential using gis and regional climate projections for Hawai'i island--an application to macadamia nut and coffee* (Doctoral dissertation, [Honolulu]:[University of Hawaii at Manoa],[August 2014]).

Hammond, A. P. (1997). *Late quaternary landscape evolution of western Hawke's Bay, North Island, New Zealand: a thesis presented in partial fulfilment of the requirements for the degree of Doctor of Philosophy in Earth Science at Massey University, Palmerston North, New Zealand* (Doctoral dissertation, Massey University).

Hargreaves, G. H., & Samani, Z. A. (1985). Reference crop evapotranspiration from temperature. *Applied engineering in agriculture*, *1*(2), 96-99.

Hartkamp, A. D., De Beurs, K., Stein, A., & White, J. W. (1999). Interpolation techniques for climate variables.

Hedley, C. B., Yule, I. J., & Bradbury, S. (2010, August). Analysis of potential benefits of precision irrigation for variable soils at five pastoral and arable production sites in New Zealand. In *19th World Soil Congress* (pp. 1-6).

Hengl, T., Heuvelink, G. B., & Stein, A. (2004). A generic framework for spatial prediction of soil variables based on regression-kriging. *Geoderma*, *120*(1), 75-93.

Hengl, T. (2009). *A practical guide to geostatistical mapping*(Vol. 52). Hengl.

Hengl, T., Heuvelink, G. B., Tadić, M. P., & Pebesma, E. J. (2012). Spatio-temporal prediction of daily temperatures using time-series of MODIS LST images. *Theoretical and applied climatology*, *107*(1-2), 265-277.

Heron, D. W. (2014). *Geological Map of New Zealand 1: 250 000: Digital Vector Data 2014*. GNS Science.

Hewitt, A. E. (2010). New Zealand soil classification. *Landcare research science series*, (1).

Hopkirk, C. L. (2011). *Forecasting Lake Waikaremoana Water Availability for Hydro Power* (Doctoral dissertation, University of Waikato).

Hofstra, N., Haylock, M., New, M., Jones, P., & Frei, C. (2008). Comparison of six methods for the interpolation of daily, European climate data. *Journal of Geophysical Research: Atmospheres*, *113*(D21).

Horne, D. J., & Scotter, D. R. (2016). The available water holding capacity of soils under pasture. *Agricultural Water Management*, *177*, 165-171.

Hutchinson, M. F., & Gessler, P. E. (1994). Splines—more than just a smooth interpolator. *Geoderma*, *62*(1-3), 45-67.

Hutchinson, G., & McIntosh, P. (2000). A case study of integrated risk assessment mapping in the Southland region of New Zealand. *Environmental Toxicology and Chemistry: An International Journal*, *19*(4), 1143-1147.

idcommunity - Demographic Resources. (n.d.). Retrieved August, 2018, from https://profile.idnz.co.nz/.

Irmak, S., Allen, R. G., & Whitty, E. B. (2003). Daily grass and alfalfa-reference evapotranspiration estimates and alfalfa-to-grass evapotranspiration ratios in Florida. *Journal of Irrigation and Drainage Engineering*, *129*(5), 360-370.

Jarvis, C. H., & Stuart, N. (2001b). A comparison among strategies for interpolating maximum and minimum daily air temperatures. Part II: The interaction between number of guiding variables and the type of interpolation method. *Journal of Applied Meteorology*, *40*(6), 1075-1084.

Jensen, M. E., & Allen, R. G. (Eds.). (2016, April). Evaporation, evapotranspiration, and irrigation water requirements. American Society of Civil Engineers.

Jessen, M., & Landcare Research New Zealand. (1999). *Land Use Capability Classification of the Gisborne - East Coast Region: A report to accompany the second-edition, New Zealand Land Resource Inventory* (Landcare Research science series; no. 21). Lincoln, N.Z.: Manaaki Whenua Press.

Jiang, Z. J. (2011). *Stratigraphy and sedimentology of Pliocene limestones, Wairoa District, Northern Hawke's Bay* (Doctoral dissertation, University of Waikato).

Jin, M., & Dickinson, R. E. (2010). Land surface skin temperature climatology: Benefitting from the strengths of satellite observations. *Environmental Research Letters*, *5*(4), 044004.

Johnson, A. K. L., & Cramb, R. A. (1991). Development of a simulation based land evaluation system using crop modelling, expert systems and risk analysis. *Soil use and management*, *7*(4), 239-246.

Jones, P., Jedlovec, G., Suggs, R., & Haines, S. (2004, September). Using MODIS LST to estimate minimum air temperatures at night. In *13th Conference on Satellite Meteorology and Oceanography* (pp. 13-18). Norfolk: American Meteorological Society.

Jones, H. G., & Tardieu, F. (1998). Modelling water relations of horticultural crops: a review. *Scientia Horticulturae*, *74*(1-2), 21-46.

Jones, A., Stolbovoy, V., Rusco, E., Gentile, A. R., Gardi, C., Marechal, B., & Montanarella, L. (2009). Climate change in Europe. 2. Impact on soil. A review. *Agronomy for sustainable development*, *29*(3), 423-432.

Kalogirou, S. (2002). Expert systems and GIS: an application of land suitability evaluation. *Computers, environment and urban systems*, *26*(2-3), 89-112.

Kenk, E., & Cotic, I. (1983). *Land Capability Classification for Agriculture in British Columbia* (Vol. 1). Kelowna: BC Ministry of Agriculture and Food.

King, J. M., Krausse, M. K., & Butcher, G. V. (1995). *The impacts of land use change in Wairoa*.

Klingebiel, A., & Montgomery, P. (1961). Land Use Capability Classification, USDA Agriculture Handbook No. 210

Koordinates (2018). Retrieved from https://koordinates.com/

Krige, D. G. (1951). A statistical approach to some basic mine valuation problems on the Witwatersrand. *Journal of the Southern African Institute of Mining and Metallurgy*, *52*(6), 119-139.

Laubscher, N. (2014). Improvement in soil water availability in pastures by excavating and mixing buried soil horizons from multilayered Pumice Soils (Vitrands) at Galatea, central North Island, New Zealand. *(Master's Thesis,* University of Waikato, Hamilton, New Zealand). Retrieved from http://researchcommons.waikato.ac.nz/bitstream/handle/10289/8709/thesis.pdf?sequence=3&isAllowed=y

Leathwick, J. R., & Stephens, R. T. T. (1998). Climate surfaces for New Zealand. *Landcare Research Contract Report LC9798*, *126*, 1-19.

Lee, J. M., Bland, K. J., Townsend, D. B., & Kamp, P. J. J. (2011). Geology of the Hawke's Bay area. *Institute of Geological and Nuclear Sciences*, *1*(250), 000.

Lilburne, L., Hewitt, A., Webb, T. H., & Carrick, S. (2004, December). S-map: a new soil database for New Zealand. In *SuperSoil 2004: Proceedings of the 3rd Australian New Zealand Soils Conference, Sydney, Australia* (pp. 5-9).

Lilburne, L. R., Hewitt, A. E., & Webb, T. W. (2012). Soil and informatics science combine to develop S-map: A new generation soil information system for New Zealand. *Geoderma*, *170*, 232-238.

Linacre, E., & Geerts, B. (1997). *Climates and weather explained*. Routledge.

Loomis, T. (2012). Wairoa Business Survey, Vision Projects.

Lowe, D. J., Blaauw, M., Hogg, A. G., & Newnham, R. M. (2013). Ages of 24 widespread tephras erupted since 30,000 years ago in New Zealand, with re-evaluation of the timing and palaeoclimatic implications of the Lateglacial

cool episode recorded at Kaipo bog. *Quaternary Science Reviews*, *74*, 170-194.

Lowe, D. J. & Walker, J. D. (1992). Lakes. In Soons, J., & Selby, M. (1992). *Landforms of New Zealand* (2nd ed.). Auckland, N.Z.: Longman Paul.

LRIS, (2018). Retrieved from https://lris.scinfo.org.nz/

Lynn, I. H., Manderson, A. K., Page, M. J., Harmsworth, G. R., Eyles, G. O., Douglas, G. B., ... & Newsome, P. J. F. (2009). Land Use Capability Survey Handbook–a New Zealand handbook for the classification of land. *Hamilton: AgResearch*.

Malczewski, J. (1999). *GIS and Multicriteria Decision Analysis*. New York: J. Wiley & Sons

Malczewski, J. (2004). GIS-based land-use suitability analysis: A critical overview. *Progress in Planning*, 62, 3-65. doi:10.1016/j.progrss.2003.09.002

Malone, B. P., Minasny, B., & McBratney, A. B. (2017). *Using R for digital soil mapping*. Springer International Publishing.

Mason, E. G., Salekin, S., & Morgenroth, J. A. (2017). Comparison between meteorological data from the New Zealand National Institute of Water and Atmospheric Research (NIWA) and data from independent meteorological stations. *New Zealand Journal of Forestry Science*, *47*(1), 7.

Massawe, B. H. J. (2015). *Digital Soil Mapping and GIS-based Land Evaluation for Rice Suitability in Kilombero Valley, Tanzania*. *(*Doctoral dissertation*,* Ohio State University, Ohio, United States of America). www.maximus.co.nz/Products/iButton-Products/Hygrochron-Temperature-Humidity-Loggers/DS1921G

Mazengarb, C., & Speden, I. G. (Eds.). (2000). *Geology of the Raukumara area* (Vol. 6). Institute of Geological & Nuclear Sciences.

McAneney, K. J., & Judd, M. J. (1983). Pasture production and water use measurements in the central Waikato. *New Zealand journal of agricultural research*, *26*(1), 7-13.

McCarty, L. B., Hubbard, L. R., & Quisenberry, V. L. (2016). *Applied soil physical properties, drainage, and irrigation strategies*. Springer International Publishing.

McLaren, R., & Cameron, K. (1996). *Soil science: Sustainable production and environmental protection* (2nd. ed.). Auckland: Oxford University Press.

McIndoe, I., Brown, P., Rajanayaka, C. & Birendra. K. (2017). Guidelines for Reasonable Irrigation Water Requirements in the Otago Region. Christchurch, Otago Regional Council. C15000.

McVicar, T. R., Li, L. T., Van Niel, T. G., Hutchinson, M. F., Mu, X. M., & Liu, Z. H. (2005). Spatially distributing 21 years of monthly hydrometeorological data in China: Spatio-temporal analysis of FAO-56 crop reference evapotranspiration and pan evaporation in the context of climate change.

Meng, Q., Liu, Z., & Borders, B. E. (2013). Assessment of regression kriging for spatial interpolation–comparisons of seven GIS interpolation methods. *Cartography and geographic information science*, *40*(1), 28-39.

Milne, J. D. G., Clayden, B., Singleton, P. L., & Wilson, A. D. (1995). *Soil description handbook*. Manaaki Whenua Press.

Molloy, L. (1988). Soils in the New Zealand landscape: the living mantle. *Soils in the New Zealand landscape: the living mantle.*

Monteith, J. L. (1965, July). Evaporation and environment. In *Symp. Soc. Exp. Biol* (Vol. 19, No. 205-23, p. 4).

Nwer, B. A. B. (2006). The Application of Land Evaluation Technique in the north-east of Libya. *(*Doctoral dissertation*,* Cranfield University, Cranfield, United Kingdom).

Mostovoy, G. V., King, R. L., Reddy, K. R., Kakani, V. G., & Filippova, M. G. (2006). Statistical estimation of daily maximum and minimum air temperatures from MODIS LST data over the state of Mississippi. *GIScience & Remote Sensing*, *43*(1), 78-110.

Mueller, L., Schindler, U., Mirschel, W., Shepherd, T. G., Ball, B. C., Helming, K., ... & Wiggering, H. (2010). Assessing the productivity function of soils. A review. *Agronomy for Sustainable Development*, *30*(3), 601-614.

Newsome, P. F. J., Wilde, R. H., & Willoughby, E. J. (2008). *Land Resource Information System Spatial Data Layers: Data Dictionary*. Landcare Research New Zealand.

Ninyerola, M., Pons, X., & Roure, J. M. (2007). Monthly precipitation mapping of the Iberian Peninsula using spatial interpolation tools implemented in a Geographic Information System. *Theoretical and Applied Climatology*, *89*(3-4), 195-209.

NIWA, R. (2009). CliFlo: NIWA's National Climate Database on the Web.

Oke, T. R. (2002). *Boundary layer climates*. Routledge.

Oukabli, A., Bartolini, S., & Viti, R. (2003). Anatomical and morphological study of apple (Malus× domestica Borkh.) flower buds growing under inadequate winter chilling. *The Journal of Horticultural Science and Biotechnology*, *78*(4), 580-585.

Page, M., & National Water Soil Conservation Authority. (1988). *Land Use Capability Classification of the Northern Hawke's Bay Region: A bulletin to accompany the New Zealand Land Resource Inventory Worksheets* (Water & soil miscellaneous publication; no. 109). Wellington, N.Z.: Published for the National Water and Soil Conservation Authority by the Water and Soil Directorate, Ministry of Works and Development.

Pearse, L., Johnston, D., & Becker, J. (2001). Managing natural hazards in the Hawke's Bay, New Zealand. *Australian Journal of Emergency Management, The*, *16*(3), 37.

Penman, H. L. (1948). Natural evaporation from open water, bare soil and grass. Proc. R. Soc. Lond. A, 193(1032), 120-145.

Penman, H. L. (1956). Estimating evaporation. *Eos, Transactions American Geophysical Union*, *37*(1), 43-50.

Penman, H. T. (1951). Some physical aspects of assimilation and transpiration. In *Symposia Soc. Exptl. Biol.* (Vol. 5, pp. 115-129).

Pereira, L. S., Allen, R. G., Smith, M., & Raes, D. (2015). Crop evapotranspiration estimation with FAO56: Past and future. *Agricultural Water Management*, *147*, 4-20.

Pike, G. (2013). *Understanding temporal and spatial temperature variation at the local scale in a high latitude environment* (Doctoral dissertation, University of Portsmouth).

Pouteau, R., Rambal, S., Ratte, J. P., Gogé, F., Joffre, R., & Winkel, T. (2011). Downscaling MODIS-derived maps using GIS and boosted regression trees: the case of frost occurrence over the arid Andean highlands of Bolivia. *Remote Sensing of Environment*, *115*(1), 117-129.

Priestley, C. H. B., & Taylor, R. J. (1972). On the assessment of surface heat flux and evaporation using large-scale parameters. Monthly weather review, 100(2), 81-92

Pullar, W., & Ayson, E. (1965). *Soils and agriculture of Wairoa Valley, Hawke's Bay, N.Z.* (N.Z. Soil Bureau report; 2/1965). Wellington, [N.Z.]: Department of Scientific and Industrial Research.

Purdie, J., Hutchinson, G., & Allen, D. (1999). Topoclimate South: integrated climate and soil mapping in Southland. *Weather and Climate*, 15-22.

Rajanayaka, C., Brown, P., & Jaramillo, A. (2016). Guidelines for Reasonable Irrigation Water Requirements in the Waikato Region. Hamilton, Waikato Regional Council. H12002803.

Richards, K., & Baumgarten, Y. (2003). Towards Topoclimate Maps of Frost and Frost Risk for Southland, New Zealand.

Rijkse, W. C. (1979). Soils of part Tiniroto-Wairoa area, North Island, New Zealand.

Rijkse, W. C. (1980). Soils of Mohaka-Aropaoanui area, North Island, New Zealand. *Soils of Mohaka-Aropaoanui area, North Island, New Zealand.*, (55).

Riveira, I. S., & Maseda, R. C. (2006). A review of rural land-use planning models. *Environment and Planning B: Planning and Design*, *33*(2), 165-183.

Rosa, D., Moreno, J. A., Garcia, L. V., & Almorza, J. (1992). MicroLEIS: a microcomputer-based Mediterranean land evaluation information system. *Soil Use and Management*, *8*(2), 89-96.

Rossiter, D. G. (1996). A theoretical framework for land evaluation. *Geoderma*, *72*(3-4), 165-190.

Sadeghi, L., & Shamseldin, A. Y. (2014). Application of the standardized precipitation index (SPI) in Hawke's Bay, New Zealand. *Drought: Research and Science-Policy Interfacing*, 139.

Salinger, M. J., & Kenny, G. J. (1995). Climate and kiwifruit cv.'Hayward'2. Regions in New Zealand suited for production. *New Zealand Journal of Crop and Horticultural Science*, *23*(2), 173-184.

Salvacion, A. & Asaad, A. (2014). ALUES (Agricultural Land Use Evaluation System). Technical report, raster vignette.

Sansom, J., & Tait, A. (2004). Estimation of long-term climate information at locations with short-term data records. *Journal of Applied Meteorology*, *43*(6), 915-923.

Scotter, D. R., Clothier, B. E., & Turner, M. A. (1979). The soil water balance in a gragiaqualf and its effectt on pasture growth in central New Zealand. *Soil Research*, *17*(3), 455-465.

Scotter, D., & Heng, L. (2003). Estimating reference crop evapotranspiration in New Zealand. *Journal of Hydrology (New Zealand)*, 1-10.

Shepherd, T., Manawatu-Wanganui . Horizons Regional Council, & BioAgriNomics. (2009). Visual soil assessment (2nd ed.). Palmerston North, N.Z.: Horizons Regional Council.

Söderström, M., & Magnusson, B. (1995). Assessment of local agroclimatological conditions—a methodology. *Agricultural and Forest Meteorology*, *72*(3-4), 243-260.

Sohrabinia, M., Zawar-Reza, P., & Rack, W. (2015). Spatio-temporal analysis of the relationship between LST from MODIS and air temperature in New Zealand. *Theoretical and applied climatology*, *119*(3-4), 567-583.

Soil Moisture (2018). Retrieved from https://www.soilmoisture.com

Stöckle, C. O., Donatelli, M., & Nelson, R. (2003). CropSyst, a cropping systems simulation model. *European journal of agronomy*, *18*(3-4), 289-307.

Sturman, A. P., & Tapper, N. J. (2006). *Weather and climate of Australia and New Zealand*. Oxford University Press.

Suleiman, A. A., & Hoogenboom, G. (2007). Comparison of Priestley-Taylor and FAO-56 Penman-Monteith for daily reference evapotranspiration estimation in Georgia. *Journal of Irrigation and Drainage Engineering*, *133*(2), 175-182.

Tait, A., & Woods, R. (2007). Spatial interpolation of daily potential evapotranspiration for New Zealand using a spline model. *Journal of Hydrometeorology*, *8*(3), 430-438.

Tait, A., & Zheng, X. (2003). Mapping frost occurrence using satellite data. *Journal of Applied Meteorology*, *42*(2), 193-203.

Thompson, S., Gruner, I., & Gapare, N. (2003). New Zealand land cover database. Version 2. Illustrated guide to target classes. Technical user guide. Version 4.0. _April 2004. Ministry for the Environment. *Ministry for the Environment*.

Thornthwaite, C. W. (1948). An approach toward a rational classification of climate. *Geographical review*, *38*(1), 55-94.

Tobler, W. R. (1970). A computer movie simulating urban growth in the Detroit region. *Economic geography*, *46*(sup1), 234-240.

Tsoumakas, G., & Vlahavas, I. (1999). ISLE: an Intelligent System for Land Evaluation. *Proceedings ACAI*, *99*, 26-32.

Turner, A., & Fitzharris, B. (1986). Mapping warm season degree days at the local scale. *New Zealand Geographer*, *42*(2), 57-64.

Tveito, O. E., Wegehenkel, M., van der Wel, F., & Dobesch, H. (2008). COST Action 719: The Use of Geographic Information Systems in Climatology and Meteorology: Final Report. *EUR-OP, Luxembourg: Office for Official Publications of the European Communities*.

Vandergoes, M. J., Hogg, A. G., Lowe, D. J., Newnham, R. M., Denton, G. H., Southon, J., ... & Almond, P. C. (2013). A revised age for the Kawakawa/Oruanui tephra, a key marker for the Last Glacial Maximum in New Zealand. *Quaternary Science Reviews*, *74*, 195-201.

Voogd, H. (1983). *Multicriteria evaluation for urban and regional planning* (Vol. 207). London: Pion.

Wall, C., Dozier, W., Ebel, R. C., Wilkins, B., Woods, F., & Foshee, W. (2008). Vegetative and floral chilling requirements of four new kiwi cultivars of Actinidia chinensis and A. deliciosa. *HortScience*, *43*(3), 644-647.

Wan, Z. (2014). New refinements and validation of the collection-6 MODIS land-surface temperature/emissivity product. *Remote Sensing of Environment*, *140*, 36-45.

Webb, M. A., Hall, A., Kidd, D., & Minansy, B. (2016). Local-scale spatial modelling for interpolating climatic temperature variables to predict agricultural plant suitability. *Theoretical and Applied Climatology*, *124*(3-4), 1145-1165.

Webb, T. H. & Wilson, A. D. (1994). *Classification of land according to its versatility for orchard crop production*. Manaaki Whenua Press.

Webster, R., & Oliver, M. A. (2007). *Geostatistics for environmental scientists*. John Wiley & Sons.

Whaley, K., & New Zealand Protected Natural Areas Programme. (2001). Tiniroto, Waihua, Mahia and Matawai ecological districts: Survey report for the Protected Natural Areas Programme. Gisborne, N.Z.: Dept. of Conservation, East Coast Hawke's Bay Conservancy.

Wood, S.R. & Dent, F.J., 1983. LECS: a land evaluation computer system. AGOF/1NS/78/006. Vols. 5 (Methodology) & 6 (User's Manual), Ministry of Agriculture, Government of Indonesia, Bogor

Woodward, S. J. R., Barker, D. J., & Zyskowski, R. F. (2001). A practical model for predicting soil water deficit in New Zealand pastures. *New Zealand Journal of Agricultural Research*, *44*(1), 91-109.

Wong, M. T. F., & Asseng, S. (2006). Determining the causes of spatial and temporal variability of wheat yields at sub-field scale using a new method of upscaling a crop model. *Plant and Soil*, *283*(1-2), 203-215.

Wright, J. L. (1982). New evapotranspiration crop coefficients. *Proceedings of the American Society of Civil Engineers, Journal of the Irrigation and Drainage Division*, *108*(IR2), 57-74.

Yang, J., Li, B., & Shiping, L. (2000). A large weighing lysimeter for evapotranspiration and soil-water–groundwater exchange studies. *Hydrological processes*, *14*(10), 1887-1897.

Yang, Y. Z., Cai, W. H., & Yang, J. (2017). Evaluation of MODIS land surface temperature data to estimate near-surface air temperature in northeast China. *Remote Sensing*, *9*(5), 410.

Yoder, R. E., Odhiambo, L. O., & Wright, W. C. (2005). Evaluation of methods for estimating daily reference crop evapotranspiration at a site in the humid southeast United States. *Applied engineering in agriculture*, *21*(2), 197-202.

Yoshino, M. M. (1975). Climate in a small area. *University of Tokyo, Tokyo*.

Zhu, W., Lű, A., & Jia, S. (2013). Estimation of daily maximum and minimum air temperature using MODIS land surface temperature products. *Remote Sensing of Environment*, *130*, 62-73.

Appendix 1

```
#setting up workspace
import arcpy
import os
from datetime import datetime
start = datetime.now()
import subprocess
arcpy.env.overwriteOutput=True
MODIStsp_full = os.getcwd()

##CS = os.path.join(MODIStsp,"CS.shp")
#defining path to climate station raster - 1by1 window or 3by3 window
##CS_ras = os.path.join(MODIStsp,"CS.tif")
#CS_ras = os.path.join(MODIS,"GEO","CS_3by3.tif")
CS = os.path.join(MODIStsp_full,"WD_CS.shp")
CS_ras = os.path.join(MODIStsp_full,"WD_CS.tif")

#setting up directories
image_dir = MODIStsp_full+"\\Images"
input_dir = MODIStsp_full+"\\Input"
output_dir = MODIStsp_full+"\\Output"
hdf_dir = MODIStsp_full+"\\HDF_Images"
summary_stats = os.path.join(output_dir,"summary_stats.dbf")
prm_file = "E:\\MODIStsp_test\\Parameter_files\\MOD2015201.prm"
out_prm = "E:\\MODIStsp_test\\Parameter_files\\parameters.prm"
arcpy.CheckOutExtension("Spatial")
arcpy.CheckOutExtension("Data Analysis")

#defining order of processing
def main():
   MRTtool()
   ZonalStats()
   finish = datetime.now() - start
   print("Finished. Total time %i:%i"%((finish.seconds / 60), (finish.seconds % 60)))
   print ("Job done, Jonno is AWESOME")

#defines process of MRT tool to be used as one function
def MRTtool():
   HDF_list=[]
   for fname in os.listdir(hdf_dir):
      if fname.endswith (".hdf"):
         in_HDF = os.path.join(hdf_dir, fname)
         out_name = fname[0:3]+fname[9:16]+'.tif'
         out_HDF = os.path.join(input_dir, out_name)
         #print in_HDF
         print out_HDF
```

```
        prm_lines = ""
        with open(prm_file, 'rb') as prm:
            for line in prm: if "INPUT_FILENAME =
D:\\2015\\MOD11A1.A2015201.h31v12.006.2016223151529.hdf" in line:
                print line
                prm_lines +=line.replace("INPUT_FILENAME =
D:\\2015\\MOD11A1.A2015201.h31v12.006.2016223151529.hdf",
                "INPUT_FILENAME = %s"%in_HDF)
            elif "OUTPUT_FILENAME = D:\\2015\\Images\\MOD2015210.tif" in line:
                prm_lines +=line.replace("OUTPUT_FILENAME =
D:\\2015\\Images\\MOD2015210.tif","OUTPUT_FILENAME = %s"%out_HDF)
            else:
                #print line
                prm_lines += line

        #print prm_lines

        with open(out_prm, 'wb') as prm:
            prm.write(prm_lines)

        command = "C:\\MRT\\bin\\resample -p %s"%out_prm
        subprocess.call(command)

#defines zonal stats table function, which is then able to be put in order of
processing later on
def ZonalStats():
    image_list=[]
    for fname in os.listdir(input_dir):
        if fname.endswith (".tif"):
            #print fname
            imagename=fname.split(".")[0]
            #print imagename +
            if imagename not in image_list:
                image_list.append(imagename)
    print image_list

#names each image to be processed
    in_image = os.path.join(input_dir, image_list[0] + '.LST_Night_1km.tif')
    #print in_image
    #allows CS pixels to align to those used in MODIS images:
    arcpy.env.cellSize = in_image
    arcpy.env.snapRaster = in_image
    arcpy.env.outputCoordinateSystem = in_image
    print in_image

    table_list=[]
    LST_list = ["Night"]
```

```
  #for loop in which main processing done. tables created and manipulated producing final summary statistics table
  for image in image_list:
    for Night in LST_list:
      in_image = os.path.join(input_dir, image + '.LST_%s_1km.tif'% Night)
      out_table = os.path.join(output_dir, image + 'LST_%s_zstat.dbf'% Night)
      in_image2 = os.path.join(input_dir, image + '.%s_view_time.tif'% Night)
      out_table2 = os.path.join(output_dir, image + '%s_zstat.dbf'% Night)
      print in_image
      #produces table stats(pizel values) for each MODIS image in 1km2 pixel around each climate station
      arcpy.sa.ZonalStatisticsAsTable (CS_ras, "VALUE", in_image, out_table, "DATA", "MEAN")
      #adds field to table then calculates temp in C from temp K
      arcpy.AddField_management (out_table, "Temp_C", "DOUBLE","15","2")
      arcpy.CalculateField_management (out_table, "Temp_C", "!Mean!*0.02-273.15", "PYTHON")
      #table join MODIS Temp C table to climate station to add CS name to MODIS temp data
      arcpy.JoinField_management (out_table, "VALUE", CS_ras, "Value", ["CS_ref"])
      #produces table stats(pizel values as view time image taken) for each MODIS image in 1km2 pixel around each climate station then calculates hour.minute image taken
      arcpy.sa.ZonalStatisticsAsTable (CS_ras, "VALUE", in_image2, out_table2, "DATA", "MEAN")
      arcpy.AddField_management (out_table2, "Time", "DOUBLE","15","2")
      arcpy.CalculateField_management (out_table2, "Time", "!MEAN!*0.1", "PYTHON")
      #table join MODIS view time table to climate station to add CS name to MODIS view time data
      arcpy.JoinField_management (out_table2, "VALUE", CS_ras, "Value", ["CS_ref"])
      arcpy.JoinField_management (out_table, "CS_ref", out_table2, "CS_ref", ["Time"])
      #adds new column to stat table lablled as "MODIS_ref" then adds image reference name to each row
      arcpy.AddField_management (out_table, "MODIS_ref", "TEXT")
      arcpy.CalculateField_management (out_table, "MODIS_ref", "'"+image+"'", "PYTHON")
      #adds new column to stat table labelled "MOD_day" then adds either "Night" or "Day" to each row
      arcpy.AddField_management (out_table, "MYD_Night", "TEXT")
      arcpy.CalculateField_management (out_table, "MYD_Night", "'"+Night+"'", "PYTHON")
      #appends all zstats data to one summary table
      table_list.append(out_table)

  #print table_list, "\n\n"
```

```
   #makes list of tables then "pops" or removes one out to become the "target
table" to append all other table data to
   table= table_list.pop()
   #print table_list, "\n\n"
   #print table
   arcpy.CopyRows_management (table, summary_stats)
   arcpy.Append_management (table_list, summary_stats, "TEST","","")
```